List of Abbrevattions

A: Acceptor
AO: Atomic Orbital
ALT: Accelerated Life Testing
BHJ: Bulk HeteroJunction
BHJSC: Bulk HeteroJunction Solar Cell
CB: Conduction Band/ Chlorobenzene
CV: Cyclic Voltammetry
d: doublet
D: donor
DSC: Differential Scanning Calorimetry
E_g: band gap
FF: Fill Factor
FT-IR: Fourier Transform-Infra Red
H-H: Head-Head
H-T: Head-Tail
HOMO: Highest Occupied Molecular Orbital
I_{sc}: Short Circuit current
J_{sc}: Short Circuit current density
LED: Light Emitting Diode
LUMO: Lowest Unoccupied Molecular Orbital
m: multiplet
MO: Molecular Orbital
Mpp: Maximum power point
MTDSC: Modulated Temperature Differential Scanning Calorimetry
NMR: Nuclear Magnetic Resonance
OFET: Organic Field Effect Transistor
OLED: Organic Light Emitting Diode
P3AT: Poly(3-alkylthiophene)
P3HT: Poly(3-alkylthiophene)
PA: Poly(Acetylene)
Pc: Phthalocyanine
PCE: Power Conversion Efficiency
PLED: Polymer Light Emitting Diode
PPV: poly(*p*-phenylenevinylene)
PSC: Polymer Solar Cell
PT: Poly(Thiophene)
q: Quadruplet

RR: Regio Regular
RCS: Refrigerator Cooling System
s: singlet
t: triplet
T_g :glass transition temperature
TLC : Thin Layer Chromatography
TMS: TetraMethylSilane
T-T: Tail-Tail
VB: Valence Band
V_{oc}: Open Circuit Voltage

Table of Contents

Chapter One:
General introduction

Abstract: This chapter introduces the relation between structure and materials properties for conjugated polymers and more specifically for poly(3-alkylthiophenes). Several synthetic routes for these materials are discussed, since these will determine the regioregularity, affecting (supra)-molecular structure and performance in bulk heterojuction solar cells.

In everyday life, the use of synthetic polymers and their presence in society increased exponentially since the first commercialized synthetic polymer "Bakelite" was reported in 1907.[1] More and more plastics and polymers became available in different applications and influenced many aspects of civilization in the 20th century. The evolution of this class of materials was driven by the development of science and technology in this field. Now, at the beginning of the 21st century, more recent materials and their possible applications stimulate the development of new technologies. Some of these new technological applications are based on conjugated polymers.

1. Structure – properties relationship in conjugated polymers

Conjugated polymers were discovered to have semi-conductive properties by the end of the 1970's.[2] Whereas classical non-conjugated polymers are known for their electrical insulating properties, conjugated polymers combine the desirable properties of the polymer-class materials such as light weight, low cost and high mechanical strength and flexibility with semi-

conducting characteristics. The electronic properties of these materials are a consequence of the molecular structure. The semi-conductive properties result from delocalization in the conjugated system, the alternating single and double bonds along the polymer backbone. Poly(acetylene) (PA) and poly(thiophene) (PT) are well known examples of conjugated polymers (figure 1).

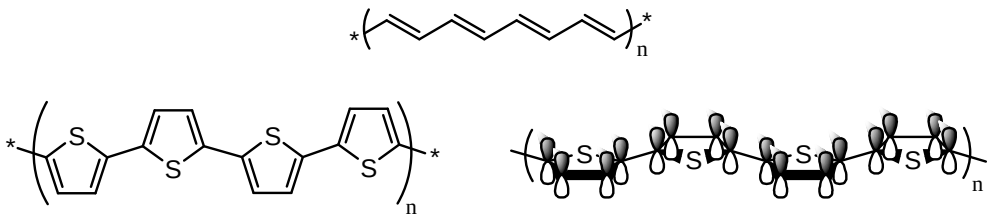

Figure 1: Poly(acetylene) and poly(thiophene)

Overlapping atomic orbitals (AO) combine into molecular orbitals (MO). The single covalent bonds (σ-bond) along the backbone of a polymer are formed by overlap of sp^2-orbitals (figure 2a). In a conjugated polymer, a second bond (π bond) is formed by sideway overlapping p_z orbitals, perpendicular to the planar polymer backbone, as displayed in figure 1 for PT.

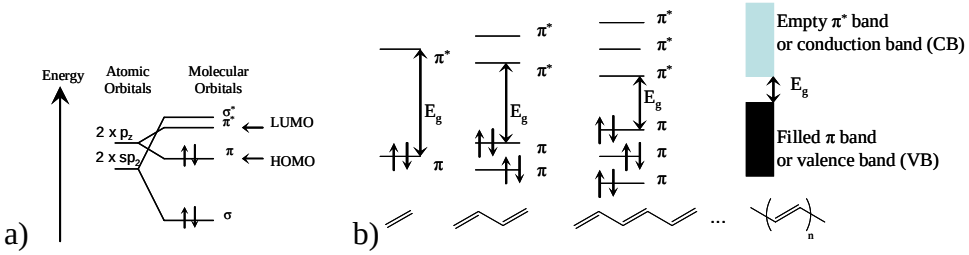

Figure 2: a)Molecular orbital formation in ethylene, b) band gap in poly(acetylene)

The combination of several orbitals results in energy bands, that move closer in energy as the size of the conjugated system increases.[3] The Highest Occupied Molecular Orbital (HOMO) or conduction band (CB) and the Lowest Unoccupied Molecular Orbital (LUMO) or valence band (VB) are separated by an energy difference: the band gap (E_g), as displayed in figure 2b. The band gap of materials determines the possible applications. Electrons in the HOMO may be excited into the LUMO when a sufficient amount of energy is absorbed. According to equation 1, the energy (E) of a photon corresponds to a certain wavelength (λ). When the values of Planck's constant h and the light velocity c are filled in, the relation between E (eV) and λ (nm) is written as equation (2).

$$E = \frac{hc}{\lambda} \quad (1) \qquad E = \frac{1240}{\lambda} \quad (2)$$

For conjugated polymers, the energy that is necessary to excite an electron corresponds to a part of the radiation that is emitted by the sun. In solar cells, the part of the energy that is absorbed can be transformed into electricity. In the opposite situation, energy is set free when electrons are introduced in the LUMO, and fall back to the HOMO-level. This energy is emitted as heat or radiation. If the wavelength of the emitted radiation corresponds to the wavelength of visible light, the material is useful for display applications. Because the E_g of some conjugated polymers matches with the energy of visible light, these materials are useful in applications, a few examples are shown in Figure 3.

1.1 Unique material properties lead to new applications

Due to the combination of desirable electronic and physical properties in organic semi-conductors, new applications with these materials were

developed and conjugated polymers will enter the society as active materials in electronic devices. Together with other functional polymers, these materials will influence again the daily routine by creating new possibilities.

In the field of organic electronics, the development of new technological applications has lead to the first commercially available items today, for example in several display applications. Also the first applications of polymer solar cells are being developed and will be appearing on the market.

Figure 3: Applications with organic light emitting materials: SONY XEL-1 OLED TV (www.sony.com), Philips Lumiblade (www.lighting.philips.com), a mobile phone: Nokia N85 (www.nokia.com)

2. Poly(3-alkylthiophenes)

The class of conjugated polymers contains very promising materials.[4] More specifically, PTs are environmentally stable conjugated polymers with a high hole mobility. PT is an insoluble solid material because the delocalized π system in one chain experiences a strong π- π attraction with the different neighbouring chains. The supramolecular structure in Poly(3-Alkylthiophene)s (P3ATs) is governed by the self-ordering of planar conjugated backbones. The π- π stacking of the conjugated system is a

driving force for crystallization of P3ATs.[5] Insertion of an alkyl side chain on the backbone of PT increases the distance between polymer chains and decreases the attraction between the chains, resulting in a more soluble polymer. Good solubility and processability of a conjugated polymer are first demands to process the materials and to apply them in a device. Poly(3-hexylthiophene) (P3HT, figure 4) is an example of such a soluble conjugated polymer and has been extensively investigated for application in organic photovoltaics.

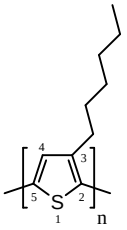

Figure 4: Poly(3-hexylthiophene), an example of a poly(3-alkylthiophene)

The position of the alkyl chains in several repeating units of the conjugated polymer determines the material properties. A combination of several diades is possible: Head-Tail (H-T), Head-Head (H-H) or Tail-Tail (T-T), as displayed in figure 5a. In a 100% regioregular (RR) structure, with only H-T bonds, all chains are in the same position relative to the connections with other repeating units at the 2 and 5' positions. The planar polymer backbones can self-assemble into a crystalline structure. In a more regiorandom or non-RR structure, the sterical hindrance of two side chains causes two repeating units in the backbone to twist out of plane (figure 5b). The supramolecular order in the system decreases, since the stacking of the π systems is disturbed by the twisting backbone. This also interrupts the aromatic system and delocalization of electrons and decreases the effective conjugation length.

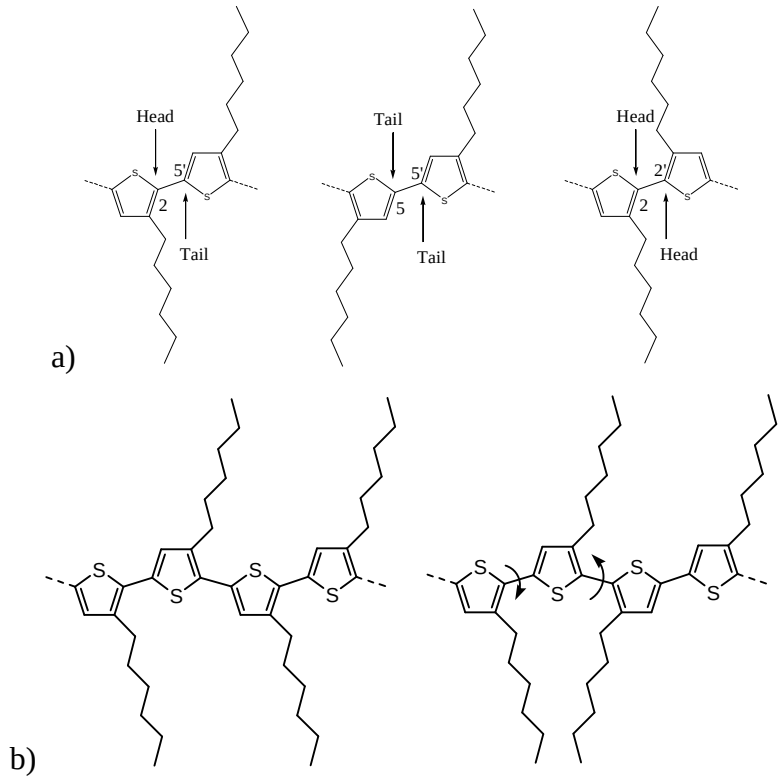

Figure 5: a) H-T or 2-5', T-T or 5-5' and H-H or 2-2'coupling of 3-hexylthiophene; b) Regioregular and non-regioregular P3ATs

2.1 Synthesis of Poly(3-alkylthiophenes)

The synthesis of P3ATs is a tool to control the desired materials properties. The synthesis of both RR as non-RR P3ATs is well documented and reviewed.[8, 9] For several synthetic routes, polymers containing functional groups in the side chains or functionalized end groups were reported.[9] In this thesis, both the oxidative polymerization with $FeCl_3$ and the Rieke method are used for the synthesis of P3ATs. Therefore, the introduction focuses on these synthetic routes. The discussed synthetic methods were used to produce functionalized P3HT-based copolymers: by inserting functional groups in the side chains, certain material properties were

modified. By changing the percentage of functionalized side chains and the nature of the inserted functional groups, the properties of the material were varied. In addition, an overview is given of other synthetic methods to produce P3ATs.

2.1.1 Oxidative polymerization with $FeCl_3$

The oxidative polymerization using $FeCl_3$ yields non-RR P3AT, containing 60 to 80% H-T bonds. The non-RR P3HT in a bulk heterojunction solar cell (BHJSC) is inferior to RR materials in absolute efficiency,[6] but can lead to more stable devices.[7]

The mechanism is proposed to proceed at the surface of solid $FeCl_3$ particles.[10] A slurry in chloroform as a reaction medium was found to give the best results. At the surface of $FeCl_3$, the thiophene is oxidized while $FeCl_2$ is formed. Functional P3AT copolymers can be obtained using a variety of synthetic procedures. Using oxidative polymerization with $FeCl_3$, it is possible to incorporate a wide variety of functional groups in the side chains of P3AT. P3AT copolymers including several ester, alkoxy, alcohol, bromine and other functionalities on side chains have been reported. In the mechanism of the polymerization reaction (figure 6), there is no or little control for bonds to be formed in a H-T fashion, and no or little steric hindrance at the catalysts surface for a highly regioregular structure to be formed preferably.

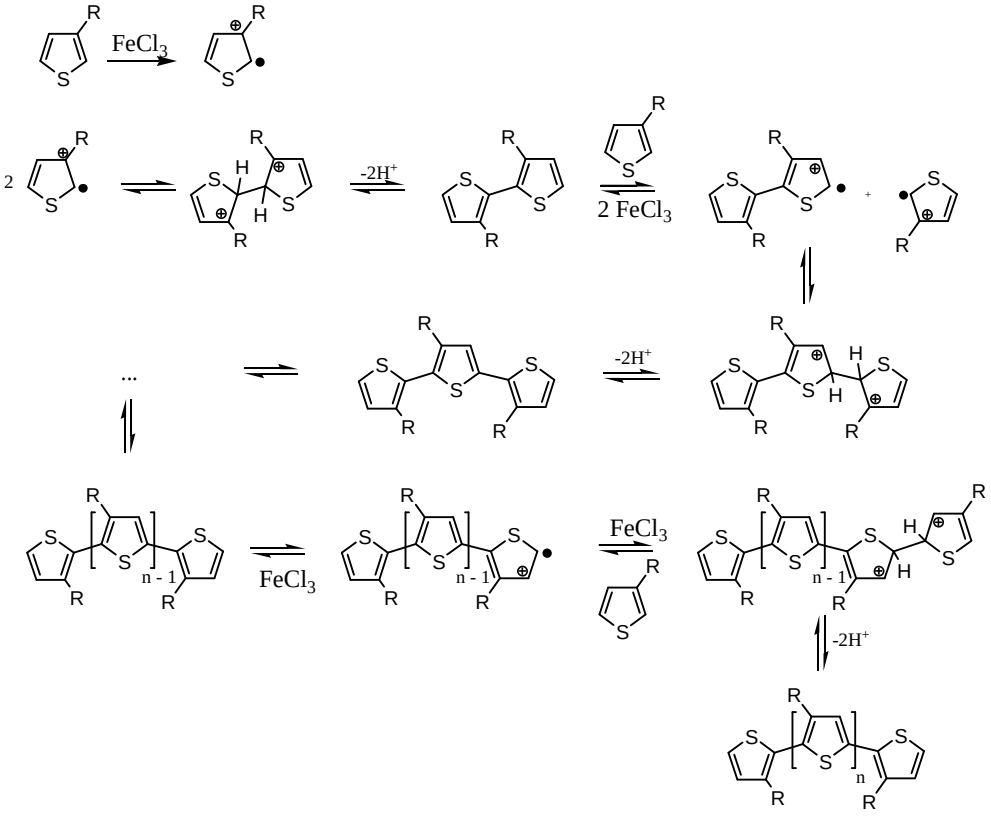

Figure 6: Mechanism of the oxidative polymerization using $FeCl_3$ as proposed by Niemi *et al.*[10]

2.1.2 Rieke method

Soon after publication of the McCullough method in 1992,[11] the Rieke method for production of highly RR P3ATs was reported (figure 7, Table 1). Chen and Rieke showed that by using Nickel catalysts instead of Pd catalysts, a regioregular structure was obtained.[12] Together with the evolution of synthetic methods and the ability to produce RR P3ATs, the insight in the relationship between molecular and supramolecular structure developed.[5, 13, 14] Because of the selective oxidative addition of active zinc to the aromatic bromine, the Rieke method is compatible with several functional groups.[15] Therefore, this route was chosen to synthesize side-chain functionalized RR copolymers of P3HT.

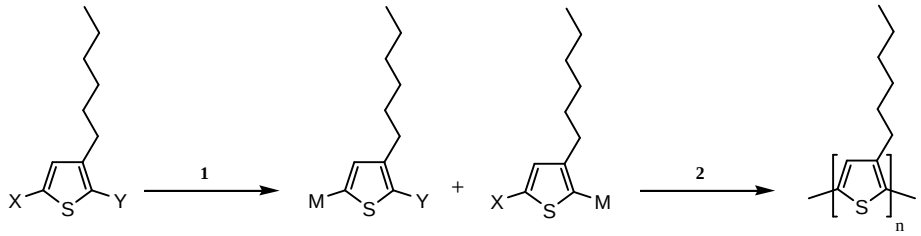

Figure 7: Metal- or halogen substituted 3-HT as building blocks for P3HT

Table 1: Synthetic methods for synthesis of poly(3-alkylthiophenes)[9]

Method	H-T (%)	Yield (%)	X,Y	Reaction 1	Reaction 2	M_n
Oxidative polymerization	60-80	60-70	H,H	$FeCl_3$	-	30k-300k
Rieke	>90	~75	Br,Br	Zn*, THF	$Ni(dppp)Cl_2$	25k-35k
McCullough	95-99	45-65	H,Br	i)LDA/THF ii)$MgBr_2.Et_2O$	$Ni(dppp)Cl_2$	20k-40k
GRIM	>99	40-60	Br,Br	RMgX	$Ni(dppp)Cl_2$	20k-35k

2.1.3 McCullough method and Grignard metathesis (GRIM)

The McCullough method produces P3ATs containing a high percentage of H-T bonds. It has been applied for synthesis of homopolymers containing alkoxy and ether-functionalized side-chains.[16] In 1999, the Grignard metathesis (GRIM), a method to produce RR P3AT without cryogenic reaction conditions was reported.[17] Using this method, several end-group functionalized RR P3ATs [18] or block copolymers have been synthesized.[19, 20]

Several experimental studies were performed to elucidate the mechanism of the Nickel catalyzed cross coupling reaction. It was proposed that a catalytic cycle of three consecutive steps was involved in this mechanism. The

reaction is initiated by the oxidative addition of a thiophene compound to the catalyst. The polymerization proceeds by transmetallation and reductive elimination (figure 8), via a living chain-growth mechanism.[21] The quasi-living nature of the GRIM method allows production of well defined block copolymers.[19] Recently, the GRIM route is often the polymerization method of choice in literature, since this method yields highly regioregular P3ATs and there is no need for cryogenic reaction conditions.

2.1.4 Suzuki and Stille coupling in polymerization of 3-alkylthiophenes

Other synthetic methods for the production of regioregular poly(3-alkylthiophenes) were also reported. In the Suzuki method, an organoboron compound is used, while for the Stille coupling a tributylstannane is applied to produce regioregular P3ATs. Phosphonic ester functionalized P3ATs have been synthesized with the Stille coupling.[22]

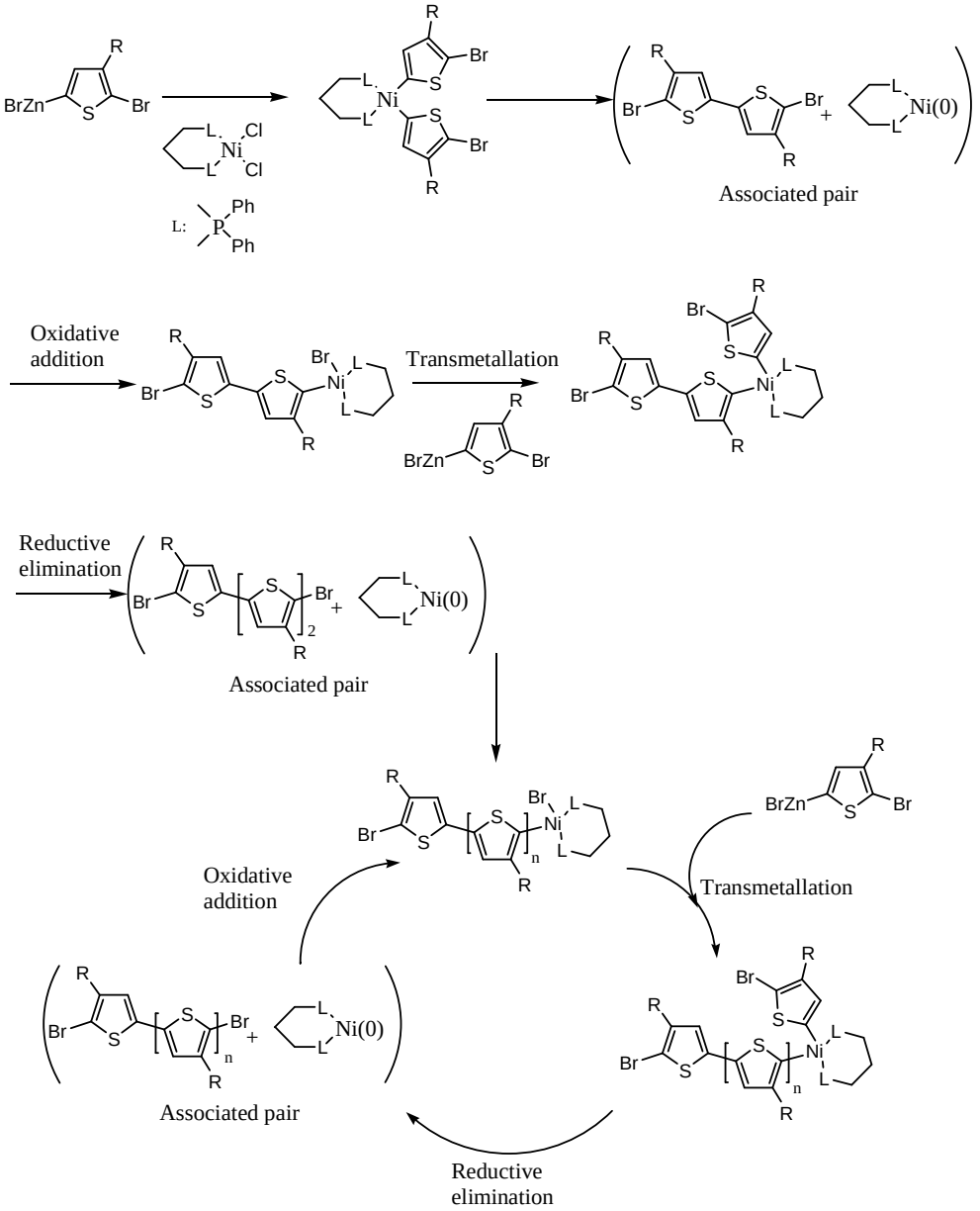

Figure 8: Mechanism for the nickel initiated cross-coupling mechanism proposed by Sheina et al.[21]

2.2 Application of P3ATs

As described before, conjugated polymers may absorb energy which is emitted by the sun (solar cells) or may emit energy in the form of visible light (lighting or display applications).

Polythiophenes are conjugated polymers with good thermal stability. If a sufficient regioregularity is reached, the mobility of charge carriers in these materials is appropriate for application in polymer solar cells (PSC)[23] or organic field effect transistors (OFETs).[24-26] Electroluminescence makes these polymers a candidate for organic light emitting diodes (OLEDs).[27-29]

In the following paragraph, a description of polymer:fullerene solar cells is given.

Semi-conductors are substances where the conductivity increases with higher temperature. At the injection of charge carries in one of the energy bands, these charges may be delocalized along the conjugated system. With a directional movement of these charges along or between polymer backbone(s), an electrical current is created in an organic material. When electrons are moving in otherwise empty energybands, it is an **n-type** semi-conductor as for example C_{60}. In PTs, mostly electrons are brought into an excited state, leaving holes in the LUMO, allowing electrons to move. This is a **p-type** semiconductor.

2.2.1 Polymer:fullerene solar cells

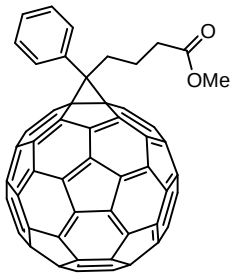

Figure 9: Phenyl C_{61} Butyric acid Methyl ester, a soluble fullerene often used in combination with a conjugated polymer, in a polymer solar cell

In a solar cell, several materials may be used as light absorbing material. Because of the great promise that solar energy applications hold, the search for other materials and methods to produce organic or hybrid solar cells is ongoing.[30-32] Usually, a polymer acts as a p-type semiconductor and serves in a polymer solar cell as an electron donor in combination with an n-type semiconductor, which acts as an electron acceptor. The observed photo-induced electron transfer between a conjugated polymer and a buckminsterfullerene initiated the search for high efficiency polymer:fullerene solar cells.[33]

For the mechanism of energy production in such a solar cell, the following model was developed.[34] When energy is absorbed, an electron is brought in an excited state (Figure 10, step 1). The result is an electron in the LUMO and a hole in the HOMO. These separate opposite charges are bound by Coulomb attraction. This bound electron-hole pair is called an **exciton**.

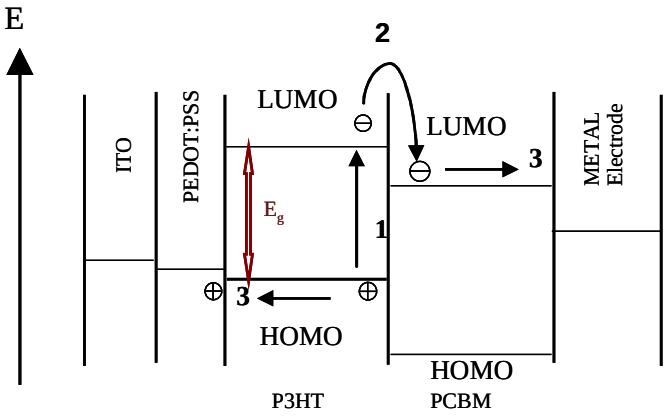

Figure 10: Scheme of the energy levels and model for energy production in a P3HT:PCBM solar cell

The exciton can migrate, typically for a distance of 10 nm in organic semi-conductors, before the electron falls back to its ground state and recombination occurs. If the exciton reaches an interface surface of a donor (D) and acceptor (A), the excited electron is transferred to the LUMO of the acceptor (step 2) if the energy difference between LUMO of the donor and LUMO of the acceptor is sufficiently high. Still an electrically bound state, the **charge transfer complex** may be separated by the internal electric field which is caused by the asymmetric work function of the metal electrodes. Then the separated charges can migrate to their respective electrodes (step 3). This model is applicable on several combinations of materials in active layer, electrodes and contact layers. For P3HT, the bandgap is around 2 eV, with the HOMO at 5.2 eV and the LUMO at 3.2 eV.[35] P3HT therefore absorbs wavelengths of 600 nm and shorter. The absorbed energy may be transferred to several e-acceptors. In solar cells, P3HT has been combined with C_{60} and derived molecules e.g. PCBM[33], ZnO_x or TiO_x.and others.[36] For this work, P3HT:PCBM was chosen as a reference system. Several groups have optimized the performance of this system by fine-tuning

interface layers,[37] blend morphology[38, 39] and device architecture,[40] resulting in 4 to 5% power conversion efficiency.[41-43] New materials with tailored energy bands result in even higher efficiencies,[44] with the current record certified efficiency of 6.77% produced by Solarmer Energy, Inc. Combined with the development of low-cost production techniques,[45] this brightens the future for polymer solar cells.

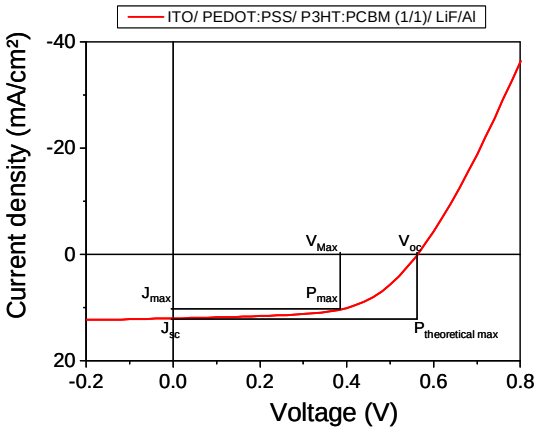

Figure 11: J-V curve of an illuminated P3HT:PCBM solar cell, with the corresponding device parameters.

The efficiency of a solar cell is determined by the amount of energy that is transferred into electrical energy. The electrical characteristics of a solar cell are obtained by measuring the current over a certain voltage range. The current density is calculated by dividing the measured current with the active area surface of the device. The obtained current density – voltage curve (*J-V* curve) allows calculation of the device parameters, displayed in figure 11. The point where the generated power reaches its maximum (P_{max}) is called the maximum power point (Mpp).[23]

$$FF = \frac{P_{\max}}{P_{theoretical\,\max}} = \frac{J_{\max}.V_{\max}}{J_{SC}.V_{SC}} \quad (3)$$

The Fill Factor (*FF*) is the ratio of P_{max} to the power at theoretical maximum (equation 3). The short circuit current (I_{sc}) is the external current that flows when no external bias is applied. More often the short current density (J_{sc}) is used, since the latter is independent of the devices' surface. The open circuit voltage (V_{oc}) is the voltage required so that no current flows through the device. In a polymer:fullerene BHJSC this parameter is attributed to the difference in energy between the HOMO of the polymer and the LUMO of the fullerene.[46-49] The efficiency of a device is calculated as the ratio of the power that is generated (P_{out}=P_{max}) to the power that is irradiated on the device (P_{in}=P_{light}).

$$\eta = \frac{P_{out}}{P_{in}} = \frac{P_{\max}}{P_{light}} = \frac{J_{\max}V_{\max}}{P_{light}} = J_{SC}.V_{OC}.FF \quad (4)$$

To rule out the dependency on light intensity or light source, usually the AM 1.5G spectrum at an intensity of 100 mW/cm² (1 Sun at a latitude of 45°N) is applied as the standard procedure to characterize the solar cells.

Bulk heterojunction morphology

According to the device model in figure 10, only excitons created near the D/A surface can be dissociated. A network where the donor-acceptor heterojunction is found throughout the bulk of the material proved to be more efficient as compared to a bilayer device.[50] In a network, the probability of an exciton to reach a D/A surface is higher. To control the

morphology of this bulk heterojunction network, first the processing solvent [38] and then the thermal annealing [39] were identified as important processing parameters for the P3HT:PCBM system. Several studies were dedicated to different aspects of the morphology of a polymer:fullerene system, first for MDMO-PPV:PCBM[51-53], and later in P3HT:PCBM.[54-61] A good morphology is obtained when the two materials are sufficiently phase-separated in a three-dimensional interpenetrating network to ensure that there are percolation paths for both charges to their respective electrodes. Too close intermixing must be avoided to prevent fast charge recombination or decreasing charge mobility.[50, 62] Ideally, each created exciton reaches a D/A interface where the charges are separated and transported to their respective electrodes, before recombination can occur. To have an appropriate morphology, several parameters have to be taken into account:[63]

- Post production treatments and thermal annealing: Thermal annealing was discovered to drastically improve the efficiency of P3HT: PCBM solar cells.[39] It was found that a thermal treatment induces crystallization of P3HT and phase demixing on a nanoscale level in the P3HT:PCBM system.[54]

- Blend ratio and concentration: The optimum blend composition was observed to be about a 1:1 ratio for P3HT:PCBM.[42, 59] Lower PCBM contents result in too few electron transport paths percolating the active layer. Higher PCBM concentrations result in PCBM clusters, which are no longer dispersed within the polymer matrix. In addition, a higher PCBM ratio leads during a thermal annealing step to the formation of clusters that can damage the cathode due to mechanical stress.[59] The

blending ratio does not only have an influence on the efficiency of the blend, but also on blend stability.[42]

❖ Solvent and processing techniques: The solubility of both compounds in the processing solvent is a first demand, and best results are obtained when the solubility of the compounds in the chosen solvent is comparable.[64] The boiling point of the solvent determines whether the solvent will be evaporated faster or slower during the spin-coating of the blend. When the solvent evaporates slowly (higher boiling point), the phase segregation proceeds further and both compounds are allowed to settle in a more phase separated state. If the polymer chains have more time to settle in an ordered fashion, P3HT will form crystalline fibrils and organize in the blend, so that higher hole mobility is achieved.[26, 58] Solvent-annealing or processing blends for solvent mixtures are techniques to give time to the molecules in the blend to self-organize and phase-separate before the solvent is evaporated completely.[43, 65-67] Using these techniques, blend morphology is tuned without thermal treatment.[60, 61]

❖ Materials purity and characteristics will determine morphology by affecting the crystallization behaviour of P3HT and PCBM. To self-organize, a certain regioregularity[5, 68], and molecular weight[69] are required.

Mophological stability

Recently, the focus in the field of polymer:fullerene solar cells was on obtaining higher efficiency.[70] Now the drive for commercialization of plastic solar cells is increasing, also more attention has gone to the stability of the polymer:fullerene solar cells.[71] The several layers of the polymer solar cell are susceptible to both chemical and physical degradation, but

these phenomena may be solved by introducing barrier layers between the solar cells and the atmosphere. If a sufficient extent of encapsulation can be obtained, these mechanisms will not determine the device lifetime.[72, 73] A problem that has been addressed recently concerns the thermal stability of the blend morphology.

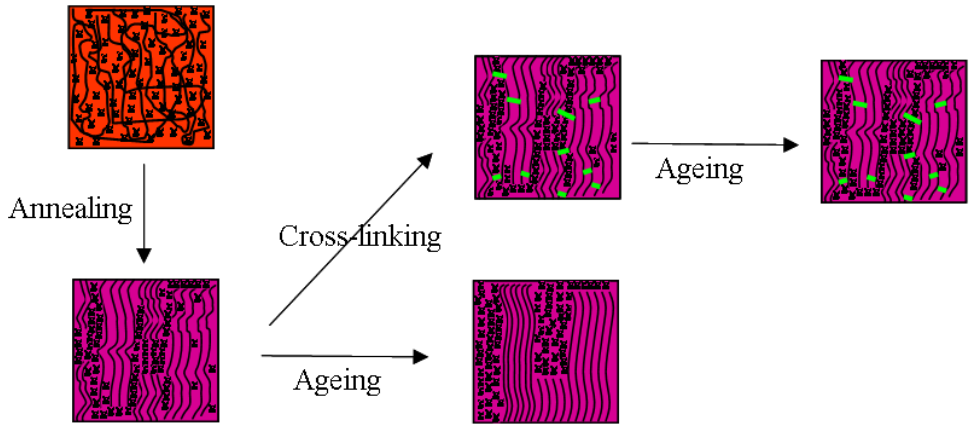

Figure 12: Crosslinking concept to prevent thermal ageing by prolonged phase seperation in a bulk heterojunction morphology

Since the BHJ morphology is a key point for a high efficiency, it needs to be stable in time at varying temperatures. A continuous demixing of the two phases in the active layer results in a decreased donor-acceptor interface surface (figure 12), so that fewer excitons are dissociated and the J_{sc} diminishes in time. During the last few years, a thermal stable morphology was achieved with crosslinkable materials,[74-76] compatibilizing compounds,[77, 78] high T_g materials[79, 80] or materials with a lower tendency to crystallize.[7, 81, 82] The crosslinking approach proved to be effective in preventing large-scale phase separation in a P3AT:PCBM BHJ morphology.[74, 75] Although Accelerated Life Testing (ALT) based on the Arrhenius model for first-order kinetic degradation was applied for

polymer:fullerene BHJSCs,[83, 84] it remains unclear what the life time expectations for the P3HT:PCBM solar cells in applications could be.[70]

3. Aim and Outline

Every following chapter was written in the form of a (draft for) manuscript for publication. Therefore, monomers (M) and polymer (P) structures are numbered again in each chapter, and the formatting of references may differ from chapter to chapter, depending on the requirements of the journal to which the chapter is to be submitted. The subject of each chapter is shortly described in this outline.

New and improved applications using conjugated polymers require new materials, with specific properties. The aim of this thesis is to investigate a method that delivers materials with tailored properties. Therefore, the synthesis of P3ATs in this work focuses on several sets of copolymers. Copolymerization is a synthetic tool to control the polymer properties. Copolymers of 3-hexylthiophene (3-HT) are synthesized to improve the performance of the related electronic devices.

In **chapter 2,** the oxidative polymerization with $FeCl_3$ is used to synthesize copolymers of P3HT. Copolymers of 3-HT with esterified analogues of thiophene monomers containing alcohol or acid groups in the side chains are prepared in several monomer molar ratios. The effect of the ester-functionalized side chains on the solubility and the compatibility of these groups with performance in a light emitting device are discussed. The introduction of an alcohol or acid group in the side chain is desirable because they can be readily functionalized. Several functional groups complementary to the acid or alcohol are used for reactions on the polymer,

thus providing the necessary tools to allow for synthesis of functionalized polythiophenes with tailored properties. If the functional group that is attached to a polymer side chain is chosen carefully, the material properties can be adapted to the needs of possible applications.

As indicated in the introduction, the molecular structure and more specifically the regioregularity of P3ATs determine the properties of the material. A method producing a non-RR polymer (the oxidative polymerization with $FeCl_3$) is reported in chapter 2. The conclusions from this work are applied in the design and synthesis of the RR functionalized polythiophenes in **chapter 3**. The Rieke method is applied to synthesize copolymers with high regioregularities and a varying percentage of functionalized side chains. The UV-Vis absorption of these polymers and of polymer blends with PCBM and solar cell performance of one copolymer series are described in function of the percentage and nature of the functional group that was introduced in the polymer side chain.

The thermal characterization, charge mobility measurements in OFETs, and impact of the side chain functionalities on the crystalline structure are given in **chapter 4**, for two copolymer series with varying percentage of ester-functionalized side chains. The application in solar cells with PCBM as an electron acceptor is discussed.

Post-polymerization functionalization is a powerful tool to synthesize from one polymer a set of materials with different properties, this will be illustrated in **chapter 5**. Here, a “click chemistry” reaction is used to functionalize conjugated polymers with Phthalocyanines, molecules that absorb longer wavelengths, to broaden the absorption window of the active layer in the solar cell. A first evaluation of the solar cell performance of these materials is presented and discussed.

The influence of the introduced functionalities on thermal stability of the morphology in a polymer:PCBM (1:1) blend is discussed in **chapter 6**. The crystallization of both compounds in the blend is investigated with optical microscopy, XRD and DSC. The performance of solar cells at higher temperature is measured as a function of time and related with the morphological stability of the blend.

4. References

1. C. E. J. Carraher. in *Seymour/Carraher's Polymer Chemistry* 738 (CRC press)
2. H. Shirakawa, E. J. Louis, A. G. Macdiarmid, C. K. Chiang and A. J. Heeger. Synthesis of Electrically Conducting Organic Polymers - Halogen Derivatives of Polyacetylene, (Ch)X *Journal of the Chemical Society-Chemical Communications* 578-580 (1977)
3. P. Atkins and J. De Paula. *Atkins' Physical Chemistry* (Oxford University Press)
4. S. R. Forrest. The path to ubiquitous and low-cost organic electronic appliances on plastic *Nature* **428**, 911-918 (2004)
5. R. D. Mccullough, S. Tristramnagle, S. P. Williams, R. D. Lowe and M. Jayaraman. Self-Orienting Head-to-Tail Poly(3-Alkylthiophenes) - New Insights on Structure-Property Relationships in Conducting Polymers *Journal of the American Chemical Society* **115**, 4910-4911 (1993)
6. M. Urien. Effect of the regioregularity of poly(3-hexylthiophene) on the performances of organic photovoltaic devices *Polymer International* **57**, 764-769 (2008)
7. C. H. Woo, B. C. Thompson, B. J. Kim, M. F. Toney and J. M. Fréchet. The influence of Poly(3-hexylthiophene) regioregularity on fullerene-composite solar cell performance *Journal of the American Chemical Society* **130**, 16324-16329 (2008)
8. R. D. McCullough. The chemistry of conducting polythiophenes *Advanced Materials* **10**, 93-116 (1998)
9. I. Osaka and R. D. McCullough. Advances in molecular design and synthesis of regioregular polythiophenes *Accounts of Chemical Research* **41**, 1202-1214 (2008)
10. V. M. Niemi, P. Knuuttila, J.-E. Österholm and J. Korvola. Polymerization of 3-alkylthiophenes with $FeCl_3$ *Polymer* **33**, 1559-1562 (1992)
11. R. D. Mccullough and R. D. Lowe. Enhanced Electrical-Conductivity in Regioselectively Synthesized Poly(3-Alkylthiophenes) *Journal of the Chemical Society-Chemical Communications* 70-72 (1992)
12. T. A. Chen and R. D. Rieke. The 1st Regioregular Head-to-Tail Poly(3-Hexylthiophene-2,5-Diyl) and a Regiorandom Isopolymer - Ni Vs Pd Catalysis of 2(5)-Bromo-5(2)-(Bromozincio)-3-Hexylthiophene Polymerization *Journal of the American Chemical Society* **114**, 10087-10088 (1992)
13. R. D. Mccullough, R. D. Lowe, M. Jayaraman and D. L. Anderson. Design, Synthesis, and Control of Conducting Polymer Architectures - Structurally Homogeneous Poly(3-Alkylthiophenes) *Journal of Organic Chemistry* **58**, 904-912 (1993)

14. T. A. Chen, X. M. Wu and R. D. Rieke. Regiocontrolled Synthesis of Poly(3-Alkylthiophenes) Mediated by Rieke Zinc - Their Characterization and Solid-State Properties *Journal of the American Chemical Society* **117**, 233-244 (1995)
15. L. Zhu, R. M. Wehmeyer and R. D. Rieke. The Direct Formation of Functionalized Alkyl(Aryl)Zinc Halides by Oxidative Addition of Highly Reactive Zinc with Organic Halides and Their Reactions with Acid-Chlorides, Alpha, Beta-Unsaturated Ketones, and Allylic, Aryl, and Vinyl Halides *Journal of Organic Chemistry* **56**, 1445-1453 (1991)
16. R. D. Mccullough and S. P. Williams. Toward Tuning Electrical and Optical-Properties in Conjugated Polymers Using Side-Chains - Highly Conductive Head-to-Tail Heteroatom-Functionalized Polythiophenes *Journal of the American Chemical Society* **115**, 11608-11609 (1993)
17. R. S. Loewe, S. M. Khersonsky and R. D. McCullough. A simple method to prepare head-to-tail coupled, regioregular poly(3-alkylthiophenes) using grignard metathesis *Advanced Materials* **11**, 250- (1999)
18. J. Liu and R. D. McCullough. End group modification of regioregular polythiophene through postpolymerization functionalization *Macromolecules* **35**, 9882-9889 (2002)
19. M. C. Iovu, E. E. Sheina, R. R. Gil and R. D. McCullough. Experimental evidence for the quasi-"living" nature of the grignard metathesis method for the synthesis of regioregular poly(3-alkylthiophenes) *Macromolecules* **38**, 8649-8656 (2005)
20. M. Jeffries-El, G. Sauve and R. D. McCullough. In-situ end-group functionalization of regioregular poly(3-alkylthiophene) using the Grignard metathesis polymerization method *Advanced Materials* **16**, 1017-+ (2004)
21. E. E. Sheina, J. S. Liu, M. C. Iovu, D. W. Laird and R. D. McCullough. Chain growth mechanism for regioregular nickel-initiated cross-coupling polymerizations *Macromolecules* **37**, 3526-3528 (2004)
22. K. K. Stokes, K. Heuze and R. D. McCullough. New phosphonic acid functionalized, regioregular polythiophenes *Macromolecules* **36**, 7114-7118 (2003)
23. C. J. Brabec, N. S. Sariciftci and J. C. Hummelen. Plastic solar cells *Advanced Functional Materials* **11**, 15-26 (2001)
24. H. Sirringhaus, P. J. Brown, R. H. Friend, M. M. Nielsen, K. Bechgaard, B. M. W. Langeveld-Voss, A. J. H. Spiering, R. A. J. Janssen, E. W. Meijer, P. Herwig and D. M. de Leeuw. Two-dimensional charge transport in self-organized, high-mobility conjugated polymers *Nature* **401**, 685-688 (1999)
25. Z. Bao, A. Dodabalapur and A. J. Lovinger. Soluble and processable regioregular poly(3-hexylthiophene) for thin film field-effect transistor applications with high mobility *Applied Physics Letters* **69**, 4108-4110 (1996)
26. J.-F. Chang, B. Sun, D. W. Breiby, M. M. Nielsen, T. I. Sölling, M. Giles, I. McCulloch and H. Sirringhaus. Enhanced mobility of poly(3-hexylthiophene) transistors by spin-coating from high-boiling-point solvents *Chemistry of Materials* **16**, 4772-4776 (2004)
27. F. Chen, P. G. Mehta, L. Takiff and R. D. McCullough. Improved electroluminescence performance of poly(3-alkylthiophens) having a high head-to-tail (HT) ratio *Journal of Materials Chemistry* **6**, 1763-1766 (1996)
28. A. Kraft, A. C. Grimsdale and A. B. Holmes. Electroluminescent conjugated polymers - Seeing polymers in a new light *Angewandte Chemie-International Edition* **37**, 402-428 (1998)
29. N. C. Greenham, I. D. W. Samuel, G. R. Hayes, R. T. Phillips, Y. A. R. R. Kessener, S. C. Moratti, A. B. Holmes and R. H. Friend. Measurement of absolute

photoluminescence quantum efficiencies in conjugated polymers *Chemical Physics Letters* **241**, 89-96 (1995)
30. P. Peumans, S. Uchida and S. R. Forrest. Efficient bulk heterojunction photovoltaic cells using small-molecular-weight organic thin films *Nature* **425**, 158-162 (2003)
31. W. Y. Wong, X. Z. Wang, Z. He, A. B. Djurisic, C. T. Yip, K. Y. Cheung, H. Wang, C. S. K. Mak and W. K. Chan. Metallated conjugated polymers as a new avenue towards high-efficiency polymer solar cells *Nature Materials* **6**, 521-527 (2007)
32. F. Yang, M. Shtein and S. R. Forrest. Controlled growth of a molecular bulk heterojunction photovoltaic cell *Nature Materials* **4**, 37-41 (2005)
33. N. S. Sariciftci, L. Smilowitz,A. J. Heeger and F. Wudl. Photoinduced electron transfer from a conducting polymer to buckminsterfullerene S*cience* **258**, 1474-1476 (1992)
34. L. J. A. Koster, E. C. P. Smits, V. D. Mihailetchi and P. W. M. Blom. Device model for the operation of polymer/fullerene bulk heterojunction cells *Physical Review B* **72**, 085205 (2005)
35. B. C. Thompson and J. M. J. Frechet. Organic photovoltaics - Polymer-fullerene composite solar cells *Angewandte Chemie International Edition* **47**, 58-77 (2008)
36. Q. Liu, Z. F. Liu, X. Y. Zhong, L. Y. Yang, N. Zhang, G. L. Pan, S. G. Yin, Y. Chen and J. Wei. Polymer Photovoltaic Cells Based on Solution-Processable Graphene and P3HT *Advanced Functional Materials* **19**, 894-904 (2009)
37. C. J. Brabec, S. E. Shaheen, C. Winder, N. S. Sariciftci and P. Denk. Effect of LiF/metal electrodes on the performance of plastic solar cells *Applied Physics Letters* **80**, 1288-1290 (2002)
38. S. E. Shaheen, C. J. Brabec, N. S. Sariciftci, F. Padinger, T. Fromherz and J. C. Hummelen. 2.5% efficient organic plastic solar cells *Applied Physics Letters* **78**, 841-843 (2001)
39. F. Padinger, R. S. Rittberger and N. S. Sariciftci. Effects of postproduction treatment on plastic solar cells *Advanced Functional Materials* **13**, 85-88 (2003)
40. J. Y. Kim, S. H. Kim, H. H. Lee, K. Lee, W. L. Ma, X. Gong and A. J. Heeger. New architecture for high-efficiency polymer photovoltaic cells using solution-based titanium oxide as an optical spacer *Advanced Materials* **18**, 572 (2006)
41. M. Reyes-Reyes, K. Kim and D. L. Carroll. High-efficiency photovoltaic devices on annealed poly(3-hexylthiophene) and 1-(3-methoxycarbonyl)-propyl-1-phenyl-(6,6)C61 blends *Applied Physics Letters* **87**, 083506 (2005)
42. W. Ma, C. Yang, X. Gong, K. Lee and A. J. Heeger. Thermally stable, efficient polymer solar cells with nanoscale control of the interpenetrating network morphology *Advanced Functional Materials* **15**, 1617-1622 (2005)
43. G. Li, V. Shrotriya, J. S. Huang, Y. Yao, T. Moriarty, K. Emery and Y. Yang. High-efficiency solution processable polymer photovoltaic cells by self-organization of polymer blends *Nature Materials* **4**, 864-868 (2005)
44. Y. Y. Liang, D. Q. Feng, Y. Wu, S. T. Tsai, G. Li, C. Ray and L. P. Yu. Highly Efficient Solar Cell Polymers Developed via Fine-Tuning of Structural and Electronic Properties *Journal of the American Chemical Society* **131**, 7792-7799 (2009)
45. C. N. Hoth, P. Schilinsky, S. A. Choulis and C. J. Brabec. Printing highly efficient organic solar cells *Nano Letters* **8**, 2806-2813 (2008)
46. C. J. Brabec, A. Cravino, D. Meissner, N. S. Sariciftci, T. Fromherz, M. T. Rispens, L. Sanchez and J. C. Hummelen. Origin of the open circuit voltage of plastic solar cells *Advanced Functional Materials* **11**, 374-380 (2001)

47. C. J. Brabec, A. Cravino, D. Meissner, N. S. Sariciftci, M. T. Rispens, L. Sanchez, J. C. Hummelen and T. Fromherz. The influence of materials work function on the open circuit voltage of plastic solar cells *Thin Solid Films* **403-404**, 368-372 (2002)
48. N. Camaioni, G. Ridolfi, G. Casalbore-Miceli, G. Possamai and M. Maggini. The effect of a mild thermal treatment on the performance of poly(3-alkylthiophene)/Fullerene solar cells *Advanced Materials* **14**, 1735-1738 (2002)
49. H. Derouiche and V. Djara. Impact of the energy difference in LUMO and HUMO of the bulk heterojunctions components on the efficiency of organic solar cells S*olar Energy Materials and Solar Cells* **91**, 1163-1167 (2007)
50. G. Yu, J. Gao, J. C. Hummelen, F. Wudl and A. J. Heeger. Polymer photovoltaic cells: enhanced efficiencies via a network of internal donor-acceptor heterojunctions S*cience* **270**, 1789-1791 (1995)
51. H. Hoppe, M. Niggeman, C. Winder, J. Kraut, R. Hiesgen, A. Hinsch, D. Meissner and N. S. Sariciftci. Nanosale morphology of conjugated polymer/fullerene-based bulk-heterojunction solar cells *Advanced functional materials* **14**, 1005-1011 (2004)
52. J. K. J. van Duren, X. Yang, J. Loos, C. W. T. Bulle-Lieuwma, A. B. Sieval, J. C. Hummelen and R. A. J. Janssen. Relating the morphology of poly(*p*-phenylene vinylene)/ methanofullerene blends to solar-cell performance *Advanced Functional Materials* **14**, 425-434 (2004)
53. X. N. Yang, J. K. J. van Duren, R. A. J. Janssen, M. A. J. Michels and J. Loos. Morphology and thermal stability of the active layer in poly(p-phenylenevinylene)/methanofullerene plastic photovoltaic devices *Macromolecules* **37**, 2151-2158 (2004)
54. X. Yang, J. Loos, S. C. Veenstra, W. J. H. Verhees, M. M. Wienk, J. M. Kroon, M. A. J. Michels and R. A. J. Janssen. Nanoscale morphology of high-performance polymer solar cells *Nanoletters* **5**, 579-583 (2005)
55. A. Swinnen, I. Haeldermans, M. vande Ven, J. D'Haen, G. Vanhoyland, S. Aresu, M. D'Olieslaeger and J. Manca. Tuning the dimensions of C-60-based needlelike crystals in blended thin films *Advanced Functional Materials* **16**, 760-765 (2006)
56. A. Swinnen, I. Haeldermans, P. Vanlaeke, J. D'Haen, J. Poortmans, M. D'Olieslaeger and J. V. Manca. Dual crystallization behaviour of polythiophene/fullerene blends *The European Physical Journal Applied Physics* **36**, 251-256 (2006)
57. T. Savenije, J. E. Kroeze, X. Yang and J. Loos. The effect of thermal treatment on the morphology and charge carrier dynamics in a polythiophene-fullerene bulk heterojunction *Advanced Functional Materials* **15**, 1260-1266 (2005)
58. T. J. Savenije, J. E. Kroeze, X. N. Yang and J. Loos. The formation of crystalline P3HT fibrils upon annealing of a PCBM : P3HT bulk heterojunction *Thin Solid Films* **511**, 2-6 (2006)
59. D. Chirvase, J. Parisi, J. C. Hummelen and V. Dyakonov. Influence of nanomorphology on the photovoltaic action of polymer-fullerene composites *Nanotechnology* **15**, 1317-1323 (2004)
60. J. Jo, S. S. Kim, S. I. Na, B. K. Yu and D. Y. Kim. Time-Dependent Morphology Evolution by Annealing Processes on Polymer:Fullerene Blend Solar Cells *Advanced Functional Materials* **19**, 866-874 (2009)
61. J. Jo, S. I. Na, S. S. Kim, T. W. Lee, Y. Chung, S. J. Kang, D. Vak and D. Y. Kim. Three-Dimensional Bulk Heterojunction Morphology for Achieving High Internal Quantum Efficiency in Polymer Solar Cells *Advanced Functional Materials* **19**, 2398-2406 (2009)

62. C. Groves, L. J. A. Koster and N. C. Greenham. The effect of morphology upon mobility: Implications for bulk heterojunction solar cells with nonuniform blend morphology *Journal of Applied Physics* **105**, 094510 (2009)
63. H. Hoppe and N. S. Sariciftci. Morphology of polymer/fullerene bulk heterojunction solar cells *Journal of Materials Chemistry* **16**, 45-61 (2005)
64. P. A. Troshin, H. Hoppe, J. Renz, M. Egginger, J. Y. Mayorova, A. E. Goryochev, A. S. Peregudov, R. N. Lyubovskaya, G. Gobsch, N. S. Sariciftci and V. F. Razumov. Material Solubility-Photovoltaic Performance Relationship in the Design of Novel Fullerene Derivatives for Bulk Heterojunction Solar Cells *Advanced Functional Materials* **19**, 779-788 (2009)
65. G. Li, Y. Yao, H. Yang, V. Shrotriya, G. Yang and Y. Yang. "Solvent annealing" effect in polymer solar cells based on poly(3-hexylthiophene) and methanofullerenes *Advanced Functional Materials* **17**, 1636-1644 (2007)
66. Y. Yao, J. H. Hou, Z. Xu, G. Li and Y. Yang. Effect of solvent mixture on the nanoscale phase separation in polymer solar cells *Advanced Functional Materials* **18**, 1783-1789 (2008)
67. J. Peet, J. Y. Kim, N. E. Coates, W. L. Ma, D. Moses, A. J. Heeger and G. C. Bazan. Efficiency enhancement in low-bandgap polymer solar cells by processing with alkane dithiols *Nature Materials* **6**, 497-500 (2007)
68. Y. Kim, S. Cook, S. M. Tuladhar, S. A. Choulis, J. Nelson, J. R. Durrant, D. D. C. Bradley, M. Giles, I. McCulloch, C. Ha and M. Ree. A strong regioregularity effect in self-organizing conjugated polymer films and high-efficiency polythiophene:fullerene solar cells *Nature Materials* **5**, 197-203 (2006)
69. P. Schilinsky, U. Asawapirom, U. Scherf, M. Biele and C. J. Brabec. Influence of the molecular weight of poly(3-hexylthiophene) on the performance of bulk heterojunction solar cells *Chemistry of Materials* **17**, 2175-2180 (2005)
70. G. Dennler, M. C. Scharber and C. J. Brabec. Polymer-Fullerene Bulk-Heterojunction Solar Cells *Advanced Materials* **21**, 1323-1338 (2009)
71. M. Jorgensen, K. Norrman and F. C. Krebs. Stability/degradation of polymer solar cells *Solar Energy Materials and Solar Cells* **92**, 686-714 (2008)
72. G. Dennler, C. Lungenschmied, H. Neugebauer, N. S. Sariciftci, M. Latrèche, G. Czeremuszkin and M. R. Wertheimer. A new encapsulation solution for flexible organic solar cells *Thin solid films* **511-512**, 349-353 (2006)
73. J. A. Hauch, P. Schilinsky, S. A. Choulis, R. Childers, M. Biele and C. J. Brabec. Flexible organic P3HT : PCBM bulk-heterojunction modules with more than 1 year outdoor lifetime *Solar Energy Materials and Solar Cells* **92**, 727-731 (2008)
74. S. Miyanishi, K. Tajima and K. Hashimoto. Morphological Stabilization of Polymer Photovoltaic Cells by Using Cross-Linkable Poly(3-(5-hexenyl)thiophene) *Macromolecules* **42**, 1610-1618 (2009)
75. B. J. Kim, Y. Miyamoto, B. Ma and J. M. J. Fréchet. Photocrosslinkable pholythiophenes for efficient, thermally stable, organic *Advanced Functional Materials* **19**, 2273-2281 (2009)
76. M. Drees, H. Hoppe, C. Winder, H. Neugebauer, N. S. Sariciftci, W. Schwinger, F. Schaffler, C. Topf, M. C. Scharber, Z. G. Zhu and R. Gaudiana. Stabilization of the nanomorphology of polymer-fullerene "bulk heterojunction" blends using a novel polymerizable fullerene derivative *Journal of Materials Chemistry* **15**, 5158-5163 (2005)
77. K. Sivula, Z. T. Ball, N. Watanabe and J. M. J. Frechet. Amphiphilic diblock copolymer compatibilizers and their effect on the morphology and performance of polythiophene: Fullerene solar cells *Advanced Materials* **18**, 206 (2006)

78. Z. Y. Zhou, X. W. Chen and S. Holdcroft. Stabilizing bicontinuous nanophase segregation in pi CP-C-60 donor-acceptor blends *Journal of the American Chemical Society* **130**, 11711-11718 (2008)
79. S. Bertho, I. Haeldermans, A. Swinnen, W. Moons, T. Martens, L. Lutsen, D. Vanderzande, J. Manca, A. Senes and A. Bonfiglio. Influence of thermal ageing on the stability of polymer bulk heterojunction solar cells *Solar Energy Materials and Solar Cells* **91**, 385-389 (2007)
80. F. C. Krebs and H. Spanggaard. Significant improvement of polymer solar cell stability *Chemistry of materials* **17**, 5235-5237 (2005)
81. Y. Zhang, H. L. Yip, O. Acton, S. K. Hau, F. Huang and A. K. Y. Jen. A Simple and Effective Way of Achieving Highly Efficient and Thermally Stable Bulk-Heterojunction Polymer Solar Cells Using Amorphous Fullerene Derivatives as Electron Acceptor *Chemistry of Materials* **21**, 2598-2600 (2009)
82. K. Sivula, C. K. Luscombe, B. C. Thompson and J. M. J. Fréchet. Enhancing the Thermal Stability of Polythiophene:Fullerene Solar Cells by Decreasing Effective Polymer Regioregularity *Journal of the American Chemical Society* **128**, 13988-13989 (2006)
83. S. Schuller, P. Schilinsky, J. Hauch and C. J. Brabec. Determination of the degradation constant of bulk heterojunction solar cells by accelerated lifetime measurements *Applied Physics a-Materials Science & Processing* **79**, 37-40 (2004)
84. R. De Bettignies, J. Leroy, M. Firon and C. Sentein. Accelerated lifetime measurements of P3HT:PCBM solar cells *Synthetic Metals* **156**, 510-513 (2006)

Chapter Two:

Processable and cross-linkable side-chain functionalized poly(3-alkylthiophene)-based copolymers for polymer electronics*

Abstract: Poly(3-alkylthiophene)- based copolymers with ester-functionalized side chains were synthesized using the oxidative polymerization with $FeCl_3$. The introduction of ester-functionalized side chains in the copolymers poly[(3-hexylthiophene-2,5-diyl)-*co*-(3-[R]thiophene-2,5-diyl)] with R = 2-acetoxyethyl (**P1**), 2-methoxy-2-oxoethyl (**P3**), 2-ethoxy-2-oxoethyl (**P4**) or 6-ethoxy-6-oxohexyl (**P5**) affected the solubility of the copolymers. Generally, a decrease in molecular weight and reaction yield was observed for copolymers with an increasing ratio of functionalized side chains. In a Polymer Light Emitting Diode, the ester-functionalized copolymer **P5** performed comparable to P3HT indicating that the charge transport is not affected by the functionalization. The functional groups in the side chains were hydrolized post-polymerization to alcohol and acid groups, before they were further functionalized with a variety of commercially available molecules. The facile decoration of the copolymers was illustrated by reaction of an alcohol function with butylisocyanato acetate, (meth)acrylic acid chloride or cinnamoylchloride and reaction of an acid group with (3-ethyl-oxetan-3-

*Submitted By Bert J. Campo, Henk J. Bolink, Kristof Colladet, Wibren D. Oosterbaan, Peter Adriaensens, Laurence Lutsen, Thomas J. Cleij and Dirk Vanderzande

yl)methanol. This way, crosslinkable functionalities following different crosslink-initiating mechanisms were introduced.

1. Introduction

The use of conjugated polymers in plastic electronics shows great promise due to the combination of their semi-conducting behaviour with beneficial properties of polymers such as light weight, high mechanical strength, solution processability and flexibility.[1] This enables the development of new low cost technologies starting from solvent-based processing or printing of active layers in plastic electronic devices.[2, 3] In polymer electronics, solubility of the conjugated polymer is a first demand for solvent based processing. A highly succesfull class of soluble semiconducting polymers are poly(3-alkylthiophenes) (P3ATs), with poly(3-hexylthiophene) (P3HT) as the most prominent example.[4-6] P3ATs have been applied in Field Effect Transistors (FETs), Polymer Solar Cells (PSCs) and Light Emitting Diodes (LEDs). [7-9] Depending on the synthetic route used for the conjugated polymer, the position of the alkyl tails on the backbone follows a pattern that defines the structure as more or less regioregular or regiorandom. The extent of regioregularity affects substantially the electro-optical properties of the polymer. Although for FETs for example a high regioregularity (>95%) is desirable,[10] it has been shown that for P3HT:fullerene solar cells a regioregularity as low as 86% is still sufficient for obtaining high efficiencies while it improves the thermal stability of the device.[11, 12]

Also the presence of functional groups in the polymer structure can affect the material properties. Functionalization of the polymer can be desirable as a tool to modify or introduce new properties into the polymer. For example,

crosslinkable conjugated polymers have been applied in LEDs, FETs and PSCs or photolithography applications.[13-17] After crosslinking, PSCs were obtained which showed improved stability of device performance as a function of time and temperature.[15, 16] Furthermore, introduction of specific functionalities may be useful to obtain grafting sites for larger molecules which are useful in biosensors.[18] The oxidative polymerization using $FeCl_3$ is a straightforward method to obtain 70-90% regioregular P3AT on a gram-scale.[4, 19] With this route, a wide range of functional groups in the side chains of homopolymers and copolymers have been reported for various purposes. Among them are bromine [20-23], ether [24-29], hydroxy [30-32], thioether and sulfanyl [33, 34], ester [17, 18, 35-40], amino [41] and urethane [42] functionalized polythiophenes. This variety of functionalized P3ATs demonstrates the compatibility of this polymerization method with many functional groups. With the introduction of functionalized alkyl side chains however, not only the desired properties are introduced, but also the polymer solubility may be affected.

In this work, a route is explored that allows for a versatile variation of functional groups in the side chains, enabling the introduction of crosslinkable groups with the aim to fundamentally improve the device operating lifetime of the PSCs. To control the percentage of functionalized side chains, copolymers of 3-HT with either an alcohol or carboxylic acid substituted 3-alkylthiophene comonomer were prepared (Scheme 1). These functional groups can be further modified by post-polymerization derivatization. They were chosen because of their versatility: further functionalization is possible with several other functionalities following different synthetic procedures.[43] To obtain a copolymer soluble in organic solvents, rather the ester-analogues of the alcohol or acid functionalized

thiophenes were used. The oxidative polymerization method was chosen because it is a straightforward experimental method which is well documented and compatible with ester functionalized monomers. By varying the percentage of functionalized comonomer, the effect of ester-functionalized side chains on the copolymer characteristics was investigated. Conversion of the ester groups to alcohol or acid groups allows reaction with complementary functional groups to introduce a variety of crosslinkable functions by several reaction types. As all these copolymers contain ester functionalities, the compatibility of the ester group with device operation was tested for a copolymer in a LED device. The presented synthesis scheme enables the preparation of functionalized P3AT materials for polymer electronics, where post-polymerization functionalization reactions allow tuning the chemical structure toward desired materials properties.

2. Experimental section

2.1 General experimental procedures

All chemicals were obtained from commercial sources and used as received unless stated otherwise. Iron(III)chloride was treated with freshly distilled thionylchloride and washed with dry pentane (dried over sodium wire and distilled) before it was dried under vacuum and stored under nitrogen. Chloroform was refluxed overnight over P_2O_5 and distilled before use. Diethylether and tetrahydrofurane were distilled under N_2 atmosphere from a blue mixture with sodium wire and benzophenone until a blue colour appeared. ^{1}H-NMR spectra were recorded on a Varian Inova 300 MHz spectrometer. Products were dissolved in 0.8 mL deuterated $CHCl_3$,

obtained from Cambridge Isotope Laboratories. Chemical shifts are reported in ppm downfield from tetramethylsilane (TMS) using the peak of residual $CHCl_3$ as an internal standard at δ = 7.24 ppm. The ratio between the hexyl tails and the ester functionalized side chains was calculated from the ratio of the integration of a CH_3-proton in the hexyl side chains (at δ = 0.89 ppm), compared to the integration of a CH_2-O proton of the functionalized side chain. The regioregularity was calculated as the fraction of the head-tail α-CH_2 around δ = 2.79 ppm to the total α-CH_2 signal integration from the hexyl side chain. Fourier-transform infrared spectroscopy (FT-IR) was performed on a Perkin Elmer Spectrum One FT-IR spectrometer using pellets in KBr or films drop-cast on a quartz disk from a $CHCl_3$ solution. Gas chromatography/mass spectrometry (GC-MS) was carried out on TSQ-70 and Voyager mass spectrometers. UV-Vis spectra were recorded on a Varian CARY 500 UV-Vis-NIR spectrophotometer from 200 to 800 nm at a scan rate of 600 nm min^{-1}. Size exclusion chromatography (SEC) was done with a 1 mg mL^{-1} polymer solution in THF, which was filtered with a 0.45 µm pore PTFE syringe filter. A Spectra Physics P90 pump equipped with two mixed-B columns (10 µm, 30 cm x 7.5 mm), Polymer Labs and a Shodex refractive index detector at 40 °C in THF at a flow rate of 1.0 mL min^{-1} were used. Molecular weight distributions were measured relative to polystyrene standards and toluene was used as a flow rate marker. OLEDs were made on glass substrates with a pattern of ITO electrodes. The glass substrates were cleaned with soapy water, sonicated in acetone, heated in isopropanol and treated with UV/O_3 for 20 minutes. Typically, 30 nm poly(ethylenedioxythiophene): poly(styrenesulfonate) (PEDOT: PSS) (HCStark) was spin-coated at 3000 rpm on the glass substrate before spin-coating the polymer from a 10 mg mL^{-1} solution in chlorobenzene at 300

rpm. 20 nm of 1,3,5-tris-(N-phenyl-benzimidazole-2-yl)benzene TBPI, 5 nm Ba and 80 nm Al were evaporated in high vacuum ($p < 3\ 10^{-6}$ mbar). The ITO electrodes were cleared before measuring current density and luminance versus voltage using a Keithley 2400 source meter, a Keithley 6485 picoampmeter and an integrating sphere. The EL spectrum was measured using an Avantes luminance spectrometer.

2.2 Monomer synthesis

3-Hexylthiophene (3-HT) was obtained from reaction of 3-bromothiophene (3-BT, Acros) and hexylmagnesium bromide (Aldrich), in the presence of a Ni catalyst. Synthesis and characterization were in accordance with literature procedures.[44] In a dried three-necked flask, 100 mL (166.0 g, 1018 mmol) 3-BT was dissolved under nitrogen atmosphere with 0.01 eq. of Ni(dppp)Cl_2 (5.2 g, 10 mmol) in 300 mL dry diethylether. 1.2 Eq. (611 mL of a 2.0 M solution in Et_2O, 1220 mmol) of hexylmagnesiumbromide was added dropwise at a temperature of 0°C. The reaction was stirred overnight at room temperature before neutralization by addition of a 1.0 M HCl solution. After extraction with Et_2O, washing with a saturated $NaHCO_3$ solution and drying over $MgSO_4$, a brown liquid was obtained. This liquid was purified by distillation to obtain 3-HT in a yield of 96 % (163.7 g, 973 mmol) at $p = 7.10^{-3}$ mbar and T = 81-84 °C. ^{1}H NMR (300 MHz, $CDCl_3$) δ 7.23 (s, 1H, H_{arom}), 6.95 (m, 1 H, H_{arom}), 6.92 (m, 1H, H_{arom}), 2.63 (t, 2H, α-CH_2, J = 7.5 Hz), 1.63 (q, 2H, β-CH_2, J = 7.5 Hz), 1.32 (m, 6H, 3 CH_2), 0.90 (t, 3H,CH_3, J = 6.5 Hz); ^{13}C NMR (75 MHz, $CDCl_3$) δ 142.8, 130.8, 110.2, 107.2, 31.5, 29.4, 29.3, 28.7, 22.5, 14.0; GC-MS 98% pure, *m/z* 168 $[M]^+$,153 $[M - CH_3]^+$, 139 $[M – CH_2CH_3]^+$, 125 $[M – (CH_2)_2CH_3]^+$, 111 $[M – (CH_2)_3CH_3]^+$, 97 $[M - (CH_2)_4CH_3]^+$, 85 $[M – (CH_2)_5CH_3]^+$; FT-IR (NaCl,

cm^{-1}): 3104 (w), 3051 (w), 2956 (vs), 2929(vs), 2856(vs), 1750 (w), 1537, 1466 (s), 1409, 1378, 1328 (w), 1234 (w), 1153(w), 1079, 936 (w), 924 (w), 856, 834, 772 (vs), 713

3-(2-Acetoxyethyl)thiophene (**M1**) was obtained after stirring 10.8 g (84 mmol) 3-(2-hydroxyethyl)thiophene (Acros) under reflux with 1.3 eq. acetic anhydride and 40 mL of pyridine during five hours.[17] The reaction was allowed to cool down to room temperature before adding 20 ml of a 4 N HCl solution. Extraction was done with 3 x 100 mL Et_2O. The extract was washed with 3 x 100 mL H_2O, dried over $MgSO_4$, filtrated and evaporated. 13.0 g (76 mmol, 91 %) **M1** was isolated after Kugelrohr (fraction at p = 2.5 10^{-3} mbar and T = 125 °C). Characterization is comparable to ref [17]. ^{1}H NMR (300 MHz, $CDCl_3$) δ 1.99 (s, CH_3), 2.92 (t, α -CH_2), 4.24 (t, β-CH_2), 6.93 (dd, H_{arom}), 6.98 (s, H_{arom}), 7.21 (dd, H_{arom}); ^{13}C NMR (75 MHz, $CDCl_3$) δ 170.9, 137.8, 128.1, 125.5, 121.4, 64.1, 29.4, 20.8; FT-IR (NaCl, cm^{-1}): 3103, 2958, 1736, 1537, 1432, 1412, 1383, 1364, 1334, 1239, 1155, 1035, 979, 942, 900, 858, 832, 777, 690, 666, 643, 626, 606; GC/MS: 98 % pure, *m/z* 170[M] $^+$, 127 [M – $COCH_3$] $^+$, 110 [M – $OCOCH_3$] $^+$, 97 [M – $CH_2OCOCH3$] $^+$

3-(2-methoxy-2-oxoethyl)thiophene (**M2**) was prepared following a modified literature procedure[45] by refluxing 10.0 g (70 mmol) thiophen-3-yl-acetic acid (Acros) in 50 mL of MeOH with 2.5 mL concentrated H_2SO_4 for 24 h. The mixture was neutralized by addition of Na_2CO_3. After evaporation of the solvent, the residue was extracted with Et_2O. The extract was washed with deionized water, dried over $MgSO_4$ and filtered. After evaporation of the Et_2O, 10.1 g (65 mmol, 92 %) of **M2** was obtained. ^{1}H NMR (300 MHz, $CDCl_3$) δ 3.64 (s, CH_2), 3.68 (s, CH_3), 7.02 (dd, H_{arom}), 7.13 (s, H_{arom}), 7.26 (dd, H_{arom}); ^{13}C NMR (75 MHz, $CDCl_3$) δ 171.4, 133.4,

128.3, 125.6, 122.7, 51.9, 35.4; FT-IR (NaCl, cm^{-1}): 3104, 2998, 2952, 2842, 1740 (s), 1436, 1336, 1268, 1231, 1201, 1152, 1083, 1013, 946, 857, 832, 765, 727, 675, 611 cm^{-1}; GC/MS 99 % pure, *m/z* 156 $[M]^+$ 141$[M - CH_3]^+$ 125 $[M - CH_3O]^+$ 97 $[M - COOCH_3]^+$

3-(2-ethoxy-2-oxoethyl)thiophene (**M3**) was prepared following a similar procedure as was applied to obtain **M2**. 10.0 g (70 mmol) of thiophen-3-yl-acetic acid (Acros) was refluxed overnight in 50 ml of EtOH with 3 ml of concentrated H_2SO_4. Short path distillation was used to obtain 10.57g (62 mmol, 89 %) of the purified compound at $p = 9.10^{-3}$ mbar and $T = 50°C$. ^1H NMR (300 MHz, $CDCl_3$) δ 1.26 (t, CH_3), 3.63 (s, CH_2), 4.14 (q, CH_2-O), 7.02 (dd, H_{arom}), 7.12 (s, H_{arom}), 7.26 (dd, H_{arom}); ^{13}C NMR (75 MHz, $CDCl_3$) δ 171.0, 133.6, 128.3 125.5 122.6 60.7 35.7 14.0; FT-IR (NaCl, cm^{-1}) 3104, 2998, 2952, 2842, 1740 (s), 1436, 1336, 1268, 1231, 1201, 1152, 1083, 1013, 946, 857, 832, 765, 727, 675, 611 cm^{-1}; GC/MS 99 % pure, *m/z* 170 $[M]^+$ 141 $[M - CH_3CH_2]^+$ 125 $[M - CH_3CH_2O]^+$, 97 $[M - CH_3CH_2OCO]^+$

3-(6-ethoxy-6-oxohexyl)thiophene (**M4**). 6-Bromo-hexanoic acid ethyl ester (20 g, 89 mmol) was added to active zinc and stirred for 2 h at room temperature under argon atmosphere.[46] The zinc particles were allowed to settle overnight. The supernatant organozinc compound was added dropwise to a solution of 16.81 g 3-BT (103 mmol) and 0.05 eq $Ni(dppp)Cl_2$ in THF.[47] The reaction was stirred for 48h at room temperature and quenched with a saturated NH_4Cl solution. After extraction with Et_2O (3 x 200 mL), the organic phase was dried over $MgSO_4$ and filtrated. 8.6 g **M4** (38 mmol, 42 %) was obtained with short path distillation at $T = 72$ °C and $p = 1.10^{-3}$ mbar. ^1H NMR (300 MHz, $CDCl_3$) δ 7.20 (m, 1H, H_{arom}), 6.90 (m, 2H, H_{arom}), 4.10 (q, 2H, O-CH_2, $J = 7.5$ Hz), 2.62 (t, 2H, α-CH_2, $J = 7.5$ Hz),

2.28 (t, 2H, β-CH_2, *J* = 7.5 Hz), 1.63 (m, 4H, 2 CH_2), 1.38 (m, 2H, CH_2), 1.23 (t, 3H, CH_3, *J* = 7.1 Hz); ^{13}C NMR (75 MHz, $CDCl_3$) δ 173.4, 142.4, 127.8, 124.8, 119.6, 59.8, 33.9, 29.8, 29.6, 28.4, 24.4, 13.8; GC/MS 95% pure, *m*/*z* 226 $[M]^+$, 181 $[M- OCH_2CH_3]^+$, 153 $[M – C(O)OCH_2CH_3]^+$, 139 $[M – CH_2C(O)OCH_2CH_3]^+$, 125 $[M – (CH_2)_2C(O)OCH_2CH_3]^+$, 111 $[M-(CH_2)_3C(O)OCH_2CH_3]^+$, 97 $[M- (CH_2)_4C(O)OCH_2CH_3]^+$; FT-IR (NaCl, cm^{-1}): 3104, 2980, 2934, 2858, 1733 (vs), 1537, 1463, 1372, 1299, 1252, 1181, 1130, 1096, 1032, 859, 833, 773

2.3 General polymerization procedure

The flasks and other glassware in which the reactions were performed were dried in an oven at 110 °C, allowed to cool down under vacuum and kept under N_2 atmosphere. $FeCl_3$ (4 eq. with respect to the total amount of monomers) was weighed in a dry three-necked flask under N_2 atmosphere before addition of dry $CHCl_3$ (20 ml g^{-1} $FeCl_3$).[19] The monomer was weighed in another dry three-necked flask and stirred while evacuation and flushing with N_2 three times. To obtain copolymers, a mixture of monomers was weighed. The monomer (mixture) was dissolved in dry $CHCl_3$ and stirred before it was added dropwise through a cannula to the vigorously stirred $FeCl_3$ slurry. The reaction was stirred at room temperature under a continuous nitrogen flow for 18h. The polymer was precipitated in 0.75 L MeOH for each gram of polymer and stirred for one hour. Then the polymer was filtered off and stirred overnight in a 1 vol % solution of hydrazine monohydrate (NH_2-NH_2.H_2O) in MeOH. The polymer was filtered off again and purified with Soxhlet extraction using MeOH and acetone. The polymers were isolated and dried after extraction with $CHCl_3$ and

precipitation in MeOH. In Table 1 the amounts of monomer are given for each mixture with the corresponding copolymer.

2.3.1 Synthesis of P3HT

The described procedure was applied after 10.8 g $FeCl_3$ was weighed in a dry three-necked flask. 1.6 g of polymer was obtained after purification. ^{1}H NMR (300 MHz, $CDCl_3$) δ 0.89 (CH_3), 1.33, 1.53 and 1.68 (ε, δ, γ, β-CH_2), 2.54 and 2.78 (α-CH_2), 6.96-7.03 (H_{arom}); FT-IR (NaCl, cm^{-1}): 2955, 2925, 2857, 1512, 1456, 1378, 823, 725.

2.3.2 Synthesis of copolymers P1 for several X/Y ratios

For example, the X/Y 0.88/ 0.12 copolymer was prepared by mixing 3-HT and the functionalized monomer in this molar ratio (for weights: see Table 1) before dissolving the mixture in dry $CHCl_3$ and performing the polymerization procedure as mentioned before. SEC and UV Vis: in film: Table 2, ^{1}H NMR (300 MHz, $CDCl_3$) δ 0.89 (CH_3, 3HT), 1.33 and 1.67 (ε, δ, γ, β-CH_2, 3HT), 2.06 (CH_3), 2.56 and 2.78 (α-CH_2, 3HT), 3.15 (α-CH_2), 4.34 (β-CH_2), 6.98 (H_{arom}); FT-IR (NaCl, cm^{-1}): 3056, 2960, 2928, 2856, 1745, 1511, 1463, 1454, 1377, 1261, 1236, 1094, 1027, 820, 801. Synthesis and characterization of copolymers for other X/Y ratios was done following a similar procedure. The amount of monomers used for each copolymerization reaction is given in Table 1.

2.3.3 The conversion of ester to alcohol functions

Polymer **P1** was stirred under reflux in the dark for 18 h in a 0.2 M NaOH solution in MeOH (50 mL g^{-1}).[17] Then the mixture was poured out in MeOH/2 N HCl (1/1, v/v) and stirred for 1 h before it was filtered off, rinsed with MeOH and H_2O and dried to obtain the copolymers in high yield

(> 90%). Characterization of polymers which were further functionalized is given here, the synthesis and characterization of copolymers for other X/Y ratios was done according to the same procedure. **P2** 0.95/0.05 ^{1}H NMR (300 MHz, $CDCl_3$) δ 0.89 (CH_3, 3HT), 1.32, 1.53 and 1.68 (ε, δ, γ, β-CH_2, 3HT), 2.55 and 2.78 (α-CH_2, 3HT), 3.15 (α-CH_2), 3.84 and 3.95 (CH_2-OH), 6.96 (H_{arom}); FT-IR (NaCl, cm^{-1}): 2954, 2925, 2855, 1464, 1393, 1336, 1154, 1084, 985, 823 cm^{-1}; **P2** 0.88/0.12 ^{1}H NMR (300 MHz, $CDCl_3$) δ 0.89 (CH_3, 3HT), 1.32 and 1.67 (ε, δ, γ, β-CH_2, 3HT), 2.55 and 2.78 (α-CH_2, 3HT), 3.15 (α-CH_2), 3.84 and 3.95 (CH_2-OH), 6.96 (H_{arom}); FT-IR (NaCl, cm^{-1}): 2954, 2925, 2855, 1464, 1394, 1337, 1154, 1084, 985, 825 cm^{-1}

2.3.4 Synthesis of P3, P4 and P5

Monomer amounts which were mixed are given in Table 1 and treated according to the previously described procedure. **P3** 0.95/0.05 ^{1}H NMR (300 MHz, $CDCl_3$) δ 0.89 (CH_3, 3HT), 1.33 - 1.66 (ε, δ, γ, β-CH_2, 3HT), 2.62 (α-CH_2, 3HT), 3.70 (CH_2), 3.70 (CH_3), 7.10 (H_{arom}); FT-IR (NaCl, cm^{-1}): 2954, 2925, 2855, 1744, 1513, 1460, 1376, 1260, 1091, 1021, 825, 801, 725 cm^{-1}. **P3** 0.50/0.50 ^{1}H NMR (300 MHz, $CDCl_3$) δ 0.88 (CH_3, 3HT), 1.26, 1.32, 1.66 (ε, δ, γ, β-CH_2, 3HT), 2.53 and 2.78 (α-CH_2, 3HT), 3.60 – 3.81 (CH_2, CH_3), 6.96- 7.19 (H_{arom}); FT-IR (NaCl, cm^{-1}): 2956, 2927, 2856, 1743, 1513, 1465, 1455, 1435, 1375, 1326, 1262, 1198, 1168, 1093, 1020, 801 cm^{-1}. **P3** 0.10/0.90 ^{1}H NMR (300 MHz, $CDCl_3$) δ 0.88 (CH_3, 3HT), 1.26, 1.32, 1.68 (ε, δ, γ, β-CH_2, 3HT), 2.53 and 2.77 (α-CH_2, 3HT), 3.60 (CH_2), 3.75 (CH_3), 6.96- 7.19 (H_{arom}); FT-IR (NaCl, cm^{-1}): 2961, 2926, 2856, 1739, 1435, 1326, 1260, 1200, 1170, 1092, 1020, 820 cm^{-1}. **P3** 0.00/1.00 ^{1}H NMR ($CDCl_3$): δ=3.6 (CH_2), 3.75 (CH_3), 7.2 (H); FT-IR (NaCl, cm^{-1}): 2963, 1739, 1436, 1267, 1090, 1020, 801 cm^{-1}.**P4** 0.95/0.05 ^{1}H NMR (300 MHz, $CDCl_3$) δ 0.89 (CH_3, 3HT), 1.32 and 1.67 (ε, δ, γ, β-

CH_2, 3HT, CH_3), 2.55 and 2.78 (α-CH_2, 3HT), 3.57 and 3.79 (α-CH_2), 4.18 (CH_2-O), 6.96 (H_{arom}); FT-IR (NaCl, cm^{-1}): 2955, 2928, 2855, 1741, 1514, 1465, 1395, 1311, 1261, 1152, 1083, 1019, 867, 800 cm^{-1}. **P4** 0.85/0.15 ^{1}H NMR (300 MHz, $CDCl_3$) δ 0.89 (CH_3 ,3HT), 1.32 and 1.68 (ε, δ, γ, β-CH_2, 3HT, CH_3), 2.55 and 2.78 (α-CH_2, 3HT), 3.56 and 3.79 (α-CH_2), 4.20 (CH_2-O), 6.96 (H_{arom}); FT-IR (NaCl, cm^{-1}): 2956, 2928, 2855, 1739, 1512, 1457, 1377, 1317, 1260, 1230, 1154, 1025, 861, 825 cm^{-1}. **P4** 0.50/0.50 ^{1}H NMR (300 MHz, $CDCl_3$) δ 0.88 (CH_3 ,3HT), 1.32 and 1.56 (ε, δ, γ, β-CH_2, 3HT, CH_3), 2.55 and 2.78 (α-CH_2, 3HT), 3.57 and 3.78 (α-CH_2), 4.18 (CH_2-O), 6.98 (H_{arom}); FT-IR (NaCl, cm^{-1}): 2955, 2928, 2855, 1740, 1509, 1458, 1377, 1314, 1230, 1153, 1093, 1021, 801 cm^{-1}.

Table 1: Amounts of monomers and FeCl3 used for the copolymerization reactions of 3-HT (X) with **M1**, **M2**, **M3** and **M4** (Y) together with the resulting polymer yields

Polymer	Molar ratio X/Y	#g (mmol) X	#g (mmol) Y	Yield (g)
P3HT	100/0	2.80 (16.6)	-	1.60
P1	0.97/0.03	3.03 (18.0)	0.08 (0.46)	2.68
P1	0.95/0.05	3.80 (22.4)	0.23 (1.17)	3.46
P1	0.88/0.12	1.68 (10.0)	0.19 (1.11)	2.17
P1	0.82/0.18	2.25 (13.4)	0.40 (2.37)	2.24
P1	0.50/0.50	0.79 (4.7)	0.80 (4.70)	1.00
P3	0.95/0.05	2.32 (14.0)	0.12 (0.70)	1.97
P3	0.50/0.50	2.90 (17.3)	2.70 (17.30)	1.63
P3	0.10/0.90	0.23 (0.6)	1.81 (5.30)	0.60
P3	0.00/1.00	-	0.50 (3.20)	0.12
P4	0.95/0.05	2.00 (11.0)	0.11 (0.60)	1.89
P4	0.85/0.15	9.35 (56.0)	1.67 (10.00)	5.73
P4	0.50/0.50	1.25 (7.4)	1.26 (7.40)	0.36
P5	0.88/0.12	2.75 (16.0)	0.51 (2.00)	1.80

P5 0.88/0.12 ^{1}H NMR (300 MHz, $CDCl_3$) δ 0.88 (CH_3, 3HT), 1.32, 1.57 and 1.67 (ε, δ, γ, β-CH_2, 3-HT), 2.36 (CH_2COO), 2.54 and 2.78 (CH_2 α), 6.96 (H_{arom}); FT-IR (NaCl, cm^{-1}): 2956, 2925, 2856, 1735, 1638, 1508, 1454, 1384, 1260, 1161, 1032, 816, 801, 725 cm^{-1}.

2.3.5 The conversion of ester to acid functions

Polymer **P5** (1.0 g) was dissolved in a minimal amount of $CHCl_3$ and added slowly to 2 M NaOH in EtOH.[48] When addition was complete, the reaction was stirred in the dark for 48h under reflux. The mixture was poured out in a MeOH/2 N HCl mixture and stirred for 1 h, before it was filtered off and rinsed with MeOH and H_2O. The polymer **P8** (0.95 g) was dried and characterized. ^{1}H NMR (300 MHz, $CDCl_3$) δ 0.88 (CH_3, 3HT), 1.32, 1.57 and 1.67 (ε, δ, γ, β-CH_2, 3-HT), 2.36 (C*H*$_2$COOH), 2.54 and 2.78 (α-CH_2), 6.96 (H_{arom}); FT-IR (NaCl, cm^{-1}): 3135, 2960, 2925, 2852, 1705, 1638, 1508, 1403, 1074, 821, 801 cm^{-1}; UV Vis in film λ_{max}= 510 nm

2.3.6 Further post-polymerization reactions (Scheme 2)

Functionalization with butylisocyanate acetate was done comparable to literature procedures.[42] Polymer **P2** 0.95/0.05 (250 mg) was dissolved in dry THF before addition of 14 mg dibutyltindilaurate and 125 mg butylisocyanatoacetate in excess amounts. The reaction was stirred during 72h under N_2. The solvent was evaporated, the polymer was redissolved in $CHCl_3$, precipitated in MeOH, filtered off, rinsed with MeOH and H_2O and dried to obtain 260 mg (99 %) of polymer **P9**. ^{1}H NMR (300 MHz, $CDCl_3$) δ 0.89 (CH_3, 3HT), 1.32 and 1.67 (ε, δ, γ, β-CH_2, 3HT), 2.05 (ζ-CH_2), 2.33 (ε-CH_2), 2.54 and 2.78 (α-CH_2 3-HT), 3.15 (α-CH_2), 3.94 (γ -CH_2), 4.12 (δ-CH_2), 4.36 (β-CH_2), 5.15 (N-H), 6.96 (H_{arom}); FT-IR (NaCl, cm^{-1}): 2957,

2927, 2855, 1730, 1512, 1459, 1393, 1300, 1260, 1193, 1152, 1080, 1020, 865, 800 cm^{-1}

Polymer **P2** 0.88/0.12 was functionalized with acrylic derivatives by reaction of the alcohol functionalities with an acid chloride.[35] For copolymers **P10**, **P11**, **P12** a similar procedure was applied: 260, 200 and 210 mg of polymer **P2** 0.88/0.12 were dissolved in 30 mL of THF, before adding 2 mL Et_3N and addition of 10 equivalents of the acid chloride in 20 mL THF. After stirring for 18h in the dark at room temperature, the solvent was evaporated. The polymer was redissolved in $CHCl_3$, precipitated in a 0.5 N HCl/ MeOH mixture (1/1, v/v), filtered off while rinsing with MeOH and H_2O and dried to obtain 250, 190 and 220 mg respectively. **P10** ^{1}H NMR (300 MHz, $CDCl_3$) δ 0.88 (CH_3, 3HT), 1.32 and 1.67 (ε, δ, γ, β-CH_2, 3HT), 2.54 and 2.78 (α-CH_2), 4.43 (CH_2-O), 5.81 (CH=C), 6.13 (C=CH_2), 6.37 (C=CH_2), 6.96 (H_{arom}); FT-IR (NaCl, cm^{-1}): 2955, 2925, 2855, 1730, 1508, 1463, 1377, 1261, 1180, 1097, 1020, 801 cm^{-1} **P11** ^{1}H NMR (300 MHz, $CDCl_3$) δ 0.89 (CH_3, 3HT), 1.32, 1.43 and 1.67 (ε, δ, γ, β-CH_2, 3HT), 1.93 (CH_3-C=C), 2.53 and 2.77 (α-CH_2), 4.4 (CH_2-O), 5.54 (CH=C), 6.09 (CH=C), 6.95 (H_{arom}); FT-IR (NaCl, cm^{-1}): 2955, 2925, 2855, 1730, 1508, 1463, 1377, 1261, 1180, 1097, 1020, 801 cm^{-1} **P12**: ^{1}H NMR (300 MHz, $CDCl_3$) δ 0.88 (CH_3 ,3HT), 1.32, 1.54 and 1.67 (ε, δ, γ, β-CH_2, 3HT), 2.54 and 2.78 (α-CH_2 3-HT), 3.22 (α-CH_2), 4.48 (CH_2-O), 6.44 (CH=C), 6.96 (H_{arom}), 7.33 and 7.48 (H_{phenyl}), 7.76 (CH=C); FT-IR (NaCl, cm^{-1}): 2956, 2926, 2856, 1780, 1712, 1683, 1612, 1578, 1513, 1495, 1450, 1422, 1380, 1315, 1288, 1261, 1163, 1108, 1025, 985, 936, 874, 805, 765, 707, 677 cm^{-1}

Functionalization with oxetane (**P13**): The esterification of the acid groups in the side chains of **P8** was performed according to literature procedures following the DCC/DMAP protocol.[49] **P8** (100 mg) was stirred at 60°C in

25 mL chlorobenzene until it was dissolved. The alcohol (3-ethyl-oxetan-3-yl)methanol (69 mg) was added before adding 15 eq. DCC and 1 eq. DMAP. The reaction was kept stirring for 48 h. The polymer was precipitated in MeOH, filtrated, rinsed with MeOH and H_2O and dried to obtain 96 mg **P13** ^{1}H NMR (300 MHz, $CDCl_3$) δ 0.89 (CH_3 3-HT), 1.23, 1.33, 1.54 and 1.69 (ε, δ, γ, β-CH_2, 3-HT), 2.36 (C*H*$_2$COOR), 2.55 and 2.78 (α-CH_2), 4.19 (CH_2-OCO), 4.36 and 4.43 (CH_2-$O_{oxetane}$) 6.96 (H_{arom}); FT-IR (NaCl, cm^{-1}): 2960, 2920, 2850, 1739, 1700, 1649, 1512, 1461, 1415, 1260, 1090, 1019, 865, 800 cm^{-1}

3. Results and discussion

As stated before, several side chain ester-functionalized poly(3-hexylthiophene)-based copolymers were prepared (Scheme 1) to investigate to what extent certain side chain functionalities may be introduced in the polymer structure without negatively affecting the polymer properties, e.g. processability.

3.1 Monomer synthesis

3-HT was obtained according to literature procedures.[44] Ester analogues of acid and alcohol functionalized thiophene compounds were used. 3-(2-acetoxyethyl)thiophene (**M1**) was obtained after esterification of 3-(2-hydroxyethyl)thiophene with acetic anhydride in pyridine.[17, 35] 3-(2-Methoxy-2-oxoethyl)thiophene (**M2**) and 3-(2-ethoxy-2-oxoethyl)thiophene (**M3**) were obtained via the acid catalyzed esterification of thiophen-3-yl-acetic acid with MeOH and EtOH, respectively. 3-(6-Ethoxy-6-oxohexyl)thiophene (**M4**) was prepared analogues to 3-HT, according to

literature procedures.[44, 47] All monomers were obtained in high yield and purity.

3.2 Synthesis of ester-functionalized copolymers

The copolymers were synthesized using the oxidative polymerization with anhydrous $FeCl_3$, by bulk copolymerization of mixtures of 3-HT and thiophene monomers containing functionalized side chains. A slurry of anhydrous $FeCl_3$ in $CHCl_3$ was stirred vigorously, while a monomer solution in dry $CHCl_3$ was added. Monomer mixtures of 3-HT with the several functionalized monomers in varying X/Y molar ratios were used to obtain copolymers with a varying percentage of functionalized alkyl side chains, as presented in Table 2. The reaction was stirred for 18 h at room temperature before precipitation in MeOH, dedoping with hydrazine and purification by Soxhlet extraction. The polymer was isolated by extraction with $CHCl_3$, precipitation in MeOH, filtration and drying. The polymer characterization was done by ^{1}H-NMR and FT-IR, for **P1** and **P3** displayed in Figure 1. In Table 2, molecular weights, reaction yields and results of UV-Vis spectroscopy of all copolymers are given. P3HT was prepared following the same procedure as for the copolymers.

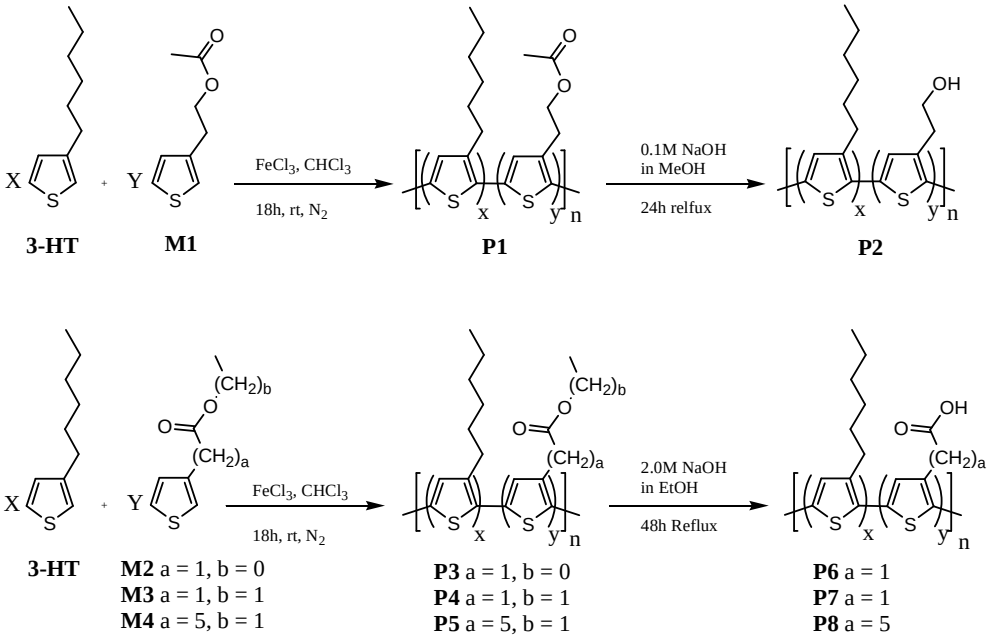

Scheme 1: Synthesis of side-chain ester-functionalized copolymers. Soluble alcohol and acid functionalized copolymers P2 and P8 were obtained after hydrolysis of the ester functions in the side chains.

Synthesis of poly[(3-hexylthiophene-2,5-diyl)-*co*-(3-[2-acetoxyethyl]thiophene-2,5-diyl)] (**P1**) has been reported previously via several routes.[17, 38] Introduction of an increasing percentage of acetoxyethyl functionalities in the side chain was proved by the appearance of an increasingly strong C=O absorption at 1740 cm^{-1} in FT-IR (Figure 1a). In ^{1}H-NMR (Figure 1b), the signals of the $-CH_2$-O protons at 4.3 ppm and CH_3-CO protons at 2.05 ppm illustrated the increasing degree of functionalization. For the **P1** 0.50/0.50 copolymer, the signal of α-CH_2 protons originating from the acetoxyethyl functionalized repeating units was clearly visible at 3.15 ppm. The x/y ratio of repeating units in the polymer was calculated using ^{1}H-NMR (Table 2).

Table 2: Molar ratios of monomers used for the copolymerization reactions of 3-HT (X) with **M1**, **M2**, **M3** and **M4** (Y) together with the resulting polymer characteristics of the several copolymers.

Polymer	Monomer molar ratio (X/Y)	x/y (^{1}H-NMR)	%RR (^{1}H-NMR)	λ_{max} (nm) in film	M_w (10^3) [a]	PD [b]	Yield (%)
P3HT	1.00/0.00	1.00/0.00	76	516	178	3.7	57
P1	0.97/0.03	0.94/0.06	71	513	113	3.4	86
P1	0.95/0.05	0.95/0.05	71	509	213	4.6	86
P1	0.88/0.12	0.87/0.13	72	480	344	5.1	86
P1	0.82/0.18	0.84/0.16	86	495	184	6.1	85
P1	0.50/0.50	0.51/0.49	72	469	180	3.9	63
P3	0.95/0.05	0.95/0.05	73	514	172	3.9	80
P3	0.50/0.50	0.64/0.36	65	453	184	6.1	32
P3	0.10/0.90	0.33/0.67	63	443	72	3.5	29
P3	0.00/1.00	0.00/1.00	59	420	20	2.1	24
P4	0.95/0.05	0.98/0.02	80	509	201	6.5	89
P4	0.85/0.15	0.97/0.03	76	509	252	4.2	52
P4	0.50/0.50	0.89/0.11	87	499	160	3.4	15
P5	0.88/0.12	0.87/0.13	80	518	374	4.1	55

[a] Weight average molecular weight in THF solution, [b] Polydispersity = M_w/M_n

In **P1**, the comonomer amount (or x/y ratio) present in the copolymers remarkably correspond to the amount (or X/Y ratio) present in the monomer mixture. This is an indication that the rate of polymerization is equal for both monomers. The obtained copolymers were soluble in common organic solvents like $CHCl_3$, chlorobenzene (CB) or tetrahydrofurane (THF). With an increasing percentage of functionalized alkyl side chains, the weight average molecular weight (M_w) first increases from 112k in the 0.97/0.03 copolymer to 213k in the 0.95/0.05 copolymer and reaches a maximum of 343k for the 0.88/0.12 copolymer. With a further increasing percentage of

functionalized comonomer, M_w decreases to 180k for the 0.82/0.18 and 0.50/0.50 copolymer. Polydispersities between 3 and 6 were observed. There is no clear relation between M_w and degree of functionalization (i.e. percentage of functionalized side chains). The regioregularities observed for most of the copolymers ranged from 59 to 87%. In UV-Vis, the absorption of 76% RR P3HT was observed between 400 and 600 nm, with a maximum at 516 nm. The wavelength of maximum absorption (λ_{max}) of **P1** copolymers shifts towards shorter wavelengths with an increasing ratio of functionalized side chains. This is probably due to the disruption of the π-π stacking by the introduction of the functionalized side chains and a decrease in effective conjugation length. An exception in this evolution is the **P1** 0.82/0.18 copolymer, indicating an increased structural order of the system due to the higher regioregularity in this copolymer compared to the regioregularity of our P3HT sample (86 % vs. 76 %).[50]

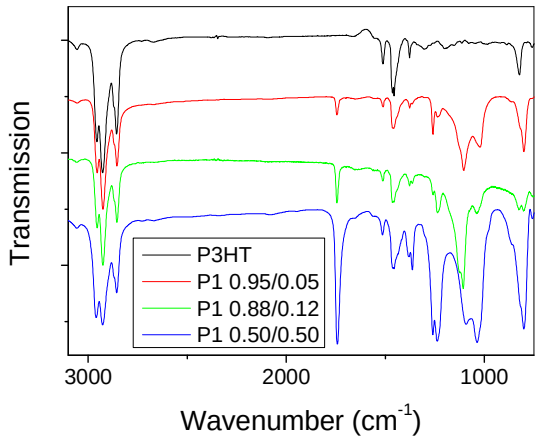
Transmission
P3HT
P1 0.95/0.05
P1 0.88/0.12
P1 0.50/0.50
3000
2000
1000
Wavenumber (cm-1)

a)

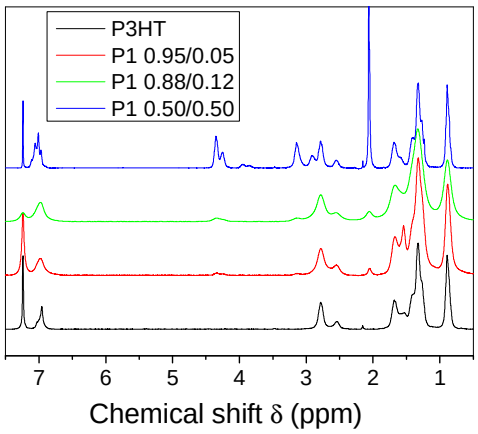
P3HT
P1 0.95/0.05
P1 0.88/0.12
P1 0.50/0.50
7
6
5
4
3
2
1
Chemical shift δ (ppm)

b)

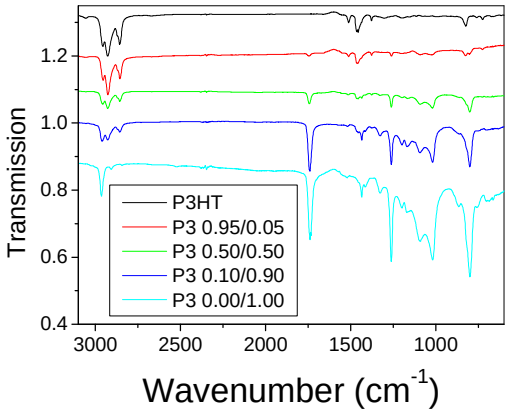

c)

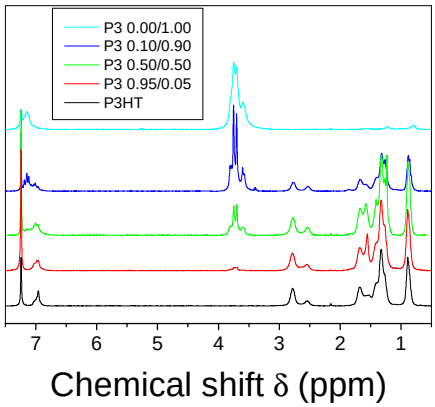

d)

Figure 1: a) FT-IR and b) ^{1}H-NMR spectra of **P1** with increasing percentage of functionalized side chains compared to P3HT; c) FT-IR and d) ^{1}H-NMR spectra of copolymers **P3** with increasing ratio ester functions in the side chains, compared to P3HT

To be able to obtain acid functionalized copolymers, an ester-protected analogue of acetic acid thiophene-3-yl was used in the copolymerization reaction. Copolymers poly[(3-hexylthiophene-2,5-diyl)-*co*-(3-[2-methoxy-2-oxoethyl]thiophene-2,5-diyl)] (**P3**) were obtained in several x/y ratios after copolymerization of 3-HT with **M2**. The resulting copolymers characteristics are displayed in Table 2. The homopolymer poly[3-(2-methoxy-2-oxo)thiophene-2,5-diyl] was also prepared. When more than 5%

of functionalized monomer was used, the percentage that is actually incorporated in the copolymer is significantly less then what was present in the feed ratio. With an increasing degree of functionalization, there is also a decrease in reaction yield and polymer M_w after purification. These observations indicate that polymer chains with a higher percentage of functionalized side chains are no longer soluble in $CHCl_3$ or THF. Insolubility of the fraction of polymer chains with higher molecular weight explains the decrease in M_w and reaction yield. Also in the **P3** copolymers, an increasing percentage of functionalities in the side chains causes a decrease in λ_{max}. FT-IR and ^{1}H-NMR spectra of copolymers **P3** with several x/y ratio and P3HT are displayed in Figure 1c and 1d. The x/y ratio in the copolymer was determined by comparing the integration of the 3 CH_3 protons of the hexyl side chain at δ = 0.89 ppm with the integration of the signal at δ = 3.7 ppm originating from the 5 protons in the **M1** units. In Figure 1d, the signal around δ = 3.7 ppm from the CH_2COOCH_3 protons in the ^{1}H-NMR spectrum of copolymers **P3** increases because of the increasing amount of functionalized side chains in the copolymer. The peaks at δ = 0.89 ppm, between δ = 1.3 and 1.7 ppm and between δ = 2.5 and 2.8 ppm, originating from the hexyl side chain, decrease in intensity with an increasing ratio of functionalized side chains. In the FT-IR spectrum (Figure 1c), there are increasingly strong signals visible due to the ester function at 1740 cm^{-1} and between 1250 and 800 cm^{-1}, while the signals of the C-H stretch of the alkyl side chains around 2900 cm^{-1} disappear. Conversion of the ester functionalities in the side chains of copolymers **P3** towards acid functionalities (**P6**) was done according to literature procedures,[18] but no complete conversion could be obtained: the ester absorption in FT-IR around 1740 cm^{-1} remains visible.

Since the solubility of the copolymers **P3** decreases with an increasing percentage of functional groups in the side chain, a series of copolymers poly[(3-hexylthiophene-2,5-diyl)-*co*-(3-[2-ethoxy-2-oxoethyl]thiophene-2,5-diyl)] (**P4)** of 3-HT with **M2** was prepared, as displayed in Table 2. Also in copolymers **P4**, the percentage of functionalized side chains in the copolymer does not correspond to the percentage of monomers with functionalized side chains in the monomer mixture. With 5 or 15 mol % of functionalized monomers in the monomer mixture, only 2 and 3 % functionalized side chains were built in the resulting copolymers as determined by ^{1}H-NMR. These copolymers display a M_w comparable to P3HT, while the reaction yield decreases with increasing percentage of functionalized monomers in the monomer mixture. In a 1/1 monomer mixture, only 11% of functionalized monomers are present in the copolymer and the reaction yield further decreases. In the **P4** copolymers, the λ_{max} does not decrease significantly compared to P3HT because of a higher regioregularity. To improve the solubility of the ethyl ester functionalized product, copolymer poly[(3-hexylthiophene-2,5-diyl)-*co*-(3-[6-ethoxy-6-oxohexyl]thiophene-2,5-diyl)] **P5** with a longer alkyl chain between conjugated backbone and functional group was prepared. Copolymer **P5** was prepared from a 0.88/0.12 monomer mixture and contains 13% of ester functionalized units in the copolymer. This copolymer has high molecular weight (323k) and was obtained in an acceptable yield of 55%.

3.3 Application of the soluble functionalized P3HT-based copolymer P5 in a PLED

To test the compatibility of ester functional groups in the copolymer with electronic functionality, Polymer Light Emitting Diode (P-LED) devices were prepared. The P-LEDs were produced on ITO patterned surfaces, after a standard cleaning procedure was applied to the substrate. PEDOT:PSS was spincoated from a filtrated aqueous solution at 3000 rpm for 60 s. Polymers were spincoated at 300 rpm from a 1 wt % solution in CB. 20 nm of the hole blocking material TBPI was evaporated onto the polymer layer to confine the holes to the polythiophene, before deposition of Ba and Ag in high vacuum ($p < 3\ 10^{-6}$ mbar) as the cathode. At low voltages (2 - 6 V), a slightly higher luminance was observed for the device containing **P5** 0.88/0.12 as compared to one containing P3HT. At 8 V, both the current densities and the luminance are similar for the above mentioned devices, indicating that the presence of the functionalized side chains in the polymer structure does not affect the electronic or photonic properties. (Figure 2b) It must be stated that the absolute performance of the PLEDs is rather poor, due to the poor photoluminescence properties of polythiophenes.[9] Both polymers emitted a bright red colour and no change in the emission spectrum was observed when the active material in the device was changed from P3HT to **P5** (Figure 2 a), demonstrating that ester groups in the active material are compatible with their use in electronic devices.

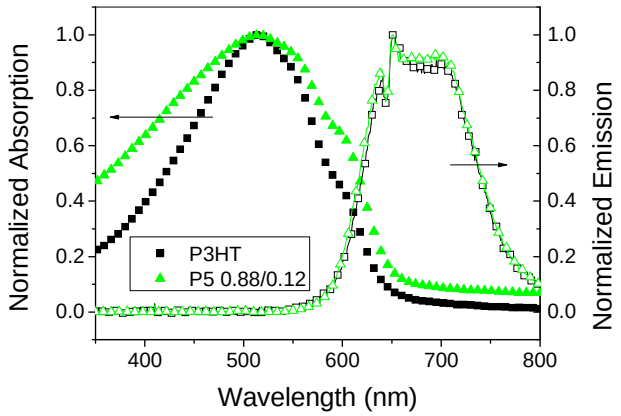

a)

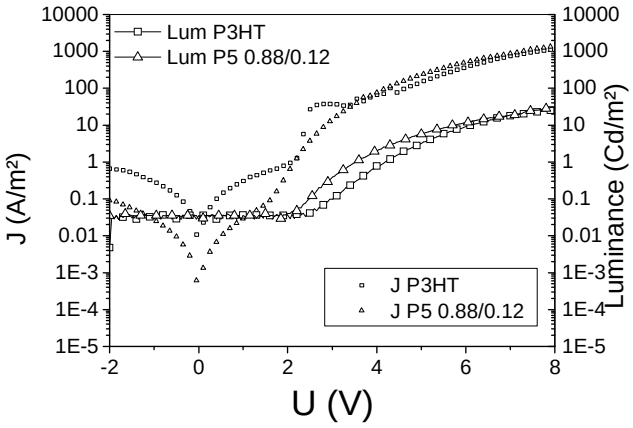

b)

Figure 2 a) Absorption of polymer films drop-cast from $CHCl_3$ solution and emission measured in PLEDs from P3HT (squares) and **P5** (triangles), b) PLED current density (scatter) and luminance (line + scatter) in ITO/ PEDOT:PSS/ Polymer/ TPBI/ Ba/ Ag

3.3 Conversion of side chain ester functionalities towards alcohol or acid

The conversion of the acetoxy ester functionalities in the side chains of copolymer **P1** towards alcohol functions in **P2** was done by stirring the finely grounded polymer in a 0.2M NaOH solution in MeOH for 18h under

reflux in the dark.[13] The polymer was crushed into a fine powder, to ensure a maximum contact surface during reaction. The complete conversion is confirmed by the absence of the acetoxy CH_3 signal in ^{1}H-NMR at δ = 2.05 ppm and the disappearance of the C=O absorption at 1740 cm^{-1} in FT-IR (Figure 3). The signal of the β-CH_2 protons in ^{1}H-NMR shifts upfield from δ = 4.3 ppm towards δ =3.9 ppm in **P2**. The conversion of the side chain functionalities affects the polymer solubility. The alcohol functionalized copolymers are soluble in organic solvents as $CHCl_3$ and CB when the amount of alcohol functionalized side chains is small (i.e. < 10%) and the product is additionally stirred at higher temperature for some time. With higher degrees of functionalization, the solubility of alcohol functionalized copolymers in CB or $CHCl_3$ is lost. For example the **P2** 0.50/0.50 copolymer is not soluble in $CHCl_3$ or CB, but it is still soluble in THF. M_w, recorded from solutions in THF (Table 3), shifted slightly upon conversion of **P1** towards **P2**. The hydrodynamic volume (related with the solubility) of the polymer chains in solution is affected by changing the nature of the functionalized side chains. For lower degrees of functionalization (up to 10%), the molecular weight of **P2** increases slightly compared to **P1** with the same x/y ratio in ^{1}H-NMR. In copolymers with around 20 or 50% of functionalized side chains, the alcohol functionalized copolymers display lower molecular weights, pointing to a lower hydrodynamic volume.

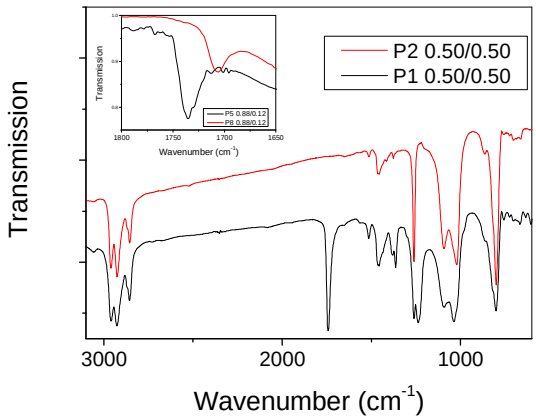

Figure 3: Conversion of ester side chain functionalities in **P1** 0.50/0.50 towards alcohol functions in **P2** 0.50/0.50. Inset: the conversion of ester functionalities in **P5** 0.88/0.12 towards acid functions in **P8** 0.88/0.12

Conversion of the ester group in the side chains towards an acid group was done in a 2 M NaOH solution in EtOH, using a similar procedure as the conversion towards alcohol. The conversion of ester in **P3** towards acid in **P6** was not complete and the resulting product is not completely soluble. On the other hand, the conversion towards **P7** was complete, but the resulting acid functionalized product is not completely soluble either. Finally, the conversion of the ester functions in **P5** towards acid functions in **P8** was complete after 48h, as indicated by the disappearance of the CH_2-O signals in ^{1}H-NMR and the shift of the C=O absorption from 1740 cm^{-1} to 1710 cm^{-1} (Figure 3, inset). Furthermore, **P8** dissolved in CB after stirring overnight at 50°C.

Table 3: Polymer characteristics of alcohol and acid functionalized copolymers **P2** and **P8**.

Polymer	X/Y	M_w (10^3) [a]	PD [b]	Yield (%)
P2	0.97/0.03	154	4.9	98
P2	0.95/0.05	294	6.6	93
P2	0.88/0.12	353	5.3	96
P2	0.82/0.18	143	6.6	97
P2	0.50/0.50	51	2.2	99
P8	0.88/0.12	366	4.9	95

[a] Weight average molecular weight in THF solution, [b] Polydispersity = M_w/M_n

From copolymer composition, reaction yield and M_w in ester-functionalized P3HT-based copolymers, it is clear that the ester side chain substantially affects the solubility of the **P3** and **P4** polymers.

Acetoxyethyl side chains were introduced in several percentages, without a major effect on solubility of **P1**. The complete conversion of ester to alcohol functionalities was obtained by reaction with NaOH. Copolymers **P2** with between 20 and 50% of alcohol functionalized side chains are not completely soluble in $CHCl_3$ or CB. Introduction of ester analogues of acid functionalized thiophenes in **P3**, **P5** and **P6** has a stronger effect on molecular weight and reaction yield, and the copolymer x/y ratio does not always correspond with the monomer ratios in the monomer feed. When **M2** is copolymerized with 3-HT, a higher percentage of these functionalities causes a decrease in solubility, indicated by a decreasing M_w and reaction yield for **P3** copolymers with higher degrees of functionalization. No complete conversion towards acid functionalities could be obtained and the resulting products **P6** are insoluble. A longer alkoxy chain in the ester function in **M2** compared to **M1** resulted in copolymers **P4** with higher M_w compared to **P3**. Complete conversion of the ester functions in **P4** to acid

functionalities in **P7** was achieved, but the resulting acid functionalized **P7** is not completely soluble and therefore could not be completely analyzed. Introducing a longer alkyl chain spacer between the conjugated backbone and the functionality in copolymer **P5** allows synthesis of a copolymer with 10% of acid functionalities in the side chains (**P8**), still soluble in CB. The molecular weight of **P8**, measured in a THF solution, is comparable to the parent **P5** copolymer, indicating that solubility in this solvent did not change much upon conversion of the side chain functionality.

3.4. Further functionalization of conjugated polymers with crosslinkable side chains by diverse post-polymerization reactions

The obtained alcohol and acid functionalized copolymers **P2** and **P8** were subjected to further functionalization reactions (Scheme 2). Post-polymerization functionalization procedures have several advantages, one of those being the easy work-up of the reaction.[43] The conversion of the alcohol or acid functionalities is driven to completion by addition of an excess of functionalized small molecules. The discussed examples are displayed in Scheme 2. The excess of non-reacted reagents is easily removed by precipitation of the polymer in MeOH, and subsequent filtration. Purification was done by rinsing the precipitated polymer with MeOH and water, which are solvents for the small molecules and non-solvents for the copolymer. The complete removal of small molecules was indicated by the absence of any eluating products on TLC. Soxhlet extractions with MeOH did not affect the ^{1}H-NMR integrations or the FT-IR spectra, indicating that all small molecules were removed by extensive rinsing of the precipitated polymer. The acid functionalized copolymer **P8** was functionalized towards the oxetane functionalized **P13** by reaction of

the acid function in the side chain with an alcohol according to the DCC/DMAP procedure.[49] The polymer characteristics are given in Table 3. The ^{1}H-NMR spectrum of **P13** is displayed in Figure 4a, together with the spectra of the polymers where the polymer was derived from. The CH_2-O protons of the ester function and the oxetane function in **P13** were visible around δ = 4.4 ppm, the CH_2COOR protons at δ = 2.4 ppm. The acid C=O absorption in **P8** shifted towards the ester C=O absorption around 1740 cm^{-1} in **P13**.

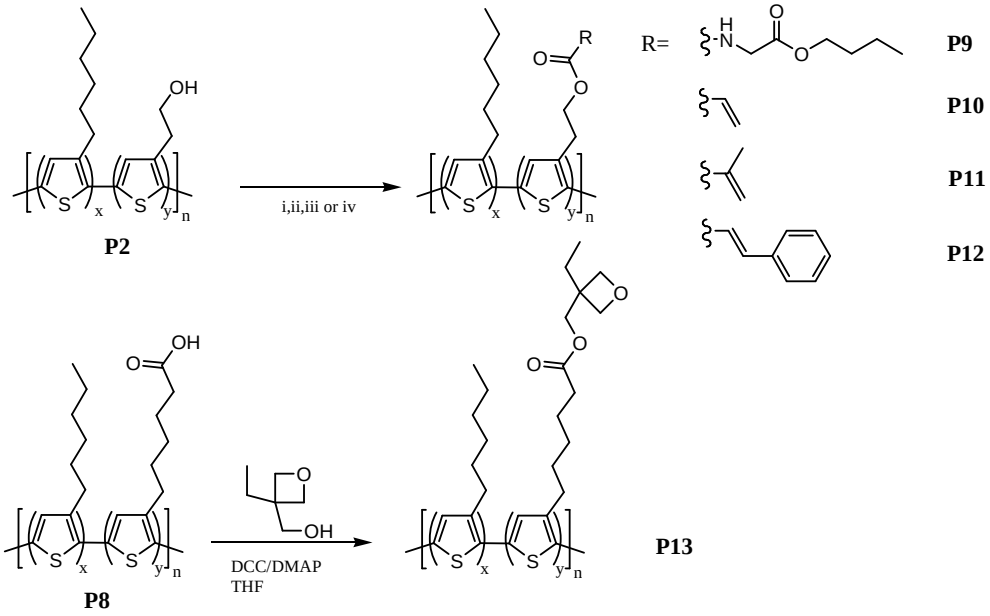

Scheme 2: Post-polymerization functionalization reactions on alcohol and acid functionalized copolymers **P2** and **P8**: decoration with several commercially available molecules. Added reagents were i: dibutyltindilaurate and butyl isocyanatoacetate (**P9**) ii: acrylic acid chloride and Et_3N (**P10**) iii: methacrylic acid chloride and Et_3N (**P11**) iv: cinnamoyl chloride and Et_3N (**P12**)

The alcohol functions in the side chains of the copolymers were functionalized using two different kinds of reagents. To test the post-polymerization functionalization reactions, the reaction of **P2** 0.95/0.05 with butyl isocyanato acetate was performed comparable to literature procedures

and yielded a copolymer with 5% of urethanes in **P9**, indicating that functionalization was complete.[42] The N-H and the butyl CH_2-O protons are visible in ^{1}H-NMR around δ = 4 ppm, as displayed in Figure 4b. Crosslinkable functions other than the oxetane function were introduced by functionalization of the alcohol functionalities with acrylic, methacrylic and cinnamoylchlorides. In copolymers **P10**, **P11** and **P12**, 10% of these functional groups proved to be present in the side chains. The CH_2 protons of the ester functions are visible around δ = 4 ppm for the three different copolymers. In **P10**, the alkene protons appear around δ = 6 ppm. Also in **P11,** there are alkene protons visible in this region, while the methacryl CH_3 protons are at δ = 1.9 ppm. In **P12**, the alkene signals shifts to 6.5 and 7.8 ppm. The protons on the phenyl ring are visible in the region around δ = 7 ppm on ^{1}H-NMR. On FT-IR, the C=O absorption of the acid in **P8** around 1710 cm^{-1} shifts towards the C=O ester absorptions in **P13** around 1740 cm^{-1}. For **P12**, the FT-IR absorptions of the ester C=O is visible at 1710 cm^{-1}, somewhat lower as compared to other C=O absorptions due to conjugation.

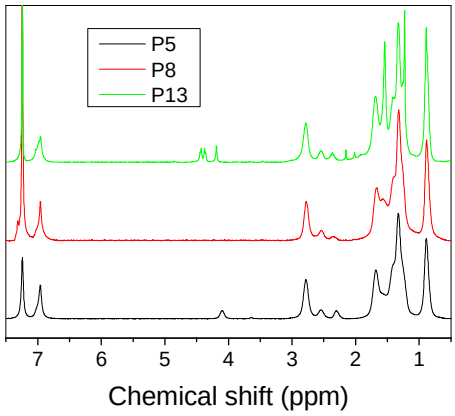

a)

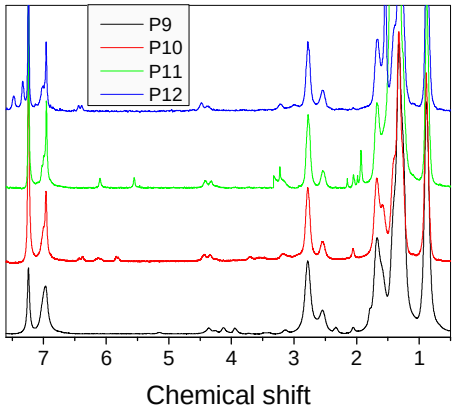

b)

Figure 4: a) ^{1}H NMR spectra of **P5**, **P8** and **P13** b)^{1}H-NMR spectra of **P9**, **P10**, **P11**, **P12**

Functionalization with different kinds of molecules affects the copolymer solubility and UV-Vis absorptions. The molecular weigths and λ_{max} in UV-Vis of films drop-cast from solution in $CHCl_3$ are given in Table 3.

Table 3: Polymer characteristics of post-polymerization functionalized copolymers

Polymer	**x/y**	**λ_{max}** (nm) in film	**M_w** (10^3) [a]	**PD** [b]
P9	0.95/0.05	515	217	4.3
P10	0.90/0.10	509	290	4.8
P11	0.90/0.10	501	102	3.5
P12	0.90/0.10	480	238	5.5
P13	0.90/0.10	506	163	3.2

[a] Weight average molecular weight in THF solution, [b] Polydispersity = M_w/M_n

Thus we introduced several crosslinkable functions using post-polymerization functionalization procedures. This way, crosslinkable functional groups following different initiator mechanisms for several complimentary purposes were introduced. The oxetane function in **P13** is a

crosslinkable moiety with low volume shrinkage,[51] the crosslinking reaction is based on acid catalyzed ring opening polymerization.[52] The use of photo-acids as UV initiators was demonstrated for this crosslinking mechanism.[53] The acrylic functions in **P10** and **P11** are susceptible to thermal or radical initiation.[16] The phenyl substituted double bonds (i.e. cinnamoylfunctions) are known to undergo a cyclisation reaction according to a [2+2] photo initiated cycloaddition mechanism.[54] This could be appropriate for systems where the addition of an initiator is not desirable. Crosslinking experiments are subject of a forthcoming paper.

4. Conclusion

P3HT-based copolymers were prepared using the oxidative polymerization with $FeCl_3$. Acetoxyester functionalized copolymers **P1** were soluble for several percentages of functionalized side chains. The x/y molar ratio in the copolymer was generally the same as the content of ester functionalized comonomer in the monomer feed. The ester functionalities were converted post-polymerization to the corresponding alcohol groups. Copolymers **P3** of 3-HT with 2-methoxy-2-oxoethyl side chains were prepared. With increasing ester ratio the molecular weight and yield decreased, since the high molecular weight fraction of the polymer was insoluble in $CHCl_3$. 2-Ethoxy-2-oxoethyl as functionalized side chain in copolymers **P4** yielded higher molecular weight, but the x/y molar ratio increased only moderately with increasing amounts of functionalized comonomer in the monomer feed. Post-polymerization conversion towards the corresponding acid is easier for the ethyl ester in **P4** as compared to the methyl ester in **P3**. Copolymer **P5** with 6-ethoxy-6-oxohexyl as functionalized side chain, are copolymers where the functional groups are separated from the conjugated backbone by

a longer carbon tail. The x/y molar ratio in the copolymer corresponds to the X/Y molar ratio in the monomer feed. The ester functions in **P5** were converted towards acid functional groups in copolymer **P8**. The ester functionalities in the side chain of **P5** do not influence the performance of the thiophene copolymer in a P-LED device compared to P3HT. Crosslinkable functional groups susceptible to various initiating mechanisms were introduced using post-polymerization functionalization procedures on the alcohol and acid functionalities in the side chain.

5. Acknowledgements

The authors gratefully acknowledge the funding of the Ph.D. grant of Bert J. Campo by the Institute for the Promotion of Innovation through Science and Technology in Flanders (IWT-Vlaanderen), as well as the European Science Foundation (ESF) for the ORGANISOLAR Network Program 'New Generation of Organic based Photovoltaic Devices'.

6. References

[1] McNeill CR, Greenham NC, Advanced Materials 2009;21, 1-11.
[2] de Gans BJ, Duineveld PC, Schubert US, Advanced Materials 2004;16(3):203-213.
[3] Hoth CN, Schilinsky P, Choulis SA, Brabec CJ, Nano Letters 2008;8(9):2806-2813.
[4] Leclerc M, Diaz FM, Wegner G, Makromolekulare chemie 1989;190; 3105-3116.
[5] McCullough RD, Advanced Materials 1998;10(2):93-116.
[6] Osaka I, McCullough RD, Accounts of Chemical Research 2008;41(9):1202-1214.
[7] Zen A, Pflaum J, Hirschmann S, Zhuang W, Jaiser F, Asawapirom U, Rabe JP, Scherf U, Neher D, Advanced Functional Materials 2004;14(8):757-764.
[8] Dennler G, Scharber MC, Brabec CJ, Advanced Materials 2009;21(13):1323-1338.
[9] Chen F, Mehta PG, Takiff L, McCullough RD, Journal of Materials Chemistry 1996;6(11):1763-1766.
[10] Sirringhaus H, Brown PJ, Friend RH, Nielsen MM, Bechgaard K, Langeveld-Voss BMW, Spiering AJH, Janssen RAJ, Meijer EW, Herwig P, de Leeuw DM, Nature 1999;401:685-688.

[11] Sivula K, Luscombe CK, Thompson BC, Fréchet JMJ, Journal of the American Chemical Society 2006;128:13988-13989.
[12] Woo CH, Thompson BC, Kim BJ, Toney MF, Fréchet JM, Journal of the American Chemical Society 2008;130(48):16324-16329.
[13] Yang C, Hou J, Zhang B, He C, Fang H, Ding Y, Ye J, Li Y, Macromolecular Chemistry and Physics 2005;206:1311-1318.
[14] Lu K, Guo YL, Liu YQ, Di CA, Li T, Wei ZM, Yu G, Du CY, Ye SH, Macromolecules 2009;42(9):3222-3226.
[15] Kim BJ, Miyamoto Y, Ma B, Fréchet JMJ, Advanced Functional Materials 2009;19(14):2273-2281.
[16] Miyanishi S, Tajima K, Hashimoto K, Macromolecules 2009;42(5):1610-1618.
[17] Lowe J, Holdcroft S, Macromolecules 1995;28:4608-4616.
[18] Buga K, Kepczynska K, Kulszewicz-Bajer I, Zagórska M, Demadrille R, Pron A, Quillard S, Lefrant S, Macromolecules 2004;37(3):769-777.
[19] Niemi VM, Knuuttila P, Österholm J-E, Korvola J, Polymer 1992;33(7):1559-1562.
[20] Costa-Bizarri P, Lanzi M, Paganin L, Della Casa C, Bertinelli F, Casalboni M, Sarcinelli F, Quatella A, Macromolecular Chemistry and Physics 2003;204:1982-1988.
[21] Lanzi M, Paganin L, Costa-Bizarri P, Della Casa C, Fraleoni A, Macromolecular Rapid Communications 2002(23):630-633.
[22] Ng SC, Ma YF, Chan HSO, Dou ZL, Synthetic Metals 1999;100(3):269-277.
[23] Pomerantz M, Liu MLX, Synthetic Metals 1999;101(1-3):95-95.
[24] Lanzi M, Paganin L, European Polymer Journal 2008;44:3987-3996.
[25] Lanzi M, Paganin L, Caretti D, Polymer 2008;49:4942-4948.
[26] Zhao XY, Hu X, Yue CY, Xia XL, Gan LH, Thin Solid Films 2002;417(1-2):95-100.
[27] Ganapathy HS, Kim JS, Jin S-H, Gal Y-S, Lim KT, Synthetic Metals 2006;156(1):70-74.
[28] Kijima M, Akagi K, Shirakawa H, Synthetic Metals 1997;84:237-238.
[29] Fraleoni-Mogera A, Della Casa C, Lanzi M, Costa-Bizarri P, Macromolecules 2003;36:8617-8620.
[30] Ng SC, Fu P, Yu WL, Chan HSO, Tan KL, Synthetic Metals 1997;87(2):119-122.
[31] Della Casa C, Salatelli E, Andreani F, Costa-Bizarri P, Die makromolekulare chemie: macromolecular symposia 1992;59:233-246.
[32] Helwig JA, Chen X, Gonsalves KE, Polymeric Materials Science and Engeneering 1995;73:306-307.
[33] Cagnoli R, Lanzi M, Mucci A, Parenti F, Schenetti L, Polymer 2005;46(11):3588-3596.
[34] Barbarella G, Melucci M, Sotgiu G, Advanced Materials 2005;17:1581-1593.
[35] Kock TJJM, de Ruiter B, Synthetic Metals 1996;79:215-218.
[36] Yanagida S, Senadeera GKR, Nakamura K, Kitamura T, Wada Y, Journal of photochemistry and photobiology A: chemistry 2004;166:75-80.
[37] Lanzi M, Bizzarri PC, Paganin L, Cesari G, European Polymer Journal 2007;43(1):72-83.
[38] Lee C, Kim KJ, Rhee SB, Synthetic Metals 1995;69295-296.
[39] Costa-Bizarri P, Andreani F, Della Casa C, Lanzi M, Salatelli E, Synthetic Metals 1995;75:141-147.
[40] Kim B, Chen L, Gong J, Osada Y, Macromolecules 1999;32:3964-3969.

[41] Ogawa K, Stafford JA, Rothstein SD, Tallman DE, Rasmussen SC, Synthetic Metals 2005;152(1-3):137-140.
[42] Chittibabu KG, Journal of Macromolecular Science: part A: Pure and Applied Chemistry 1996;33(9):1283-1300.
[43] Gauthier MA, Gibson MI, Klok H-A, Angewandte chemie international edition 2009;48:48-58.
[44] Tamao K, Kodama S, Nakajima I, Kumada M, Minato A, Suzuki K, Tetrahedron 1982;38(22):3347-3354.
[45] Chotpatatananont D, Sirivat A, Jamieson AM, Colloid and Polymer Science 2004;282:357-365.
[46] Chen TA, Wu XM, Rieke RD, Journal of the American Chemical Society 1995;117(1):233-244.
[47] Dai J, Sellers JL, Noftle RE, Synthetic Metals 2003;139:81-88.
[48] Buga K, Majkowska A, Pokrop R, Zagórska M, Djurado D, Oddou J-L, Lefrant S, Chemistry of Materials 2005;17(23):5754-5762.
[49] Neises B, Steglich W, Angewandte Chemie-International Edition in English 1973;17(7):522-524.
[50] Mccullough RD, Tristramnagle S, Williams SP, Lowe RD, Jayaraman M, Journal of the American Chemical Society 1993;115(11):4910-4911.
[51] Nuyken O, Bacher E, Braig T, Faber R, Mielke F, Rojahn M, Wiederhirn V, Meerholz K, Müller D, Designed Monomers and Polymers 2002;5(2-3):195-210.
[52] Crivello JV, Lam JHW, Journal of Polymer Science: Polymer Chemistry Edition 1979;17:977-999.
[53] Crivello JV, Journal of Polymer Science part A: Polymer Chemistry Edition 1999;37(23):4242-4254.
[54] Kato M, Hirayama T, Matsuda H, Minami N, Okada S, Nakanishi H, Macromolecular Rapid Communications 1994;15(9):741-750.

Chapter Three:

Design and Synthesis of Side-chain Functionalized Regioregular Poly(3-hexylthiophene)-based Copolymers and Application in Polymer:Fullerene Bulk Heterojunction Solar Cells[†]

Abstract: A set of novel regioregular poly(3-hexylthiophene)-based random copolymers containing varying ratios of ester functionalized alkyl side chains were synthesized using the Rieke method. The percentage of functionalized side chain varied between 10 and 50 mol% for each copolymer. Using post-polymerization reactions, the ester functions in the alkyl side chain were hydrolyzed to yield an alcohol or acid group. These groups are available for further functionalization reactions, so a wide variety of secondary functionalities may be covalently attached to the conjugated polymer. The copolymers were applied in polymer: fullerene bulk heterojunction solar cells (BHJSCs) with [6,6]-phenyl -C_{61}-butyric acid methyl ester (PCBM) as electron acceptor. The influence of side-chain functionalities on absorption, device performance and layer morphology depends on the ratio and nature of the functionalized side chains. For a 9/1 copolymer, containing 10% of functionalized side chains, behaviour and efficiency in BHJSCs comparable to P3HT:PCBM solar cells were observed.

[†]Published in *Proceedings of SPIE*, vol. 7416, 74161G (2009) by B. J. Campo, W. D. Oosterbaan, J. Gilot, T. J. Cleij, L. Lutsen, R. A. J. Janssen, D. Vanderzande

1. Introduction

The observation of electron transfer between a conjugated polymer and a C_{60} molecule,[1] and the development of the bulk-heterojunction concept in polymer:fullerene devices,[2, 3] have lead together with several developments in materials and device design to polymer solar cells nearing 6% efficiency.[4] A well-documented example of a polymer:fullerene bulk heterojunction solar cell (BHJSC) is the poly(3-hexylthiophene) (P3HT): [6,6]-phenyl -C_{61}-butyric acid methyl ester (PCBM) solar cell, a material combination for which several research groups have reported efficiencies near 5%.[5-7] Further progress in efficiency may be possible by further improving device architecture and/or by designing suitable donor and/or acceptor materials.[8, 9] A careful design of the materials molecular structure may deliver tailored electronic properties to enhance the performance in devices. Often, a compromise between several materials properties is necessary, within the boundaries of what is possible with the current tools in materials synthesis. In the past years, the main focus of device and material development has been on increasing the efficiency by changing material properties, using several material combinations or improving processing conditions, interface contacts and device geometry.[10-16] Recently, increasing attention is going also towards improving life-time and stability of these solar cells,[17] since device stability is a necessity if the polymer solar cells are ever going to be economically viable.[18] The stability of the BHJSC performance is, beside other parameters, based on the stability of the active layer morphology. The optimum morphology of the blend as found for P3HT:PCBM consists of a nanoscale interpenetrating network of crystalline polymer rich and fullerene rich areas.[19] This morphology is the result of phase separation obtained

during active layer deposition. The specific characteristics are determined by the properties of the materials which are used in the blend, by blend composition,[6] solvent or solvent mixtures,[20-22] post-production heat treatment and solvent annealing.[23, 24] The morphology of the blend where the polymer and fullerene phases are separated is a key issue for good solar cell efficiency. When energy from the sun is absorbed, a bound electron hole pair (exciton) is created in either the polymer or fullerene phase. The phase-separated areas should not be too large, so that the created excitons can reach the donor/acceptor interface, where charge separation can occur. A certain extent of phase separation is required, so that the generated charges are able to reach their respective electrodes and do not recombine. Since the typical diffusion length of an exciton in organic semiconductors is only several nanometers, the optimum domain size of the phase-separated compounds is at the nano-meter scale. The desired nano-morphology however, is thermodynamically not stable and the phase separation will progress in time, depending on temperature.[25] The continued phase segregation of the blend materials is one of the stability issues that need to be addressed before a long term stable solar cell could be produced. In other degradation mechanisms, chemical degradation of the active materials may be caused by interface reactions between metal(oxide) electrodes or reactions with residual water or solvent molecules in the blend.[17] These problems can be tackled by encapsulation or the use of air-stable materials.[26] The thermal stabilization of the active layer morphology has been pursued using various strategies. It has been demonstrated that the stability of film morphology may be improved by the use of crosslinkable polymers or fullerenes,[27-31] the use of other materials,[32]compatibilizers or block copolymers,[33, 34] decreasing the P3AT regioregularity,[35, 36] or by

increasing the glass transition temperature of the conjugated polymer.[37] Recently, a thermal crosslinkable regioregular P3AT and a photocrosslinkable P3HT-copolymer for application in thermally stable morphology have been reported.[30, 38] Miyanishi et al. synthesized a derivative of poly(3-hexylthiophene) (P3HT) containing a double bond at the end of the side chain. This polymer was evaluated in devices showing initial device performance comparable to that of P3HT. A reduction of the degradation speed compared to P3HT:PCBM solar cells was observed at 150°C, although J_{sc} decreased with more than 20% after 10h. [30] Kim et al. presented a photocrosslinkable regioregular P3AT copolymer. With 10 % photocrosslinkable groups, a 10% decrease in solar cell efficiency after 50h at 150°C was demonstrated.[38] Our approach to stabilization of the blend morphology encompasses the use of a photo-induced pericyclic cycloaddition of a cinnamoyl functionality in specially designed copolymers of P3HT.

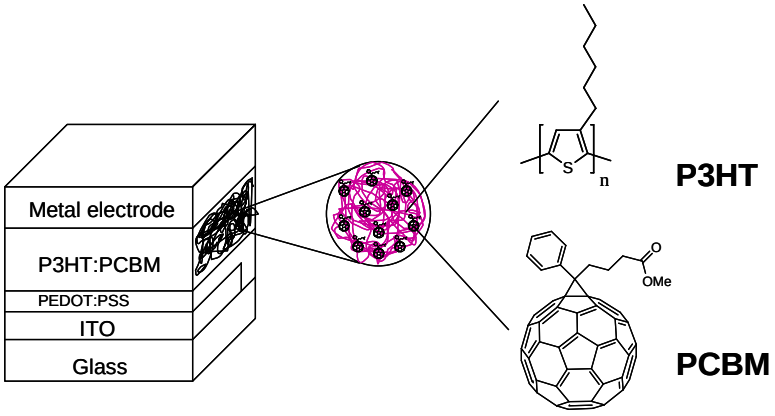

Figure 1: Typical device structure of a P3HT:PCBM solar cell: ITO/PEDOT:PSS/P3HT:PCBM blend/metal electrode. In this paper, the metal electrode is typically 100nm Al with a 1nm LiF intermediate layer.

Previously, the synthesis of functionalized regioregular poly(3-alkylthiophene)s (P3AT)s has been reported via several synthetic routes.[39]

Various functionalized homopolymers, end-group functionalized polymers or functionalized block copolymers and post-polymerization functionalization reactions for several applications have been reported using the McCullough or the Grignard metathesis method (GRIM).[40-47] Phosphonic acid functionalized homopolymers have been reported using the Stille coupling.[48] With the Rieke method, synthesis of several P3ATs has been reported. [49, 50] The Rieke method is compatible with various functional groups, since the oxidative addition proceeds selectively to the aromatic halide. [51] Within one class of materials, the materials properties may be adapted by introducing functional groups. In the case of P3HT, a certain degree of functionalization may be necessary to improve for example the thermal stability of the BHJ morphology. Functional groups may also be useful to improve interface contacts between layers, or they can be used to covalently bind other molecules to the alkyl side chains, for example an additional absorber.

In this work, the influence of alkyl side-chain functionalization on the optical absorption and performance in BHJSC is presented. First, the synthesis of regioregular side-chain ester-functionalized P3HT-based random copolymers is presented. We aimed for copolymerization, so that the desired properties of P3HT, like good processability and high hole mobility would be maintained. After synthesis of the random copolymers, photo-crosslinkable groups were introduced into the molecular structure of the conjugated polymer using straightforward post-polymerization procedures.[52] These copolymers were evaluated in BHJSC with PCBM as the electron acceptor. This study aims to evaluate the initial effect of functionalized side chains, e.g. cinnamoyl functional group, on the properties of the polymer and in the blend of a BHJSC.

2. Experimental details

Synthesis

The synthetic routes are depicted in Figure 2. 2,5-Dibromo-3-hexyl thiophene (**M1**) was obtained by bromination of 3-hexylthiophene (3-HT) with *N*-bromosuccinimide.[53] 3-HT was obtained by reacting 3-bromothiophene (3-BT) with *n*-hexylmagnesium bromide according to literature procedures.[54] The functionalities in the side chains of the functionalized monomers were chosen to be ester analogues of alcohol or acids groups, which are tolerated by active zinc.[51] 2,5-dibromo-3-(2-acetoxyethyl)thiophene (**M_2**) was obtained by dibromination of 2-(3-thienyl)ethanol followed by esterification of the formed 2,5-dibromo-3-(2-hydroxyethyl)thiophene with acetic anhydride and pyridine.[53, 55] **M_3** was obtained using a similar procedure as was utilized to obtain **M_1**, starting from 6-bromoethylhexanoate and 3-BT.[54, 56] Copolymers **P1** and **P4** were synthesized following the Rieke method using active zinc (Zn^*) and a nickel catalyst according to literature procedures.[49] The monomer solution in THF was added to Zn^* at -78°C to obtain an organozinc compound. This compound was added to a solution of 0.002 mol % nickel-catalyst in THF and stirred at 60°C for 18 h under inert atmosphere. The polymers were precipitated in a 2/1 (v/v) mixture of methanol and 2M HCl and purified using a Soxhlet extraction with methanol, pentane and acetone. The polymer was isolated by extraction with chloroform, precipitated in MeOH, filtered and dried. To obtain copolymers with different ratios of hexyl (x) and functionalized (y) side chains, monomer mixtures of various molar compositions were used. The various x/y ratios in the monomer feed before reaction with Zn^* allowed to obtain copolymers with different x/y ratios of

functional groups. As a reference compound for absorption measurements, P3HT was synthesized following the same literatures procedures.[49, 50] Hydrolysis of the ester functionalities in the side chain was performed by refluxing the polymer in a NaOH solution.[55] Functionalization reactions of copolymer **P2** were performed following literature procedures.[57]

Polymer characterization

All copolymers were characterized by ^{1}H-NMR and FT-IR. These data will be reported elsewhere. Size exclusion chromatography (SEC) was done with a 1weight-% polymer solution in THF, which was filtered with a 0.45µm pore PTFE syringe filter. A Spectra Physics P100 pump equipped with two mixed-B columns (10µm, 2x30cm, Polymer Labs) and a Shodex refractive index detector at 40°C in THF at a flow rate of 1.0 ml/min were used. Molecular weight distributions were measured relative to polystyrene standards. Toluene was used as a flow rate marker. UV-Vis absorption spectra of the polymer compounds and blends are presented. UV-Vis spectra were recorded on a Varian CARY 500 UV-Vis-NIR spectrophotometer from 200 to 800 nm at a scan rate of 600 nm/ min. A film of the polymer compounds was drop casted from a 0.1% solution in $CHCl_3$ on a quartz substrate. The absorption was normalized to 1 at the wavelength of maximum absorption (λ_{max}) between 300 and 800 nm. For polymer: PCBM (1:1) blends, the absorption was measured of films spin coated from a 10 mg mL^{-1} polymer solution in CB, mixed with PCBM in a 1:1 (w/w) ratio, before and after a thermal annealing step of 15 minutes at 100°C. The absorption of polymer: PCBM (1:1) blends, spin coated from 1 wt % polymer solution in CB with 2.5 mg dibromooctane (DBO) per ml CB added, was also recorded. The absorption of the copolymer blends was

scaled to the absorption of the P3HT:PCBM blend at λ = 335 nm to equalize the contribution of PCBM in the absorption.

Device structure, preparation and characterization

To measure the influence of the introduction of functionalized side-chains on solar cell performance, a typical device structure as displayed in figure 1 was used for the polymer: PCBM solar cells. ITO-patterned glass substrates were sonicated in acetone, soapy water and isopropanol and treated with UV/ozone for 15 minutes. Typically, 50nm poly(ethylenedioxythiophene):poly(styrenesulfonate) (PEDOT PSS) (Clevios™ P VP AI 4083, HC Starck) was spin coated at 3000 rpm on the glass substrate. A 1.5 wt % solution of PCBM in a dibromooctane (DBO, 24 mg/ml)/chlorobenzene solution was added to the polymer in a (1:1) (w/w) ratio and stirred at 50°C until the polymer dissolved completely. The blend solution was spin coated at several spinning speeds to investigate the influence of active layer thickness. The preparation of P3HT:PCBM solar cells was done with P3HT obtained from Rieke Metals. 1nm of LiF and 100nm of Al were evaporated on the active layer in high vacuum (10^{-7} mbar). *J-V* curves were measured measured under simulated solar light (100 mW/ cm^2) from a tungsten-halogen lamp filtered by a Schott GG385 UV filter and a Hoya LB120 daylight filter using a Keithley 2400 source meter. Spectral response was measured with monochromatic light from a 50 W tungsten halogen lamp (Philips focusline) in combination with a monochromator (Oriel, Cornerstone 130) and a lock-in amplifier (Stanford research Systems SR830). A calibrated Si cell was used as reference. The device was kept behind a quartz window in a nitrogen filled container. To

measure the cell under appropriate operating conditions, the cell was illuminated by a bias light from a 532 nm solid state laser (Edmund Optics).

3. Results and discussion

Two series of ester-functionalized copolymers **P1** and **P4** were synthesized using the Rieke method for production of regioregular P3ATs. The percentage of functionalized side chains was varied for each copolymer from 10 mol%, over 30 mol% to 50 mol%. The products of the bulk copolymerization are random copolymers, based on observations in ^{1}H-NMR. The **M1**/**M2** or **M1**/**M3** (Figure 2: X/Y) ratio in the monomer solution corresponded to the x/y ratio in the copolymers. The solubility of functionalized copolymers **P1** and **P4** was comparable to the solubility of P3HT in organic solvents like chlorobenzene (CB), chloroform ($CHCl_3$) or tetrahydrofurane (THF). The hydrolysis of the ester functions to alcohol or acid groups reduced the copolymer solubility. For example, **P2** and **P5** 1/1 copolymers were soluble in THF, but insoluble in CB and $CHCl_3$. The obtained regioregularities of the copolymers were higher then 93% for the **P1** series, with a decrease of molecular weight as the degree of functionalization (i.e. the percentage of functionalized alkyl side chains) increased. The weight average molecular weight (MW) measured for **P1** copolymers dissolved in THF were 47.8 k, 45.0 k and 26.8 k with polydispersity (D) of 1.9, 2.1 and 1.5 for the 9/1, 7/3 and 1/1 copolymers, respectively. For the **P2** series, the 9/1 copolymer displayed a regioregularity of 93%. For the 7/3 and 1/1, regioregularities of about 90% were obtained. The **P2** copolymer MW increased with an increasing percentage of functionalized side chains: from 56.7 k with D=1.9 for the 9/1 copolymer to 90.5 k , D=2.3 and 199.5 k , D=2.7 for the 7/3 and 1/1

copolymers, respectively. The ester functionalities in the side chains were converted with sodiumhydroxide as a base to obtain the corresponding alcohol or acid functionalities. A sample was taken and analyzed with FT-IR. The reaction was stopped when hydrolysis was complete.

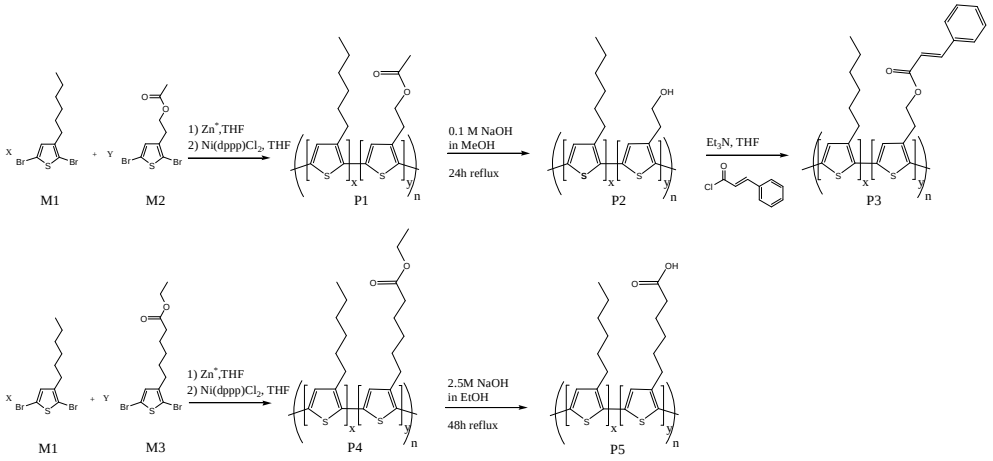

Figure 2: Copolymerization of **M1**/**M2** to acetoxyester-functionalized copolymers **P1** and M1/M3 ethyl ester-functionalized copolymers **P2**. The copolymerization was done in several ratios for both series: X/Y= 9/1, 7/3 and 1/1. All copolymers were hydrolyzed with NaOH until conversion towards alcoholgroups for copolymers **P2** or acid functionalities for copolymers **P5** was complete. The **P2** series was functionalized post-polymerization with an acidchloride in the presence of Et_3N to obtain cinnamoyl-functionalized copolymers **P3**.

For **P2**, this was typically after stirring 24h under reflux in a 0.1 M NaOH solution in methanol, while usually at least 48h in a 2.5 M NaOH solution in ethanol was necessary to obtain complete conversion towards **P5.** Post-polymerization reactions for several purposes are possible on alcohol and acid-functions in the polymer side chains.[55] The example of functionalization that we show here is the post-polymerization reaction of the alcohol groups in **P2** with cinnamoylchloride in the presence of triethylamine. After 18 h of reaction at room temperature in the presence of an excess of reagentia, the functionalization reaction is complete, as

determined by ^{1}H-NMR and FT-IR. This reaction was performed for the **P2** 9/1, 7/3 and 1/1 copolymers, to obtain the corresponding cinnamoyl functionalized copolymers **P3**.

The UV-Vis absorption spectra of drop-casted films of the copolymers and P3HT are compared in Fig 3a. For P3HT an absorption band between 400 and 600 nm is observed that has a distinct vibrational progression and peaks around 550 nm. The intensity of the maximum at 600 nm relative to the intensity at the maximum absorption at 550 nm is indicative for the order in the system. In a more regioregular structure, the order increases and the absorption at 600 nm will be higher than in a system where there is less order.[58, 59] The polymer films were drop casted on quartz substrates from $CHCl_3$ and the spectra were normalized to 1. The intensity of the peak at 600 nm relative to the absorption maximum at 555 nm is a measure for the structural order in the polymer film. In the absorption spectra of **P1** copolymer films, for the several ratios of functionalized side chains, the effect of functionalization is visible mainly by a reduction in intensity of the shoulder at λ=600 nm. This indicated that the introduction of functionalized side chains decreased the order in copolymer **P1** with respect to that of P3HT, but only noticeably for the 1/1 copolymer. For copolymer **P3**, 10% side-chain functionalities slightly increased the relative absorption intensity at 600 nm, which in general is indicative for more order. On the other hand, the absorption band has become broader and the vibrational structure is less pronounced than for P3HT. Increasing percentages of side-chain functionality (30 and 50 mol %) cause a further reduction in the absorption intensity at 600 nm. Most likely, the polymer stacking is disturbed by introducing the side-chain functionality. The slightly reduced regioregularity of 90 % vs 93% for 1/1 and 7/3 vs 9/1 and the slightly

reduced molecular weight of 9/1 as compared to 7/3 and 1/1 may also have contributed to the observed effect. In the absorption spectra of copolymers **P3**, the increasing amount of functionalized side chains was illustrated by the increase of the cinnamoyl absorption around λ=275 nm. The effect of the presence of the larger functionalities was visible as a general shift to shorter wavelengths and a decrease of the shoulder at λ=600 nm for 7/3 and 1/1 copolymers. Since **P3** was obtained from **P1** by post-polymerization reactions, bulk properties of the conjugated polymer backbone as molecular weight distribution and regioregularity should have remained the same for the both copolymer series. Therefore, the difference in behaviour between the two materials can only be caused by the nature and size of the functionalized side chains. Consequently, the bulky cinnamoyl functions are responsible for the decrease in structural order, because the functionalized groups are too big to fit in the P3HT lattice. In the absorption of copolymers **P4**, the presence of 10% side-chain functionalities also increased the absorption intensity at 600 nm. A higher percentage of functionalized side chains caused a decrease of the shoulder in the absorption spectra, indicating a loss of order. This is, similarly to the **P3** copolymers, probably due to a disturbance of the polymer crystalline structure.

UV-Vis absorption spectra of (1:1) (w/w) blends with PCBM spin-coated at 1000 rpm from a 1 wt % polymer solution in chlorobenzene and thermally annealed for 15 minutes at 100°C are displayed in Fig 3b. Generally, the same trends as observed for the pure polymer films are observed for the blends. The absorption of **P1** copolymer blends changes little with an increasing amount of functionalized side chains, except for the 1/1 copolymer. The functional groups in the side chains for **P1** are rather small, so the effect of the presence of a lower percentage of functionalized side

chains on the self organization of the polymer by π-π stacking and on the crystallinity of the polymer is limited. Since the crystallinity of the polymer in the blend is proportional to the absorption intensity,[60] the change in absorption of **P1** films can be related to the effect of the ester-functionalized side-chains on the crystallinity, compared to P3HT. For **P3** and **P4**, the functionalized side chains are larger and therefore the effect on the polymer stacking is larger and absorption is lower. The absorption of the **P3** copolymer blends decreases with an increasing amount of the bulky cinnamoyl functionalities. In the **P3** 7/3 and 1/1 copolymer blends, the absorption shifts to lower wavelengths, with only a very slight inflection at λ = 600nm, indicating that most of the structural order of the polymer phase in the blend is gone, even for 30% of functionalized side chains. Also in thermally annealed **P4**:PCBM blends, the absorption intensity and wavelength of maximum absorption decreases. Generally, the influence of functionalized side chains in the polymers on the absorption of copolymer:PCBM blends is dependent on the percentage of the side chain and its nature. Enhanced crystallinity and phase separation can be obtained by spincoating the blend from a solution which contains a high boiling co-solvent like octanedithiol or dibromooctane (DBO).[12, 20] In the absorption spectra, displayed in Fig 3c, the absorption maximum of the blends has shifted from around 500 nm for thermally annealed blends to about 550 nm for blends spin coated with DBO. This indicates a better stacking of the polymer conjugated backbones in the blend, which results in better phase-separated morphologies in blends prepared from a CB/DBO solution. The wavelength of maximum absorption increased in blends processed from CB solutions with DBO compared to thermally annealed blends for most of the copolymers. For the **P3** and **P4** 1/1 copolymers however, a more blue

shifted absorption was observed compared to the blends which were prepared by thermal annealing. For the organization in these copolymer blends, the spin coating with a co-solvent seemed less favourable.

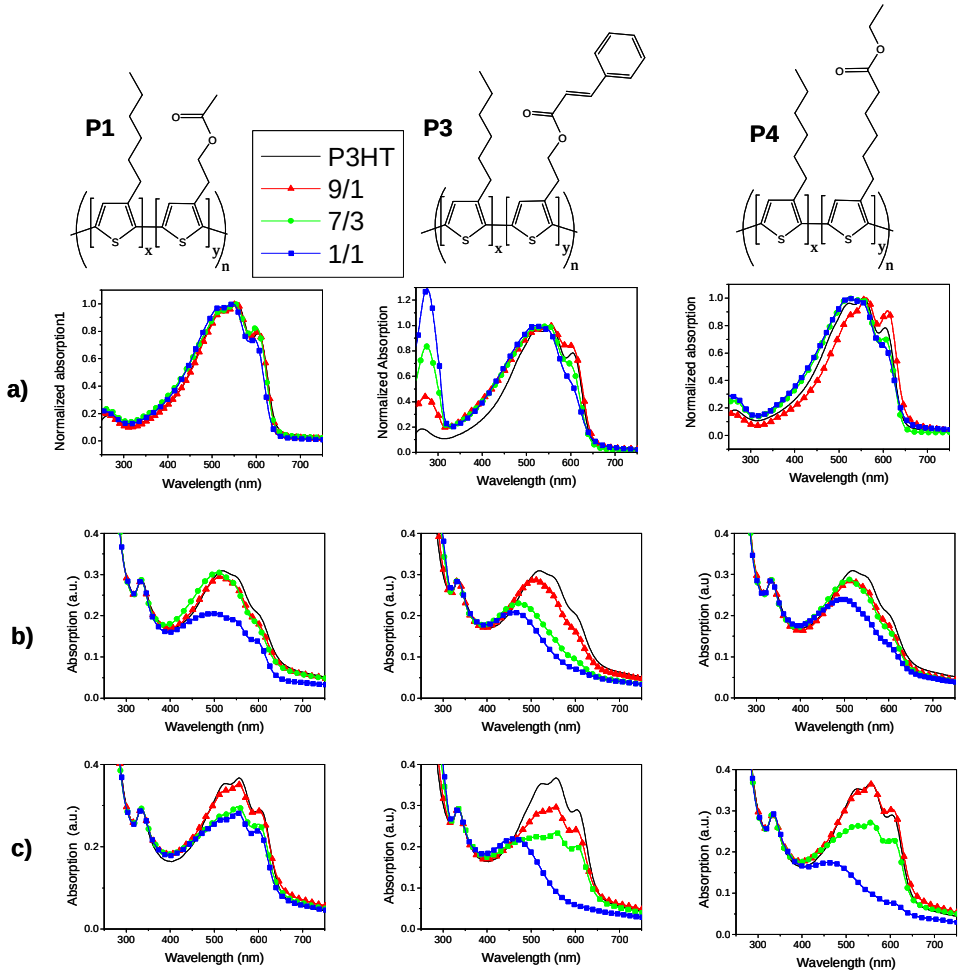

Figure 3: Absorption of copolymers **P1**, **P3**, **P4** with several ratios of functionalized side chains. a) polymer films drop-cast from solutions in $CHCl_3$ on a quartz substrate, absorptions were normalized to 1; b) polymer:PCBM (1:1) blend spin-coated on a quartz substrate at 1000 rpm from 10 mg mL^{-1} polymer solution in CB and thermally annealed at 100°C; c) polymer:PCBM (1:1) blend spin-coated on a quartz substrate at 1000 rpm fom a 10 mg mL^{-1} solution in CB with 25 mg mL^{-1} dibromooctane as high boiling co-solvent. The legend in the figures indicate the ratio of the hexyl side chain to the functionalized side chains for each series, i.e. 9/1 (triangles), 7/3 (circles) or 1/1 (squares)

The effect of the presence of the relatively large cinnamoyl ester groups in copolymers **P3** on the optical absorption spectra (Fig 3) was stronger as compared to the effect of the presence of smaller functionalized side chains in copolymers **P1** and **P4.** To evaluate the effect of the present functionalities on the performance in BHJSC, copolymer: PCBM solar cells were made with the **P3** 9/1, 7/3 and 1/1 copolymers. Solar cells with the copolymers and PCBM in a (1:1) blend, typically showed low fill factors after thermal annealing at several temperatures. With a thermal annealing step, no sufficient phase-separated morphology could be obtained, inducing increased charge recombination. With the addition of DBO as a co-solvent, a better phase separation and better fill factors were obtained. Blends were spin coated from solutions in CB with 25 mg/ ml DBO at several spinning speeds to obtain a variation of layer thickness. The solubility of the 1/1 copolymer in CB was not very good, which led to inhomogeneous spin coated layers. In Figure 4, the solar cell characterization is displayed as a function of layer thickness. With an increasing amount of functionalized side chains, a decrease was observed in the short circuit current (J_{sc}), Fill Factor (*FF*) and open circuit voltage (V_{oc}), and therefore also in the *MPP*. The copolymer with the lowest percentage of functionalized side chains generated solar cells with the best performance. The 9/1 copolymer performed comparable to P3HT:PCBM solar cells with the same layer thickness. The V_{oc} observed in the copolymer: PCBM solar cells produced with DBO was lower compared the P3HT:PCBM solar cell. This is probably due to the extensive stacking of the polymer chains by spin coating with DBO. The increased crystallinity influences the energy levels of the material and therefore also the V_{oc} in the solar cell.

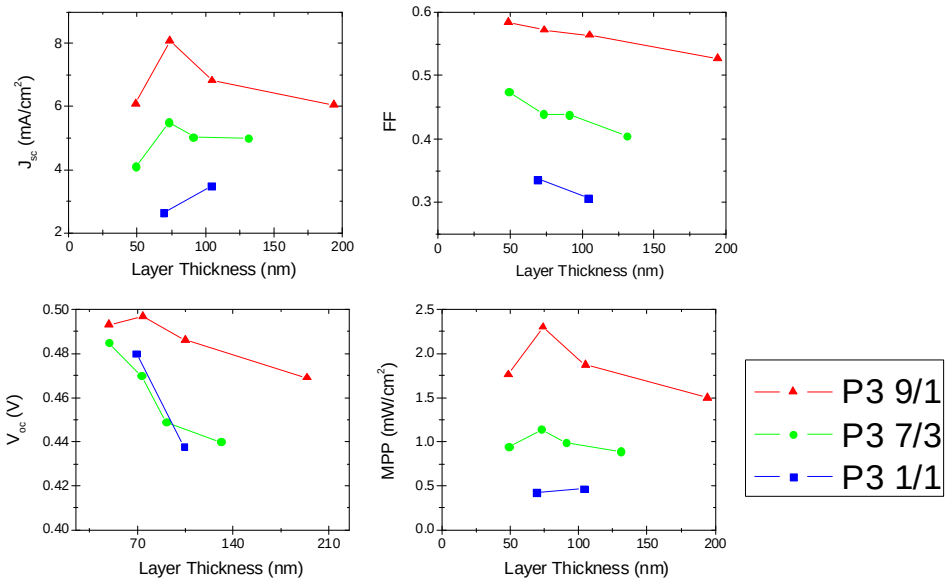

Figure 4: J_{sc}, V_{oc}, FF and MPP in ITO/PEDOT:PSS~50nm/**P3**:PCBM/LiF~1nm /Al~100 nm solar cells for blends with varying thickness made with the **P3** 9/1 (triangles), 7/3 (circles) and 1/1 (squares) copolymers.

The *J-V* curves of the best solar cells are displayed for each **P3** copolymer in figure 5. The characteristics of the solar cells are given in table 1. For the **P3** 9/1 and 7/3 copolymer solar cells, the external quantum efficiencies (*EQE*) were measured. A correction of J_{sc} was performed to obtain an estimated efficiency, which is displayed in table 1. The performance of the **P3** 9/1 copolymer with 10% of side chains remains comparable to the performance of pristine commercially available P3HT in a polymer: PCBM BHJSC. With a further increasing degree of functionalization, a decrease in J_{sc}, V_{oc} and *FF* was observed.

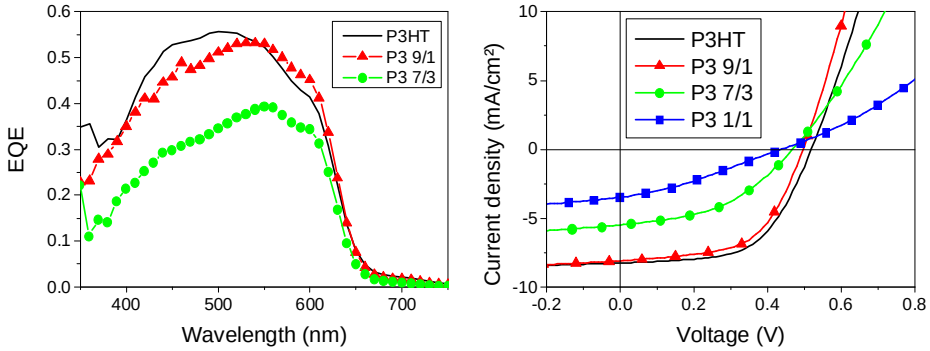

Figure 5: EQE and J-V curves of solar cells with the structure ITO/ PEDOT:PSS/ polymer:PCBM/ 1nm LiF/100 nm Al made with P3HT (full line) and the **P3** 9/1(triangles), 7/3 (circles) and 1/1 (squares) copolymer

Table 1: Characteristics of the **P3** solar cells displayed in figure 4.

x/y	J_{sc} * (mA/cm²)	V_{oc} (V)	*FF*	η	Layer thickness (nm)
P3HT	7.44	0.52	0.579	2.48	82
9/1	7.17	0.50	0.57	2.04	74
7/3	5.01	0.47	0.44	1.14	73
1/1	3.43	0.44	0.30	0.47	104

* J_{sc} under AM 1.5 conditions was obtained from the spectral response and convolution with the solar spectrum and, except for the 1/1 copolymer, this J_{sc} was used to calculate the estimated efficiency η

4. Conclusion

Processable regioregular P3HT-based random copolymers were obtained with 10, 30 and 50 % of ester functionalized side chains. Post polymerization reactions were used to convert the ester groups in the side chains to alcohol and acid functionalities. Photo-crosslinkable cinnamoyl groups were covalently attached to the functionalized alkyl side chains by esterification of the alcohol groups with the corresponding acidchloride. The introduction of the side chain functionalities influenced the UV-Vis

absorption in copolymer: PCBM blends. For 9/1 copolymers, containing 10% functionalized side chains, the absorption was comparable to the absorption of P3HT. The absorption decreased further in copolymer films and copolymer blends with an increasing percentage of functionalized side chains, probably due to the disturbance of the polymer self-organization by π- π stacking. The effect of the presence of the large cinnamoyl functions in **P3** and the ester functionalized side chains in **P4** was stronger in the 7/3 and 1/1 copolymers, containing 30 and 50 % of functionalized side chains respectively, compared to the effect of the smaller ester functionalized side chains in **P1**. In blends with **P3** and **P4** also the wavelength of maximum absorption decreased for higher degrees of functionalization. For most of the copolymers, the introduction of 25 mg mL^{-1} DBO in the spin-coating solution resulted in better organized polymer phases in the blend. This caused an increase in wavelength of maximum absorption and solar cells with better phase separated morphologies and higher fill factors were obtained. From copolymer:PBCM (1:1) blends in chlorobenzene with DBO, BHJSCs were made with several active layer thicknesses. The **P3** 9/1 copolymer, containing 10 % of functionalized side chains, was applied to obtain BHJSCs with initial power efficiency comparable to that of P3HT. Therefore, it is possible to introduce a certain amount of functionalized side chains into the polymer molecular structure and maintain solar cell performance comparable to the pristine P3HT, even for larger side chain functionalities as for example the photo-crosslinkable cinnamoyl function. The functionalization of conjugated copolymers allows modified material properties, for example the crosslinking of the active layer and potentially an improved stability of the blend morphology in the active layer of a

BHJSC can be obtained. Future work aims to investigate this approach in detail, using the photoinitiated [2+2] cycloaddition of the cinnamoyl group.

5. Acknowledgements

The authors gratefully acknowledge the funding of the Ph.D. grant of Bert Campo by the Institute for the Promotion of Innovation through Science and Technology in Flanders (IWT-Vlaanderen)

6. References

[1] Sariciftci, N. S., Smilowitz, L., Heeger, A. J. and Wudl, F., "Photoinduced electron transfer from a conducting polymer to buckminsterfullerene", Science 258, 1474-1476 (1992)
[2] Halls, J. J. M., C.A., W., Greenham, N. C., Marseglia, E. A., Friend, R. H., Moratti, S. C. and Holmes, A. B., "Efficient photodiodes from interpenetrating networks", Nature 376, 498-500 (1995)
[3] Yu, G., Gao, J., Hummelen, J. C., Wudl, F. and Heeger, A. J., "Polymer photovoltaic cells: enhanced efficiencies via a network of internal donor-acceptor heterojunctions", Science 270, 1789-1791 (1995)
[4] Kim, J. Y., Lee, K., Coates, N. E., Moses, D., Nguyen, T. Q., Dante, M. and Heeger, A. J., "Efficient tandem polymer solar cells fabricated by all-solution processing", Science 317(5835), 222-225 (2007)
[5] Li, G., Shrotriya, V., Huang, J. S., Yao, Y., Moriarty, T., Emery, K. and Yang, Y., "High-efficiency solution processable polymer photovoltaic cells by self-organization of polymer blends", Nature Materials 4(11), 864-868 (2005)
[6] Ma, W., Yang, C., Gong, X., Lee, K. and Heeger, A. J., "Thermally stable, efficient polymer solar cells with nanoscale control of the interpenetrating network morphology", Advanced Functional Materials 15, 1617-1622 (2005)
[7] Reyes-Reyes, M., Kim, K. and Carroll, D. L., "High-efficiency photovoltaic devices on annealed poly(3-hexylthiophene) and 1-(3-methoxycarbonyl)-propyl-1-phenyl-(6,6)C_{61} blends", Applied Physics Letters 87(083506), (2005)
[8] Scharber, M. C., Wuhlbacher, D., Koppe, M., Denk, P., Waldauf, C., Heeger, A. J. and Brabec, C. L., "Design rules for donors in bulk-heterojunction solar cells - Towards 10 % energy-conversion efficiency", Advanced Materials 18(6), 789 (2006)
[9] Thompson, B. C. and Frechet, J. M. J., "Organic photovoltaics - Polymer-fullerene composite solar cells", Angewandte Chemie International Edition 47(1), 58-77 (2008)
[10] Lee, K., Kim, J. Y., Ma, W. and Heeger, A. J., "New architecture for thermally stable high efficiency polymer solar cells", Proceedings of SPIE 5938, 59380B1-12 (2005)
[11] Kim, J. Y., Kim, S. H., Lee, H. H., Lee, K., Ma, W. L., Gong, X. and Heeger, A. J., "New architecture for high-efficiency polymer photovoltaic cells using solution-based titanium oxide as an optical spacer", Advanced Materials 18(5), 572 (2006)

[12] Peet, J., Kim, J. Y., Coates, N. E., Ma, W. L., Moses, D., Heeger, A. J. and Bazan, G. C., "Efficiency enhancement in low-bandgap polymer solar cells by processing with alkane dithiols", Nature Materials 6, 497-500 (2007)
[13] Brabec, C. J., Shaheen, S. E., Winder, C., Sariciftci, N. S. and Denk, P., "Effect of LiF/metal electrodes on the performance of plastic solar cells", Applied Physics Letters 80(7), 1288-1290 (2002)
[14] Moulé, A. J., Bonekamp, J. B., Ruhl, A., Klesper, H. and Meerholz, K., "The effect of active layer thickness on the efficiency of Polymer solar cells", Proceedings of SPIE 5938, 593808 1-7 (2005)
[15] Hadipour, A., de Boer, B. and Blom, P. W. M., "Organic tandem and multi-junction solar cells", Advanced Functional Materials 18(2), 169-181 (2008)
[16] Gilot, J., Barbu, I., Wienk, M. M. and Janssen, R. A. J., "The use of ZnO as optical spacer in polymer solar cells: Theoretical and experimental study", Applied Physics Letters 91(11), - (2007)
[17] Jorgensen, M., Norrman, K. and Krebs, F. C., "Stability/degradation of polymer solar cells", ", Solar Energy Materials and Solar Cells 92(7), 686-714 (2008)
[18] Dennler, G., Scharber, M. C. and Brabec, C. J., "Polymer-Fullerene Bulk-Heterojunction Solar Cells", Advanced Materials 21(13), 1323-1338 (2009)
[19] Yang, X., Loos, J., Veenstra, S. C., Verhees, W. J. H., Wienk, M. M., Kroon, J. M., Michels, M. A. J. and Janssen, R. A. J., "Nanoscale morphology of high-performance polymer solar cells", Nanoletters 5(4), 579-583 (2005)
[20] Yao, Y., Hou, J. H., Xu, Z., Li, G. and Yang, Y., "Effect of solvent mixture on the nanoscale phase separation in polymer solar cells", Advanced Functional Materials 18(12), 1783-1789 (2008)
[21] Shaheen, S. E., Brabec, C. J., Sariciftci, N. S., Padinger, F., Fromherz, T. and Hummelen, J. C., "2.5% efficient organic plastic solar cells", Applied Physics Letters 78(6), 841-843 (2001)
[22] Vanlaeke, P., Vanhoyland, G., Aernouts, T., Cheyns, D., Deibel, C., Manca, J., Heremans, P. and Poortmans, J., "Polythiophene based bulk heterojunction solar cells: morphology and its implications", Thin Solid Films 511-512, 358-361 (2006)
[23] Padinger, F., Rittberger, R. S. and Sariciftci, N. S., "Effects of postproduction treatment on plastic solar cells", Advanced Functional Materials 13(1), 85-88 (2003)
[24] Li, G., Yao, Y., Yang, H., Shrotriya, V., Yang, G. and Yang, Y., ""Solvent annealing" effect in polymer solar cells based on poly(3-hexylthiophene) and methanofullerenes", Advanced Functional Materials 17(10), 1636-1644 (2007)
[25] Swinnen, A., Haeldermans, I., vande Ven, M., D'Haen, J., Vanhoyland, G., Aresu, S., D'Olieslaeger, M. and Manca, J., "Tuning the dimensions of C-60-based needlelike crystals in blended thin films", Advanced Functional Materials 16(6), 760-765 (2006)
[26] Krebs, F. C., "Air stable polymer photovoltaics based on a process free from vacuum steps and fullerenes", Solar Energy Materials and Solar Cells 92(7), 715-726 (2008)
[27] Zhu, Z., Hadjikyriacou, S., Waller, D. and Gaudiana, R., "Stabilization of film morphology in polymer-fullerene heterojunction solar cells", Journal of Macromolecular Science: Part A: Pure and Applied Chemistry 41(12), 1467-1487 (2004)
[28] Drees, M., Hoppe, H., Winder, C., Neugebauer, H., Sariciftci, N. S., Schwinger, W., Schaffler, F., Topf, C., Scharber, M. C., Zhu, Z. G. and Gaudiana, R., "Stabilization of the nanomorphology of polymer-fullerene "bulk heterojunction" blends using a novel polymerizable fullerene derivative", Journal of Materials Chemistry 15(48), 5158-5163 (2005)

[29] Zhou, Z. Y., Chen, X. W. and Holdcroft, S., "Stabilizing bicontinuous nanophase segregation in pi CP-C-60 donor-acceptor blends", Journal of the American Chemical Society 130(35), 11711-11718 (2008)
[30] Miyanishi, S., Tajima, K. and Hashimoto, K., "Morphological Stabilization of Polymer Photovoltaic Cells by Using Cross-Linkable Poly(3-(5-hexenyl)thiophene)", Macromolecules 42(5), 1610-1618 (2009)
[31] Nierengarten, J. F. and Setayesh, S., "Towards polymerizable fullerene derivatives to stabilize the initially formed phases in bulk-heterojunction solar cells", New Journal of Chemistry 30, 313-316 (2006)
[32] Björstrom, C. M., Magnusson, K. O. and Moons, E., "Control of phase separation in blends of polyfluorene (co)polymers and the C_{60}-derivative PCBM", Synthetic Metals 152, 109-112 (2005)
[33] Rajaram, S., Armstrong, P. B., Kim, B. J. and Frechet, J. M. J., "Effect of Addition of a Diblock Copolymer on Blend Morphology and Performance of Poly(3-hexylthiophene):Perylene Diimide Solar Cells", Chemistry of Materials 21(9), 1775-1777 (2009)
[34] Sivula, K., Ball, Z. T., Watanabe, N. and Frechet, J. M. J., "Amphiphilic diblock copolymer compatibilizers and their effect on the morphology and performance of polythiophene: Fullerene solar cells", Advanced Materials 18(2), 206 (2006)
[35] Woo, C. H., Thompson, B. C., Kim, B. J., Toney, M. F. and Fréchet, J. M., "The influence of Poly(3-hexylthiophene) regioregularity on fullerene-composite solar cell performance", Journal of the American Chemical Society 130(48), 16324-16329 (2008)
[36] Sivula, K., Luscombe, C. K., Thompson, B. C. and Fréchet, J. M. J., "Enhancing the Thermal Stability of Polythiophene:Fullerene Solar Cells by Decreasing Effective Polymer Regioregularity", Journal of the American Chemical Society 128, 13988-13989 (2006)
[37] Bertho, S., Haeldermans, I., Swinnen, A., Moons, W., Martens, T., Lutsen, L., Vanderzande, D., Manca, J., Senes, A. and Bonfiglio, A., "Influence of thermal ageing on the stability of polymer bulk heterojunction solar cells", Solar Energy Materials and Solar Cells 91(5), 385-389 (2007)
[38] Kim, B. J., Miyamoto, Y., Ma, B. and Fréchet, J. M. J., "Photocrosslinkable pholythiophenes for efficient, thermally stable, organic photovoltaics", Advanced Functional Materials 19, 1-9 (2009)
[39] Osaka, I. and McCullough, R. D., "Advances in molecular design and synthesis of regioregular polythiophenes", Accounts of Chemical Research 41(9), 1202-1214 (2008)
[40] Loewe, R. S., Khersonsky, S. M. and McCullough, R. D., "A simple method to prepare head-to-tail coupled, regioregular poly(3-alkylthiophenes) using grignard metathesis", Advanced Materials 11(3), 250 (1999)
[41] Liu, J. and McCullough, R. D., "End group modification of regioregular polythiophene through postpolymerization functionalization", Macromolecules 35, 9882-9889 (2002)
[42] Zhai, L., Laird, D. W. and McCullough, R. D., "Soft-lithography patterning of functionalized regioregular polythiophenes", Langmuir 19(16), 6492-6497 (2003)
[43] Mccullough, R. D., Lowe, R. D., Jayaraman, M. and Anderson, D. L., "Design, Synthesis, and Control of Conducting Polymer Architectures - Structurally Homogeneous Poly(3-Alkylthiophenes)", Journal of Organic Chemistry 58(4), 904-912 (1993)
[44] Zhai, L., Pilston, R. L., Zaiger, K. L., Stokes, K. K. and McCullough, R. D., "A simple method to generate sice-chain derivatives of regioregular polythiophene via the GRIM methathesis and post-polymerization functionalization", Macromolecules 36, 61-64 (2003)
[45] Dai, C. A., Yen, W. C., Lee, Y. H., Ho, C. C. and Su, W. F., "Facile synthesis of well-defined block copolymers containing regioregular poly(3-hexyl thiophene) via anionic

macroinitiation method and their self-assembly behavior", Journal of the American Chemical Society 129(36), 11036 (2007)
[46] Sheina, E. E., Khersonsky, S. M., Jones, E. G. and McCullough, R. D., "Highly conductive, regioregular alkoxy-functionalized polythiophenes: A new class of stable, low band gap materials", Chemistry of Materials 17(13), 3317-3319 (2005)
[47] Jeffries-El, M., Sauve, G. and McCullough, R. D., "In-situ end-group functionalization of regioregular poly(3-alkylthiophene) using the Grignard metathesis polymerization method", Advanced Materials 16(12), 1017 (2004)
[48] Stokes, K. K., Heuze, K. and McCullough, R. D., "New phosphonic acid functionalized, regioregular polythiophenes", Macromolecules 36(19), 7114-7118 (2003)
[49] Chen, T. A., Wu, X. M. and Rieke, R. D., "Regiocontrolled Synthesis of Poly(3-Alkylthiophenes) Mediated by Rieke Zinc - Their Characterization and Solid-State Properties", Journal of the American Chemical Society 117(1), 233-244 (1995)
[50] Oosterbaan, W. D., Vrindts, V., Berson, S., Guillerez, S., Douhéret, O., Ruttens, B., D'Haen, J., Adriaensens, P., Manca, J., Lutsen, L. and Vanderzande, D., "Efficient formation, isolation and characterization of poly(3-alkylthiophene) nanofibres: probing order as a function of side-chain length", Journal of Materials Chemistry DOI: 10.1039/b900670b, (2009)
[51] Zhu, L., Wehmeyer, R. M. and Rieke, R. D., "The Direct Formation of Functionalized Alkyl(Aryl)Zinc Halides by Oxidative Addition of Highly Reactive Zinc with Organic Halides and Their Reactions with Acid-Chlorides, Alpha,Beta-Unsaturated Ketones, and Allylic, Aryl, and Vinyl Halides", Journal of Organic Chemistry 56(4), 1445-1453 (1991)
[52] Kato, M., Hirayama, T., Matsuda, H., Minami, N., Okada, S. and Nakanishi, H., "Photocrosslinkable Azo-Dye Polymers for 2nd-Order Nonlinear Optics", Macromolecular Rapid Communications 15(9), 741-750 (1994)
[53] Bauerle, P., Pfau, F., Schlupp, H., Wurthner, F., Gaudl, K. U., Caro, M. B. and Fischer, P., "Synthesis and Structural Characterization of Alkyl Oligothiophenes - the 1st Isomerically Pure Dialkylsexithiophene", Journal of the Chemical Society-Perkin Transactions 2 (3), 489-494 (1993)
[54] Tamao, K., Kodama, S., Nakajima, I., Kumada, M., Minato, A. and Suzuki, K., "Nickel-Phosphine Complex-Catalyzed Grignard Coupling .2. Grignard Coupling of Heterocyclic-Compounds", Tetrahedron 38(22), 3347-3354 (1982)
[55] Lowe, J. and Holdcroft, S., "Synthesis and polylithography of polymers and copolymers based on Poly(3-(2-(methacryloyloxy)ethyl)thiophene)", Macromolecules 28, 4608-4616 (1995)
[56] Dai, J., Sellers, J. L. and Noftle, R. E., "An efficient method for the synthesis of 3-alkylthiophenes bearing groups on the side chain: imides and amides", Synthetic Metals 139, 81-88 (2003)
[57] Kock, T. J. J. M. and de Ruiter, B., "A radiation-crosslinkable thiophene copolymer", Synthetic Metals 79, 215-218 (1996)
[58] Spano, F. C., "Modeling disorder in polymer aggregates: the optical spectroscopy of regioregular poly(3-hexylthiophene) thin films", The Journal of Chemical Physics 122, 234701 (2005)
[59] Spano, F. C., "Absorption in regio-regular poly(3-hexylthiophene) thin films: Fermi resonances, interband coupling and disorder", Chemical Physics 325, 22-35 (2006)
[60] Zhokhavets, U., Erb, T., Gobsch, G., Al-Ibrahim, M. and Ambacher, O., "Relation between absorption and crystallinity of poly(3-hexylthiophene)/fullerene films for plastic solar cells", Chemical Physics Letters 418(4-6), 347-350 (2006)

Chapter Four:

Effect of ester-functionalized side chains in Poly(3-hexylthiophene) on performance in polymer:fullerene bulk heterojunction solar cells[‡]

Abstract: The synthesis and characterization of two types of poly(3-hexylthiophene) (P3HT) -based random copolymers with ester functionalized alkyl side chains is presented. The polymers are of the type poly([3-hexylthiophene-2,5-diyl]-*co*-[3-(R)thiophene-2,5-diyl]) with R being 2-acetoxyethyl (**P1**) or 6-ethoxy-6-oxohexyl (**P2**) and the percentage of functionalized side chain is varied between 10 and 50 mol%. The polymers are synthesized using the Rieke method for regioregular poly(3-alkylthiophene)s, characterized and evaluated in bulk heterojunction solar cells (BHJSC) using [6,6]-phenyl-C_{61}-butyric acid methyl ester (PCBM) as an electron acceptor. Power conversion efficiencies decrease with an increasing percentage of side chain functionalities. The decrease depends on the percentage and nature of the introduced functionalities and is related to the effect of the functionalities on the crystalline structure of the polymer phase, as indicated by Differential Scanning Calorimetry, Transmission Electron Microscopy and X-Ray Diffraction. A limited loss in short circuit current and efficiency was observed for copolymers containing up to 10% of

[‡] Submitted by Bert J. Campo, Jan Gilot, Henk J. Bolink, Jun Zhao, Jean-Christophe Bolsée, Wibren D. Oosterbaan, Sabine Bertho, Bart Ruttens, Jan D'Haen, Thomas J. Cleij, Jean Manca, Laurence Lutsen, Guy Van Assche, René A. J. Janssen, *and* Dirk Vanderzande

functionalized side chains. The introduction of functionalities offers a pathway to future improvements via the demonstrated possibility of fine-tuning the chemical composition of the polymer phase in bulk heterojunction solar cells.

1. Introduction

The device efficiency of polymer:fullerene solar cells improved significantly since the electron transfer phenomenon between a conjugated polymer and a C_{60} molecule was observed, and the development of the bulk-heterojunction solar cell (BHJSC) concept was introduced.[1, 2] Both in design of devices and in materials development and post-production treatment, consecutive improvements were responsible for a progress in the performance of BHJSCs.[2-7] The past few years, poly-(3-hexylthiophene) (P3HT), a stable processable conjugated polymer with high charge carrier mobility, attracted considerable attention. P3HT is a hole conductor and was used in BHJSCs mixed with PCBM which acts as an electron acceptor. In the optimum device geometry, power conversion efficiencies near 5% were reported using a combination of these materials.[8, 9]

A variety of synthetic procedures has been reported for synthesis of P3AT.[10, 11] The nature of the synthetic route determines the structure and degree of regioregularity of the produced polymer, and therefore also the material properties. It was shown that P3ATs with higher regioregularity led to more homogeneous structures and performed better in BHJSCs.[12-14] A high percentage of head-to-tail (H-T) couplings (or high regioregularity) was required to obtain a polymer that tends to self-organize.[14] Because of the higher H-T ratio in the polymer, the structural order in the molecular

structure increased and crystalline polymer domains were formed in thin blend films with PCBM.[15] The tendency of the polymer to self-organize is important to reach a high hole mobility in the polymer phase, and to have sufficient phase separation between the p- and n-type materials in the blend which is necessary for device performance.[16, 17] A sufficient phase separation with good stacking of polymer chains and crystalline PCBM regions can be obtained by thermal or solvent annealing of the active layer, or by spin-coating the blend from high boiling solvents or from solvent mixtures. [6, 9, 18-21]

Several polythiophenes with functionalized side chains have been reported for a variety of synthetic procedures. The oxidative polymerization method with $FeCl_3$,[22] proved to be compatible with a wide variety of functional groups in the side chains, for example several (co)polymers with ester[23-26], alcohol[27], bromine[28, 29] or other functionalities[30, 31] in the side chains were synthesized. Several functional (co)polymers were subjected to further post-polymerization treatments towards several applications grafting or photolithography applications.[24, 32-36] This method, however, gives non-regular polymers. Regioregular poly(3-alkylthiophene) (*RR* P3AT) were obtained via reductive coupling methods, such as the McCullough[37], Grignard metathesis (GRIM)[38], or Rieke method.[39] Functionalized *RR* P3ATs were reported for several homopolymers or as end-group functionalized polythiophenes. [29, 40-46] The synthesis of copolymers of *RR* P3AT was also demonstrated.[47-49] Here, a series of novel alkyl side-chain ester-functionalized P3HT-based copolymers is presented. The *Rieke* method allowed for the synthesis of side-chain functionalized RR P3ATs, since it tolerates functional groups because of the selective oxidative addition of zinc to the aromatic halide.[50] A copolymerization reaction

allows control of the percentage of functionalized side chains in the polymer. The ester functionalities in the copolymer side chains were hydrolyzed post-polymerization to obtain alcohol- and acid functionalized RR P3ATs. This opens the way for a wide scale of possible functionalization reactions to tune the materials properties.[51] These possibilities may answer some of the limitations of the P3HT:PCBM system, for example, by adding additional chromophores to broaden the absorption window of the polymer. Other side-chain functionalities were added to improve the morphological stability of the BHJ solar cells. [52, 53] The polar functionalized side chains may influence surface interactions between the polymer and metal oxides which are often used as electrode materials. To evaluate the influence of the presence of a certain amount of functional groups in the side chains of P3HT, two series of ester side-chain functionalized *RR* P3HT copolymers were synthesized and characterized. The performance of the functionalized copolymers in bulk heterojunction solar cells using PCBM as electron acceptor is presented and compared to the pristine P3HT:PCBM.

2. Results and discussion

2.1 Synthesis of functionalized RR P3AT copolymers

Starting from the commercially available products 3-bromothiophene (3-BT) and hexylmagnesiumbromide, 3-hexylthiophene (3-HT) was obtained following literature procedures.[54] 2,5-Dibromo-3-hexyl thiophene (**M1**) was prepared by bromination of 3-HT in presence of N-bromosuccinimide (NBS).[55] 6-(2,5-dibromo-thiophen-3-yl)-hexanoic acid ethyl ester (**M3**)

was synthesized using similar procedures as was utilized to obtain **M1**, starting from 6-bromoethylhexanoate and 3-BT.[54, 56] 2-(2,5-dibromothiophen-3-yl)ethyl acetate (**M2**) was acquired after dibromination of 2-(3-thienyl)ethanol and esterification of the alcohol.

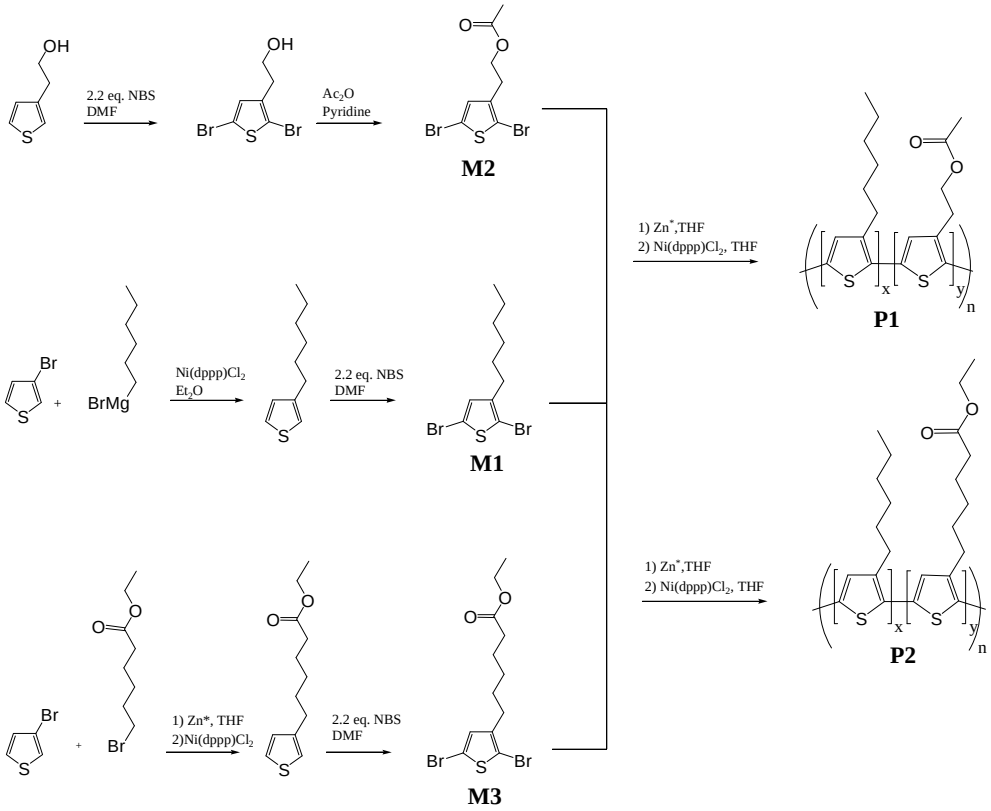

Scheme 1: Synthesis of ester-functionalized P3AT copolymers **P1** and **P2**.

The copolymers were synthesized via the Rieke polymerization method using active zinc (Zn^*) and a nickel catalyst according to literature procedures.[39, 57] For synthesis of P3HT, a monomer solution of **M1** was used. To obtain copolymers with a varying content of functionalized side chains (**Scheme 1**), monomer mixtures with various molar compositions were added to Zn^* prior to the polymerization reaction. (**Table 1**) The resulting ester copolymers were still soluble in organic solvents like chlorobenzene (CB), chloroform ($CHCl_3$) or tetrahydrofurane (THF). The

yield of the polymerization for P3HT with respect to the monomer compound, as obtained after purification by means of Soxhlet extraction, was 67%, somewhat lower compared to literature values.[39] The copolymer yield decreases with increasing percentage of functionalized side chains for both **P1** and **P2**, to around 50% for the 1/1 copolymers.

2.2 Physical characterization of copolymer compounds

2.2.1 Gel permeation chromatography

Gel Permeation Chromatography (GPC) was used to determine molecular weight distributions, relative to polystyrene standards. Since the introduced functionalized side chains may influence the hydrodynamic volume of the polymer chain in solution it could be that the observed decrease (increase) in M_n values in **P1** (**P2**) with increasing percentage of side-chain functionalized monomer is - in part - due to the smaller (larger) volume occupied by the functionalized side-chain as compared to a hexyl side chain. A decreased (enhanced) polymer solubility due to the introduction of functionalized side chains for **P1** (**P2**) may also be the cause of the lower (higher) M_n values for that polymer.

2.2.2 ^{1}H-NMR

^{1}H-NMR was used to determine the ratio between the hexyl tails and the ester functionalized side chains in the copolymers. The ratio x/y was determined on the basis of the integral ratio of the –C*H*$_3$ and –C*H*$_2$-O-(C=O)- signals of the different monomer units at 0.89 ppm and either 2.05 ppm (**P1**) or 4.1 ppm (**P2**), respectively (Table 1). It was found that the ratios of monomer units present in the copolymers correspond to the ratios present in the monomer mixture. Therefore it is possible to easily control the

desired content of ester-functionalized alkyl side chains in the copolymer. Furthermore, it indicates that the reactivity of the functional monomers **M2** and **M3** is very similar to that of **M1**. The degree of regioregularity is the ratio of the area that is originating from the H-T couplings (δ 2.8 ppm) to the area from the other couplings (δ 2.5 ppm) in the polymer backbone. For P3HT, a regioregularity higher than 96% was obtained. The introduction of increasing percentages of ester-functionalized monomer units in the copolymers increasingly lowered the *RR*s to values of 93 and 89 % for **P1** and **P2**, respectively. (Table 1)

Table 1: Polymer **P1** and **P2** characterization

Polymer	X/Y molar ratio[a]	x/y [b]	Yield [%]	RR [%] [c]	M_n (10^3) [d]	M_w (10^3) [e]	D [f]
P3HT	1/0	100/0	67	96	27.8	53.5	1.9
P1	9/1	90.7 / 9.3	61	94	24.7	47.7	1.9
P1	7/3	67.1 / 32.9	52	93	21.6	45.0	2.1
P1	1/1	53.0 / 47.0	51	93	17.3	26.8	1.5
P2	9/1	90.3 / 9.7	74	93	30.0	56.7	1.9
P2	7/3	69.8 / 30.2	62	90	39.3	90.5	2.3
P2	1/1	48.9 / 51.2	53	89	44.5	119.5	2.7

[a] monomer ratio in reaction feed [b] ratio of repeating units in copolymer, determined by ^{1}H-NMR [c] regio regularity determined on ^{1}H-NMR [d] number average molecular weight in THF [e] weight average molecular weight in THF [f] polydispersity in THF

The nature of the obtained copolymer (block, alternating or statistical) was observed by ^{1}H-NMR. The aromatic proton signal around δ = 6.9 ppm is

visible as three peaks originating from four different dyads, as displayed for the **P1** 7/3 copolymer in **Figure 1**. Due to the proximity of the polar ester groups to the aromatic protons on the polymer backbone, the chemical shift of the aromatic proton changed. The ratio of the integration areas from these signals indicated that the ratio of functionalized monomer units neighbouring each other or a 3-hexylthiophene unit is proportional to the percentage of the monomer units in the copolymer. For the 9/1 and 1/1 copolymers, the results were similarly to what is expected for a random copolymer. In a monomer mixture, no preference for bonding with an identical or a different monomer existed, leading to a random copolymer.

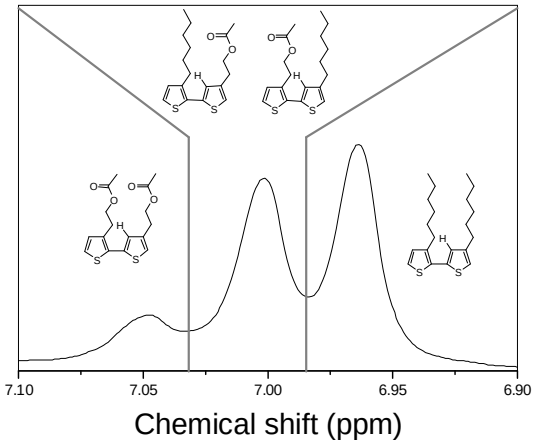

Figure 1: Three aromatic signals in the ^{1}H-NMR spectrum of the **P1** 7/3 copolymer in $CDCl_3$ due to the four different dyads with indicated molecular structures. Integration of the indicated regions gives an integral ratio that very well corresponds to that for a random copolymer (0.09/0.42/0.49)

2.2.3 UV-Vis absorption spectroscopy

The UV-Vis absorption spectra of the polymers were obtained from thin films drop-cast from a $CHCl_3$ solution on a quartz disk (**Figure 2**). For **P1**, no major change in absorption was observed, the wavelength of maximum

absorption was maintained at λ = 555 nm. Except for the **P1** 1/1 copolymer, the shoulder at λ = 605 nm was less pronounced compared to P3HT. The intensity of the absorption at 600 nm relative to the intensity at the maximum absorption at 550 nm is indicative for order in the system.[58] Here, the relative decrease of absorption at 600 nm indicates a loss of structural order. This can be explained if the presence of ester functionalized alkyl side chains prevent partially the π-π stacking of the conjugated back-bone, this leads to less crystalline order in the solid state. For **P2**, the effect of the presence of the ester functionalized alkyl side chains on crystalline order is stronger, because the functionalized side chains have a larger molar volume as compared to the functionalized side chains in **P1**. For the **P2** 9/1 copolymer however, a stronger absorption at λ = 605 nm was observed as compared to P3HT, while for the **P2** 7/3 and **P2** 1/1 copolymer, the shoulder is less pronounced. The same trends were observed in copolymer:PCBM (1:1) blends.[51]

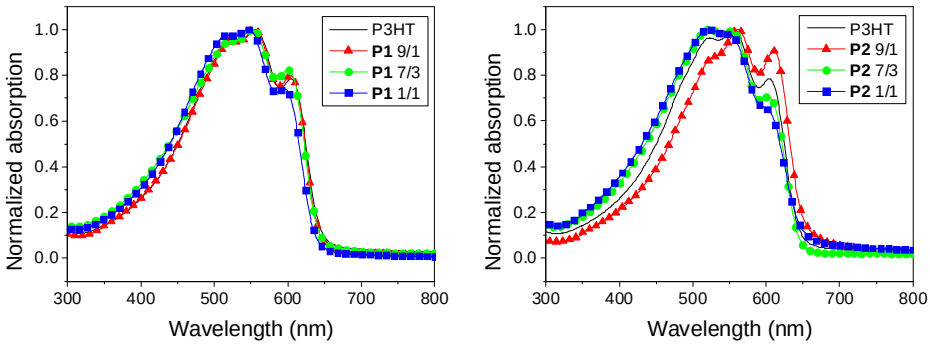

Figure 2: UV-Vis absorption of polymer compounds in films drop-cast from solution in $CHCl_3$. Absorption is normalized at wavelength of maximal absorption (λmax)

2.2.4 Thermal characterization

For both copolymers, the melting temperature (T_m) and the melting enthalpy (ΔH_m) were measured with Differential Scanning Calorimetry (DSC), while glass transition temperatures (T_g) were measured with Modulated Temperature DSC (MTDSC). For **P1**, the introduction of side-chain functionalization causes an increase of T_g: for **P1** 1/1 T_g is almost 50°C higher than for P3HT. (**Table 2**)

Table 2: Polymer **P1** and **P2** thermal characterization and hole mobility measured in organic field effect transistors, see § 2.2.6 (OFET)

Polymer	T_g [°C] [a]	T_m [°C] [b]	ΔH_m [J g^{-1}] [c]	μ [$m^2V^{-1}s^{-1}$]
P3HT	-15 ± 6	231 ± 1	22.9 ± 1.0	$1.3\ 10^{-3} \pm 3\ 10^{-4}$
P1 9/1	-10 ± 10	233 ± 1	18.5 ± 1.0	$4.4\ 10^{-4} \pm 2\ 10^{-4}$
P1 7/3	21 ± 6	238 ± 1	17.5 ± 0.5	$2.5\ 10^{-4} \pm 1.5\ 10^{-4}$
P1 1/1	33 ± 1	224 ± 2	14.8 ± 1.0	$2.0\ 10^{-4} \pm 1\ 10^{-4}$
P2 9/1	-20 ± 6	220 ± 1	20.5 ± 1.0	$1.4\ 10^{-4} \pm 3\ 10^{-5}$
P2 7/3	4 ± 6	189 ± 1	10.6 ± 0.5	$1.0\ 10^{-4} \pm 1\ 10^{-5}$
P2 1/1	-4 ± 2	179 ± 1	9.1 ± 0.5	$1.3\ 10^{-5} \pm 2.\ 10^{-6}$

[a] Glass transition temperature Tg measured by MTDSC and DSC and estimated error; [b] melting temperature Tm and [c] melting enthalpy ΔHm measured by DSC and estimated errors

For **P2**, T_g also shows an overall increasing trend with a higher amount of functionalized side chains, but the total change is less than 20°C. Also the melting behavior was affected by the introduction of functionalized side chains. For **P2**, the introduction of functionalized side chains caused a marked decrease in T_m (more than 50°C lower for **P2** 1/1 compared to

P3HT). In contrast, for **P1**, much smaller changes in T_m were observed: compared to P3HT T_m augmented ca. 7°C for **P1** 7/3 and dropped ca. 7°C for **P1** 1/1. In general, also the melting enthalpy ΔH_m was lower for both copolymers **P1** and **P2**. The effect of introduction of functionalized side chains was stronger in **P2**. The effect of the larger ester functionalized side chain on the polymer crystallinity was higher with a higher degree of functionalization. The decrease in melting temperature and enthalpy are indicative for a less perfect (less stable) crystalline ordering.

2.2.5 X Ray Diffraction (XRD) and Selected Area Electron Diffraction (SAED)

Thermal characterization and UV-Vis absorption spectra indicate that the crystalline fraction of the polymer decreased and that crystal formation was disturbed by introduction of functionalized side chains. To verify the impact of ester functionalized side chains on polymer structure, X Ray Diffraction (XRD) en Selected Area Electron Diffraction (SAED) patterns were recorded for the **P1** and **P2** 1/1 copolymer films (**Figure 3**), and compared with those of a P3HT film. All films were spin-coated from solutions in CB and annealed for 15 minutes at 125 °C. The Miller indices (*hkl*) are correlated with the parameters (*abc*) of the unity cell and correspond in a P3HT lattice to the dimensions of stacking of the polymer chains. In the setup which was used for XRD, the (*100*) diffraction peak was detected at 2 θ = 5.36°, corresponding to an interlamellar distance of d = 16.5 Å, which is comparable to the values found in literature for P3HT.[12] No diffractions of other lattice planes were observed in XRD, X-rays are scattered only at planes parallel to the substrate surface, this corresponds to the lamellar polymer stacking in the *a*-direction. The interlamellar distance increased to d = 19.0 Å by the introduction of the larger functionalized side chains in

copolymer **P2**. For copolymer **P1**, containing smaller functionalized side chains, this distance decreased to d = 15.4 Å. With Transmission Electron Microscopy (TEM), a SAED pattern was recorded. From the SAED an average π-π stacking distance of 3.8 Å was observed. In the TEM setup, the diffraction originates from planes stacked in the [*020*] direction along the *b* axis, perpendicular to the substrate surface.[59] For both 1/1 copolymers it was visible in the SAED that the π-π stacking distance remains at 3.8 Å, similar to P3HT. The peak at 3.8 Å is still well visible for **P1** but is less intense for a **P2** film. The effect of the larger functionalized side chains in **P2** on the crystalline π-π stacking in the *b* direction is stronger. For the **P1** and **P2** 1/1 copolymers, containing 50 % of functionalized side chains, XRD and TEM measurements confirmed that the crystalline structure was influenced by the introduction of functionalized side chains. The observations in UV-Vis, DSC, XRD and TEM all point to a relation between the size of the introduced side chain functionality and the effect on the crystallization behavior and crystalline structure in the copolymers.

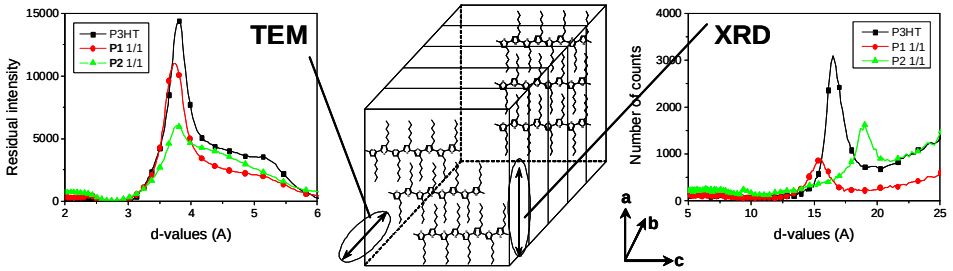

Figure 3: TEM (left) and XRD (right) diffraction patterns of P3HT (squares), **P1** 1/1 (circles) and **P2** 1/1 (triangles) polymer films, spin-coated from chlorobenzene solution on Si(100)/SiO2 substrates

2.2.6 Preparation of Organic Field Effect Transistors (OFETs) and hole mobility measurements

Organic Field Effect Transistors (OFET)s were made on bottom gate, bottom contact FET structures built on a highly n-doped Si wafer with a bare, untreated SiO_2 dielectric (204 nm thick). Gold (100 nm) on top of titanium (10 nm) electrodes were used for source and drain electrodes. Polymer layers were spincoated from solution in chlorobenzene and annealed for 15 minutes at 125°C. For each polymer, the mobility was measured for at least 4 different channels with a length varying from 20 µm to 40 µm, the channel width was 10 mm or 20 mm. For every measured channel, from the saturation and linear regimes the output characteristics were determined. (**Supporting Figure 5**) The obtained curves were typical for a p-channel in accumulation mode. Mobility measurements were performed in the linear regime. The source drain current is given by equation 1, where *W* is the channel width, L the channel length, C_0 the capacitance per unit area of the dielectric layer (C_0 = 16.9 nF cm^{-2}), R_{serial} the serial resistance including needle gold electrode contact resistance and gold polymer contact resistance and V_G, V_T, V_D are the gate, threshold and drain voltages respectively.

$$I = \frac{WC_0}{L}\mu(V_G - V_T)(V_D - IR_{serial}) \quad (1)$$

The field-effect hole mobility (μ_h) of regioregular P3HT measured in these devices from films spincoated from solutions in chlorobenzene was around 1.3 10^{-3} $cm^2V^{-1}s^{-1}$, comparable to literature values.[60] For the copolymers, lower mobilities than for P3HT were measured (Table 2). For the **P1** copolymers with different x/y ratio, the observed mobility was in the same order of magnitude. For the copolymers with three different percentages of functionalized side chains, μ_h was in the order of 10^{-4} $cm^2V^{-1}s^{-1}$. Compared

to P3HT, μ_h decreased also in **P2** with an order of magnitude to 10^{-4} $cm^2V^{-1}s^{-1}$ for the 9/1 and 7/3 copolymers and even to 10^{-5} $cm^2V^{-1}s^{-1}$ in the 1/1 copolymer. Comparing the mobility of **P1** to **P2** (**Figure 4**), the influence of the introduced side chains on μ_h depends on the ratio and nature of the introduced functional groups. Generally, the presence of 10% of functionalized alkyl side chains causes an order of magnitude decrease in μ_h compared to P3HT. A higher percentage of smaller side chain functionalities in **P1** proves to have limited impact, while the influence of higher ratios of functionalities on larger side chains in copolymer **P2** 1/1 is quite strong and decreases μ_h further.

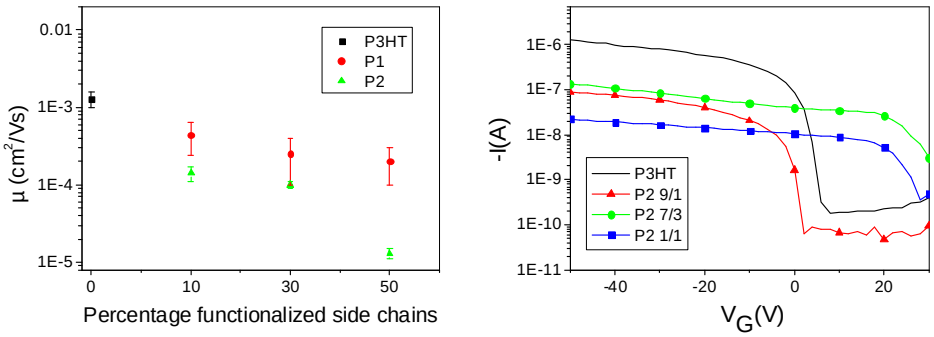

Figure 4: FET hole mobility of copolymers **P1** and **P2** as a function of the percentage of functionalized side chains (left) and transfer channels of P3HT and **P2** (right).

2.3 Application in organic photovoltaic devices

The various copolymers were evaluated in BHJSCs using a (1:1) (w/w) blend with the copolymer as electron donor and [6,6]-phenyl-C_{61}-butyric acid methyl ester (PCBM) as an electron acceptor. P3HT obtained from Rieke metals was used to prepare a P3HT:PCBM solar cell which served as a reference. All devices were made by spin-coating first a 50 nm

poly(ethylenedioxythiophene): poly(styrenesulfonate) (PEDOT:PSS) solution on ITO-patterned glass substrates. The 1:1 blend was spin-coated from a solution of 15 mg ml^{-1} polymer in chlorobenzene that contained 25 mg ml^{-1} 1,8-dibromooctane (DBO). Several spinning speeds were used to investigate the influence of layer thickness on solar cell performance. The procedure with DBO was adopted, since thermal annealing of copolymer devices resulted in low fill factors. Annealing of the copolymer blends caused an intimately mixed morphology which is insufficiently phase-separated, triggering charge recombination. By spin-coating the blends from solutions with DBO, it was possible to obtain the desired morphology with sufficient phase separation and good fill factors without post-production thermal annealing.

For the best devices based on each copolymer, the external quantum efficiency (*EQE*) was measured to estimate the short circuit current after convolution with the AM1.5G spectrum. Together with the open-circuit voltage (V_{oc}) and fill factor (*FF*) determined by the J-V curve, the overall efficiency was assessed. (Table 3) *J-V* curves and *EQE* of the solar cells with highest performance are displayed in **Figure 5** and **Figure 6** for the **P1** and **P2** copolymers respectively. The layer thickness of the best devices was usually around 80 nm. The evolution of short circuit current (J_{sc}) with layer thickness was comparable to how the J_{sc} in P3HT:PCBM devices evolves with layer thickness.[61] (Supporting Figure 1 and 2) The **P1**:PCBM solar cells had a *FF* of 0.62 and higher. With copolymer **P2**, fill factors of 0.55 and higher were observed.

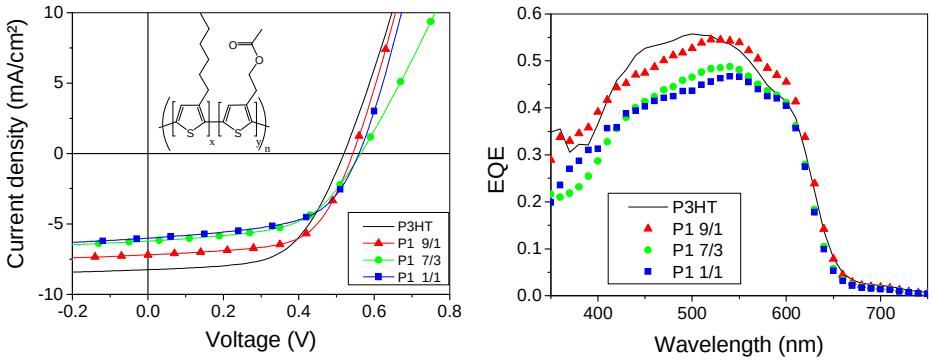

Figure 5: J-V curves and EQE of solar cells with copolymer **P1**:PCBM (1:1) blends spin-coated from 15 mg mL^{-1} polymer solution in CB with 25 mg mL^{-1} DBO

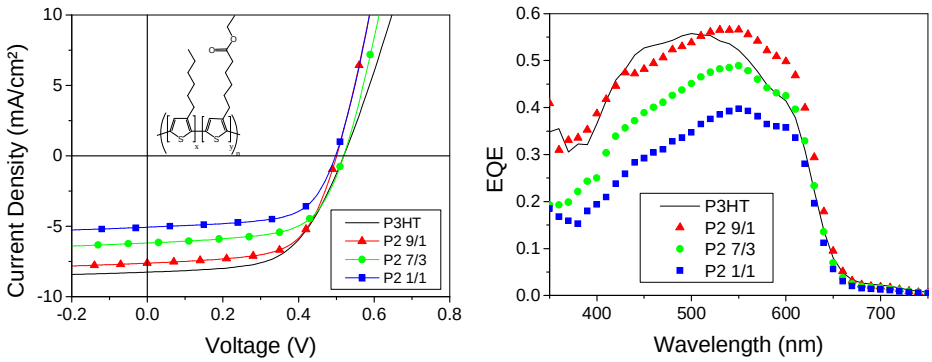

Figure 6: J-V curves and EQE of solar cells made with copolymers **P2**:PCBM (1:1) blends spin-coated from 15 mg mL^{-1} polymer solution in CB with 25 mg mL^{-1} DBO

The V_{oc} of the solar cells produced with DBO as co-solvent was lower compared to the devices produced by thermal annealing (5 minutes at 140 °C), as illustrated for the P3HT:PCBM solar cell in **Table 3**. The difference in V_{oc} caused lower device efficiencies compared to the P3HT:PCBM devices produced with thermal annealing. The presence of the co-solvent in the spin-coating solution allows the polymers to self-organize before evaporation of the co-solvent takes place.[20, 21] This results in increased order from blends spin-coated with DBO, as was also observed in UV-Vis

absorption spectra of copolymer:PCBM (1:1) blends.[51] A higher degree of crystallinity raises the HOMO of the polymer, thus lowering V_{oc}, since the latter is determined by the difference between the HOMO of the donor and the LUMO of the acceptor.[61] A lower V_{oc} has been reported previously for devices with an increasingly organized polymer phase.[62] The V_{oc} increases moderately with a higher mole percentage of functionalized side chains, since the presence of the functionalized side chains interferes with the π-π stacking.

Table 3: Device characteristics of ITO/PEDOT:PSS/polymer:PCBM (1:1)/LiF/Al solar cells. Blends were spin-coated from 1.5 wt % solution in chlorobenzene that contained 2.5 wt % 1,8-dibromooctane. The J_{sc} displayed here was corrected to AM 1.5 conditions from the spectral response and convolution with the solar spectrum.

Polymer	(x/y)	J_{sc} [mA/cm²]	V_{oc} [V]	*FF*	**PCE [%]**	Layer thickness [nm]
P3HT*		7.49	0.65	0.62	**3.00**	81
P3HT		7.44	0.52	0.58	**2.24**	82
P1	9/1	7.43	0.54	0.62	**2.49**	74
P1	7/3	6.40	0.56	0.55	**1.98**	90
P1	1/1	6.25	0.56	0.57	**1.97**	71
P2	9/1	7.85	0.50	0.62	**2.43**	71
P2	7/3	6.60	0.52	0.62	**2.13**	82
P2	1/1	5.11	0.50	0.63	**1.61**	78

*: blend processed without DBO, annealed 5 min at 140°C.

Solar cells made with copolymers are less efficient than P3HT:PCBM solar cells produced with thermal annealing. (Table 3) However, when comparing devices produced in an identical manner, with DBO as a co-solvent, the solar cell efficiencies for the **P1** and **P2** 9/1 copolymers are better than for P3HT. The increased performance, despite the lower μ_h, could be due to a slightly more beneficial morphology. The **P1** and **P2** 9/1 maximum *EQE* and J_{sc} are comparable to the reference P3HT:PCBM cell. A higher percentage of functionalized side chains decreased the *EQE* and J_{sc} and therefore also the efficiency, but the performance was not as strongly influenced in **P1** as the performance of solar cells in the **P2** copolymer series was affected. It is noteworthy that the decrease in J_{sc} from the **P1** 7/3 to the 1/1 copolymer is quite small and therefore the efficiency was not influenced strongly, either. The π-π stacking of the polymer is influenced moderately in the **P1** series, as was visible in UV-Vis, thermal and structural analysis, and mobility measurements. The **P1** series exhibited a higher efficiency for higher functionalization ratios compared to **P2**, with efficiencies of 2 % for copolymers containing 50 % of ester functionalized side chains. Devices with **P2** 9/1 show a remarkable increase in J_{sc} compared to the P3HT:PCBM reference cell processed in the same conditions. However, for solar cells made from **P2**, the J_{sc} decreased more strongly with increasing functionalization ratio (Figure 6), resulting in lower device performance. At higher functionalization ratios, the hole mobility of **P2** copolymers is low because of a decreasing structural order and π-π stacking of the copolymer conjugated backbones. Functional side chains with a larger molar volume have a stronger disturbing effect on polymer structure, causing a larger effect in device performance for higher degrees of functionalization, as was observed for the **P2** copolymers compared to **P1**.

The *EQE* and J_{sc} decrease when copolymers with a higher ratio of ester groups in the side chains are used, due to the stronger impact on the polymer organization with an increasing percentage of functionalized side chains. This observation was also made in UV-Vis spectroscopy (relative decrease at 600 nm), thermal characterization (lower T_m and ΔH_m), XRD and TEM (impact on polymer crystalline structure) and was reflected in lower field effect mobilies and now in the performance of the BHJSC. The observed decrease in *EQE* and J_{sc} with an increasing percentage of functionalized side chain is due to a hindering of the π-π stacking of the conjugated polymer backbone caused by the presence of the ester functionalized side chains.

In general, an increasing ratio of ester functions in the polymer side chains caused a decrease in J_{sc}, and had little effect on the V_{oc} and *FF*. The effect of a functional group in the side chain of the polymer structure on the electronic properties originates mainly from the effect on the polymer stacking. A planar conjugated backbone of a regioregular polymer allows the crystalline stacking along this plane. This self-organized π–π stacking is very important for the properties of conjugated polymers. In one chain (intrachain) a more planar backbone extends the aromatic system and between different polymer chains (interchain) this facilitates the hopping mechanism of charges, hence the relation with the hole mobility. From the optical and thermal characterization comes forward that the π-π stacking is not only important for the electronic properties, but is also determining for the optical absorption and the thermal properties of the conjugated polymers. As was visible in the UV-Vis spectra of copolymers **P1** and **P2**, the shoulder at λ = 600 nm decreased more for the **P2** copolymer series, where the disturbance of the π-π stacking increased for a higher degree of functionalization. Although the effect of a differing molecular weight and

regioregularity cannot be ruled out in this consideration, we also observed a stronger decrease in T_m and ΔH_m with an increasing percentage of functionalized side chains for the **P2** copolymers, compared to the **P1** series. In a BHJSC device, a relatively high amount of small side chain functionalities disturbs the π-π stacking minimally: the efficiency of the **P1** 1/1 copolymer was about 2.0% for a 80 nm thick layer. From this we derive that a functional group that does not interfere with the π-π stacking in the conjugated backbone, may be introduced in the polymer side chains in relatively high amounts with a limited influence on hole mobility and performance in the BHJSC using the right processing conditions.

3. Conclusion

The synthesis of regioregular ester-functionalized P3HT-based copolymers **P1** and **P2** succeeded using the Rieke method. Copolymers with 10, 30 and 50 mol% of ester-functionalized side chains were obtained. The ratio of ester-functionalized units in the copolymers corresponds to the ratio of ester monomers present in the starting monomer mixture that was used for copolymerization. The overall yield of the polymerization reaction decreases with an increasing content of ester-functionalized monomer in the monomer mixture. With a higher percentage of functionalized side chains the regioregularity decreases in the two types of copolymers, while the molecular weight decreases for **P1** and increases for **P2**. When smaller functionalized side chains were introduced, the self-organisation and the π-π stacking of the conjugated backbones was disturbed less. Therefore, thermal properties, the hole mobility, absorption characteristics and also the J_{sc} and efficiency in solar cells depend less on the percentage of side chains in acetoxyester-functionalized copolymer **P1** as they do for ethylester-

functionalized side chains in **P2**. In bulk heterojunction solar cells, both the **P1** and **P2** 9/1 copolymers show better power efficiency compared to a P3HT:PCBM solar cell produced in the same conditions. For copolymers with more than 10% of functionalized side chains, a decrease in external quantum efficiency and short circuit current was observed. This is because of the less perfect crystalline structure and a lower content of crystalline regions in the polymer phase and the resulting decrease in hole mobility, since the stacking of the conjugated polymer backbone is influenced by the presence of the functionalized side chains. The presented method allows the introduction of functionalized alkyl side chains in P3HT copolymers in low percentages (up to 10%) without significantly disturbing the efficiency of these materials in bulk heterojunction solar cells.

4. Experimental

Experimental details: All chemicals were used as obtained from commercial sources (Aldrich or Acros), unless stated otherwise. THF and diethylether were dried by refluxing with sodium wire and benzophenone until a blue colour appeared and freshly distilled before use. 3-Bromothiophene was distilled. ^{1}H-NMR spectra were recorded on a Varian Inova 300 spectrometer at 300MHz using a 5 mm probe. Deuterated $CHCl_3$ was obtained from Cambridge Isotope Laboratories. Chemical shifts are reported in ppm downfield from tetramethylsilane (TMS) using the peak of residual $CHCl_3$ as an internal standard at δ=7.24 ppm. Methylene protons in the side chains are assigned a symbol starting with α from the polymer backbone. If resolution was insufficient to determine the multiplicity of a signal, it was assigned as a multiplet (m). Fourier-transform infrared spectroscopy (FT-IR) was performed on a Perkin Elmer Spectrum One FT-

IR spectrometer using KBr pellets or films drop-cast on a quartz disk from a $CHCl_3$ solution. Gas chromatography/mass spectrometry (GC-MS) was carried out on TSQ-70 and Voyager mass spectrometers. UV-Vis spectra were recorded on a Varian CARY 500 UV-Vis-NIR spectrophotometer from 200 to 800 nm at a scan rate of 600 nm min^{-1}. Size exclusion chromatography (SEC) was done with a 1 mg mL^{-1} polymer solution in THF, which was filtered with a 0.45 µm pore PTFE syringe filter. A Spectra Physics P100 pump equipped with two mixed-B columns (10 µm, 30 cm x 7.5 mm), Polymer Labs and a Shodex refractive index detector at 40°C in THF at a flow rate of 1.0 mL min^{-1} were used. Molecular weight distributions were measured relative to polystyrene standards. Toluene was used as a flow rate marker.

Differential scanning calorimetry (DSC) was done to measure the melting temperature (T_m) and melting enthalpy (ΔH_m) on a TA Instruments Q2000 (Tzero^{TM}) with Refrigerator Cooling System (RCS) and nitrogen 50 mL min^{-1}, aluminum Tzero crucible at a scan rate of 10.0 K min^{-1}. The glass transition temperature (T_g) was determined with modulated temperature differential scanning calorimetry (MTDSC). Samples were quenched at 100 K min^{-1} from an upper limit temperature of 275.0 °C. Then they were heated at a rate of 2.5 K min^{-1} with a modulation of ± 0.5 K per 60 s. For DSC, the 1st cooling and 2nd heating run were used, and for MTDSC, the heating after quenching was used for discussion.

Polymer layers for XRD and TEM were spin-coated from solution in chlorobenzene on a Silicon substrate, which was cleaned by rubbing and sonicating for 30 minutes in soapy water, rinsing and sonicating in acetone for 10 minutes and heating in isopropanol. For the TEM measurements, the film was isolated by etching with 40 % hydrofluoric acid (HF) to remove

the silicon substrate and then put on a copper TEM-grid (*caution*: HF is highly toxic!). TEM-measurements were performed on a FEI Tecnai G2 Spirit Twin operating at 120 kV. The SAED patterns, recorded through TEM, originally suffered from a large background that resembled inelastic scattering. To improve the signal-to-noise ratio, integration across the complete diffraction ring was done, from which a fitted background due to inelastic scattering was subtracted (with the assumption that the film in between the crystalline P3HT is quasi-amorphous [63]. XRD measurements were done on a Siemens D5000 diffractometer in θ-2 θ mode. The incident beam used is the CuKα1 line of a Ge(111) monochromator, with a λ = 0.154056 nm.

Substrate for Organic Field Effect Transistors (OFET)s were cleaned (20 minutes ultrasonic bath in soap, 10 minutes ultrasonic bath in acetone, 10 minutes in hot isopropanol), then 15 minutes of a UV/O_3 treatment removed the hexamethylenedisilane (HMDS) monolayer from the substrate. The polymer layers were spin-coated for 60 s at 1000 rpm from a 10 mg mL^{-1} solution in CB. The samples were annealed for 15 min at 125 °C on a hotplate and allowed to cool down to room temperature during 5 minutes. The current-voltage characteristics were measured using 2 Keithley 2400 source meters. All FET preparation and measurements were performed under N_2 atmosphere.

Solar cells were made on glass slides with a pattern of ITO electrodes. The glass substrates were sonicated in acetone, cleaned with soapy water and isopropanol and treated with UV/O_3. Typically, 50 nm PEDOT: PSS (Clevios™ P VP AI 4083, HC Starck) was spin-coated at 3000rpm on the glass substrate. A 15 mg mL^{-1} solution of PCBM in a dibromooctane (DBO, 25 mg mL^{-1})/chlorobenzene solution was added to the polymer in a (1:1)

ratio and stirred at 50 °C until the polymer dissolved completely. The blend solution was spin-coated at several spinning speeds to investigate the influence of active layer thickness. The preparation of P3HT:PCBM solar cells was done with P3HT obtained from Rieke Metals. 1 nm of LiF and 100 nm of Al were thermally evaporated in high vacuum ($p = 10^{-7}$ mbar). J-V curves were measured under simulated solar light (100 mW cm^{-2}) from a tungsten-halogen lamp filtered by a Schott GG385 UV filter and a Hoya LB120 daylight filter using a Keithley 2400 source meter. Spectral response was measured with monochromatic light from a 50 W tungsten halogen lamp (Philips focusline) in combination with a monochromator (Oriel, Cornerstone 130) and a lock-in amplifier (Stanford research Systems SR830). A calibrated Si cell was used as reference. The device was kept behind a quartz window in a nitrogen filled container. To measure the cell under appropriate operation conditions, the cell was illuminated by a bias light from a 532 nm solid state laser (Edmund Optics).

Monomer synthesis: 3-Hexylthiophene (3-HT) was obtained from reaction of 100 mL (166.0 g, 1.018 mol) 3-bromothiophene (3-BT) and 1.2 Equivalent (0.611 L of a 2.0M solution in Et_2O, 1.22 mol) hexylmagnesiumbromide, in the presence 0.01 equiv of Ni(dppp)Cl_2 (5.19 g, 0.010 mol) in dry diethylether (300 mL). The reaction was performed according to literature procedures [54]. The purified compound was obtained by short path distillation in a yield of 95.6 % (163.73 g, 0.973 mol) at p= 7.10^{-3} mbar and T= 81-84 °C.

2,5-dibromo-3-hexylthiophene (**M1**) was obtained from reaction of NBS (2.2 equiv, 23.26 g, 130 mmol) and 3-HT (10g, 59 mmol) in a yield of 81% (15.50 g, 48 mmol) following literature procedures [55].

2,5-dibromo-3-(2-hydroxyethyl)thiophene was obtained by dibromination of 3-(2-hydroxyethyl)thiophene using NBS. A similar procedure as for the bromination of 3-HT was applied.[55] The resulting liquid was purified using a short path distillation to a yellow oil yield (18.66 g, 73.5 mmol, 95% yield) (fraction at p = 4.10^{-3} mbar, T = 107°C). ^{1}H NMR (300 MHz, $CDCl_3$, δ): 6.85 (s, 1H, Ar H), 3.78 (m, 2 H, CH_2-O), 2.78 (m, 2H, α CH_2), 1.65 (*br* s, 1 H, OH) ^{13}C NMR (75 MHz, $CDCl_3$, δ): 139.0 131.2 110.7 109.3 61.5 32.2 8 GC/MS (99%), *m/z* 288, 286, 284 $[M]^+$ 257, 255, 253 $[M - CH_2OH]^+$ 207, 205 $[M - Br]^+$ 175, 177 $[M – Br, CH_2OH]^+$ 125 $[M – 2Br]^+$ 95 $[M – 2Br, CH_2OH]^+$. FT-IR (film, *v*, cm^{-1}): 3325 *br*, 2951, 2926, 2879, 1668, 1542, 1470, 1417, 1348, 1244, 1196, 1044, 1002, 976, 927, 892, 824

2-(2,5-dibromothiophen-3-yl)ethyl acetate (**M2**) was obtained by reaction of 2-(2,5-dibromothiophen-3-yl)ethanol (36.2 g, 42.6 mmol) with 1.3 equiv acetic anhydride (185 mmol, 18.93 g) and an excess of pyridine [24]. The acquired product was purified with short path distillation to isolate **M2** (36.2g, 113 mmol, 78%) at p = 1.10^{-3} mbar and T = 95°C. ^{1}H NMR (300 MHz, $CDCl_3$, δ): 6.79 (s, 1H, Ar H), 4.17 (t, 2 H, CH_2-O, *J* = 6.7 Hz), 2.82 (t, 2H, α-CH_2, *J* = 6.7 Hz), 2.02 (s, 3 H, CH_3); ^{13}C NMR (75 MHz, $CDCl_3$, δ): 170.7, 138.1, 130.8, 110.7, 109.6, 62.8, 28.7, 20.8; GC/MS 97%, *m/z* 330,328,326 $[M]^+$ 271, 269, 267 $[M - OCOCH_3]^+$ 257, 255, 253 $[M – CH_2OC(O)CH_3]^+$ 205, 207 $[M – Br]^+$ 187,189 $[M – Br, OCOCH_3]^+$ 176, 174 $[M- Br, CH_2OC(O)CH_3]^+$ 108 $[M- 2Br, CH_2OC(O)CH_3]^+$, 95 $[M – 2Br, CH_2CH_2OC(O)CH_3]^+$. FT-IR (film, *v*, cm^{-1}): 3093, 2957, 1740 (vs), 1543, 1421, 1385, 1364, 1236 (vs), 1040, 1004, 936, 825, 883, 828

6-(thiophene-3-yl)hexanoic acid ethyl ester was obtained from addition of 6-bromo-hexanoic acid ethyl ester (20 g, 89.6 mmol) to active zinc and reaction with 3-BT (16.81 g, 103.1 mmol).[50, 56] 6-(thiophene-3-yl)hexanoic

acid ethyl ester was obtained with short path distillation at 72 °C and 1.10^{-3} mbar.^{1}H NMR (300 MHz, $CDCl_3$, δ): 7.20(m, 1H, Ar H), 6.90 (m, 2H, Ar H), 4.10 (q, 2H, O-CH_2, *J* = 7.5 Hz), 2.62 (t, 2H, α CH_2, *J* = 7.5 Hz), 2.28 (t, 2H, β-CH_2, *J* = 7.5 Hz), 1.63 (m, 4H, 2 CH_2), 1.38 (m, 2H, CH_2), 1.23 (t, 3H, CH_3, *J* = 7.1 Hz); ^{13}C NMR (75 MHz, $CDCl_3$, δ): 173.4, 142.4, 127.8, 124.8, 119.6, 59.8, 33.9, 29.8, 29.6, 28.4, 24.4, 13.8; GC/MS (95%) m/z: 226 $[M]^+$, 181 $[M- OCH_2CH_3]^+$, 153 $[M – C(O)OCH_2CH_3]^+$, 139 $[M – CH_2C(O)OCH_2CH_3]^+$, 125 $[M – (CH_2)_2C(O)OCH_2CH_3]^+$, 111 $[M-(CH_2)_3C(O)OCH_2CH_3]^+$, 97 $[M- (CH_2)_4C(O)OCH_2CH_3]^+$. FT-IR (film, *v*, cm^{-1}): 3104, 2980, 2934, 2858, 1733 (vs), 1537, 1463, 1372, 1299, 1252, 1181, 1130, 1096, 1032, 859, 833, 773

6-(2-5-dibromothiophene-3-yl)hexanoic acid ethyl ester (**M3**) was isolated after bromination with NBS [55] and distillation (p=1.10-3 mbar, 126°C). ^{1}H NMR (300 MHz, $CDCl_3$, δ): 6.78 (s, 1 H, Ar H), 4.08 (m, 2H, O-CH_2), 2.48 (t, 2H, ε-CH_2, *J* = 7.7 Hz), 2.26 (t, 2H, α-CH_2, *J* = 7.4 Hz), 1.62 (m, 2H, δ-CH_2), 1.53 (m, 2H, β-CH_2), 1.32 (m, 2H, γ-CH_2), 1.22 (t, 3H,CH_3, *J* = 7.1 Hz) ^{13}C NMR (75 MHz, $CDCl_3$, δ): 173.5, 142.4, 130.7, 110.3, 107.9, 60.1, 34.0, 29.0, 28.3, 24.5, 14.1; GC/MS (98%)m/z: 386, 384, 382 $[M]^+$; 341, 339, 337 $[M- OCH_2CH_3]^+$; 306, 304 $[M – Br]^+$; 257 $[M – (CH_2)_3OCH_2CH_3]^+$; 231 $[M – Br,C(O)OCH_2CH_3]^+$; 215 $[M- Br, CH_2C(O)OCH_2CH_3]^+$; 177 $[M - Br, (CH_2)_3C(O)OCH_2CH_3]^+$, 149 $[M- 2Br, (CH_2)_4C(O)OCH_2CH_3]^+$, 135 $[M- 2Br, CH_2C(O)OCH_2CH_3]^+$, 122 $[M- 2Br, (CH_2)_2C(O)OCH_2CH_3]^+$, 95 $[M- 2Br, (CH_2)_4C(O)OCH_2CH_3]^+$. FT-IR (film, *v*, cm^{-1}): 3090, 2979, 2937, 2858, 1733 (vs), 1542, 1462, 1420, 1372, 1301, 1248, 1180, 1132, 1096, 1032, 1005, 921, 857, 826, 733

Polymer synthesis: The copolymerization reaction was performed according to literature procedures [39]. Mixtures of brominated monomers were made in several molar ratios (9/1, 7/3, 1/1). Respectively 29, 25 and 20 mmol (9.41, 8.12 and 6.49 g) of **M1** and 3, 11, 20 mmol (1.05, 3.49 and 6.50 g) of **M2** were dissolved in dry THF under Ar atmosphere. These solutions were added to active Zinc at -78 °C. Solutions of 0.002 equiv Ni(dppp)Cl_2 in THF were added to the obtained organozinc solutions, and stirred under inert atmosphere at 60 °C for 18 h. The crude polymers were precipitated in a MeOH/ 2 M HCl (2/1, v/v) mixture and purified by Soxhlet extractions with methanol, hexane and acetone, subsequently. The purified polymers were extracted with chloroform and precipitated in MeOH before filtration and isolation of copolymers **P1**.

P1 9/1 (3.18 g, 60%) UV-Vis (film, λ_{max}, nm) 551, 600sh; FT-IR (KBr, *v*, cm^{-1}): 2954, 2930 and 2853 (s, C-H), 1744 (C=O), 1509 and 1456 (C=C), 1378 (CH_3), 1236, 1035 and 820 (C-H), 723 (CH_3) ^{1}H NMR (300 MHz, $CDCl_3$, δ): 7.00 and 6.96 (1H, s, Ar H), 4.36 (2H *M2*, t, β-CH_2), 3.14 (2H *M2*, t, α-CH_2), 2.79 (2H, t, H-T α-CH_2), 2.58 (2H, H-H α-CH_2), 2.05 (3H *M2*, s, CH_3), 1.70 (2 H, m, CH_2), 1.45 – 1.34 (6 H, m, γ, δ, ε-CH_2), 0.90 (3 H, t, CH_3). **P1 7/3** (3.0 g, 52%) UV-Vis (film, λ_{max}, nm) 547, 595sh; FT-IR (KBr, *v*, cm^{-1}): 2953, 2925 and 2855 (C-H), 1743 (C=O), 1509 and 1456 (C=C), 1376 (CH_3), 1363, 1234, 1037, 821 (C-H) ^{1}H NMR (300 MHz, $CDCl_3$, δ): 7.05, 7.0 and 6.96 (1H, m, Th), 4.35 (2H *M2*, br s, β-CH_2), 3.10 (2H *M2*, br s, α-CH_2), 2.78 (2H, t, H-T α-CH_2), 2.54 (2H, br s, H-H α-CH_2), 2.06 (3H *M2*, s, CH_3), 1.69 – 1.23 (8 H, m, β, γ, δ and ε-CH_2), 0.89 (3 H, s, CH_3). **P1 1/1** (2.98 g, 51%) λ_{max} (film)/nm 547, 595sh; FT-IR (KBr, *v*, cm^{-1}): 3431 (*br*, H_2O),2956, 2923 and 2853 (C-H), 1733 (C=O), 1632, 1455 (s, C=C), 1376 (CH_3), 1259, 1123, 1002, 867 ^{1}H NMR (300 MHz, $CDCl_3$, δ):

7.11, 7.06, 7.01 and 6.96 (1H, m, Th), 4.35 (2H *M2*, br s, β-CH_2), 3.10 (2H *M2*, br s, α-CH_2), 2.79 (2H, t, H-T α-CH_2), 2.56 (2H, br s, H-H α-CH_2), 2.06 (3H *M2*, s, CH_3), 1.70 – 1.23 (8 H, m, β, γ, δ and ε-CH_2), 0.89 (3 H, m, CH_3)

P2 was prepared using an analogue procedure as for **P1**. The dibrominated monomers **M1** and **M3** were mixed in several molar ratios. Respectively 26.8, 28 and 20.1 mmol **M1** (8.73, 9.13 and 6.55 g) were mixed with 3, 12 and 20.1 mmol of **M3** (1.14, 4.61 and 7.74 g) in a THF solution before applying the polymerization procedure.

P2 9/1 (3.77 g, 74%) λ_{max} (film)/nm 555, 602sh; FT-IR (film, *v*, cm^{-1}):3053, 2953, 2928 and 2854 (C-H), 1738 (C=O), 1563, 1509 and 1455 (C=C), 1376 (CH_3), 1260 (w), 1179 and 820 (C-H), 726 (CH_3) ^{1}H NMR (300 MHz, $CDCl_3$, δ): 6.96 (1H, s, Th), 4.10 (2H *M3*, q, OCH_2), 2.79 (2H, t, H-T α-CH_2), 2.56 (2H, s, H-H α-CH_2), 2.31 (2H *M3*, t, CH_2COOEt), 1.69 (2 H, br s, β-CH_2 and *M3*), 1.48 – 1.20 (10 H, m, γ, δ, ε-CH_2 and γ, δ CH_2 *M3*), 0.90 (6 H, t, CH_3 *M1* and *M3*). **P2 7/3** (4.51 g, 61.5%) λ_{max} (film)/nm 550, 600sh; FT-IR (film, *v*, cm^{-1}): 2926 and 2855 (C-H), 1736 (C=O), 1508 and 1458 (C=C), 1375 (CH_3), 1227, 1178 and 824 (C-H), 760 (CH_3) ^{1}H NMR (300 MHz, $CDCl_3$, δ): 6.96 (1H, s, Th), 4.10 (2H *M3*, q, OCH_2), 2.79 (2H, br s, H-T α-CH_2), 2.56 (2H, s, H-H α-CH_2), 2.31 (2H *M3*, t, CH_2COOEt), 1.69 (4 H, m, β-CH_2 *M1* and *M3*), 1.54 – 1.20 (10 H, m, γ, δ, ε-CH_2 and γ, δ-CH_2 *M3*), 0.89 (6 H, t, CH_3 *M1* and *M3*). **P2 1/1** (4.14 g, 53%) λ_{max} (film)/nm 550, 604sh; FT-IR (KBr, *v*, cm^{-1}):3432 (br, COOH), 2956 (C-H), 1733 (C=O), 1631 and 1454 (C=C), 1259, 1129, 1002 and 867 cm^{-1} (C-H), ^{1}H NMR (300 MHz, $CDCl_3$, δ): 6.96 (1H, s, Ar H), 4.10 (2H *M3*, q, OCH_2), 2.79 (2H, t, H-T α-CH_2), 2.54 (2H, H-H α-CH_2), 2.31 (2H *M3*, t,

CH_2COOEt), 1.69 (4 H, m, β-CH_2 *M1* and *M3*), 1.50 – 1.20 (10 H, m, γ, δ, ε-CH_2 *M1* and γ, δ-CH_2 *M3*), 0.87 (6 H, t, CH_3 *M1* and *M3*)

5. References

[1] N. S. Sariciftci, L. Smilowitz, A. J. Heeger, F. Wudl, *Science* 1992, 258, 1474.
[2] G. Yu, J. Gao, J. C. Hummelen, F. Wudl, A. J. Heeger, *Science* 1995, 270, 1789.
[3] C. J. Brabec, S. E. Shaheen, C. Winder, N. S. Sariciftci, P. Denk, *Appl. Phys. Lett*. 2002, 80, 1288.
[4] A. J. Moulé, J. B. Bonekamp, A. Ruhl, H. Klesper, K. Meerholz, *in Proceedings of SPIE*, 2005, 5938.
[5] S. E. Shaheen, C. J. Brabec, N. S. Sariciftci, F. Padinger, T. Fromherz, J. C. Hummelen, *Appl. Phys. Lett*. 2001, 78, 841.
[6] F. Padinger, R. S. Rittberger, N. S. Sariciftci, *Adv. Funct. Mater*. 2003, 13, 85.
[7] Y. Y. Liang, D. Q. Feng, Y. Wu, S. T. Tsai, G. Li, C. Ray, L. P. Yu, *J. Am. Chem. Soc.* 2009, 131, 7792.
[8] M. Reyes-Reyes, K. Kim, D. L. Carroll, *Appl. Phys. Lett.* 2005, 87, 083506.
[9] G. Li, V. Shrotriya, J. S. Huang, Y. Yao, T. Moriarty, K. Emery, Y. Yang, *Nat. Mater.* 2005, 4, 864.
[10] R. D. McCullough, *Adv. Mater*. 1998, 10, 93.
[11] I. Osaka, R. D. McCullough, *Acc. Chem. Res.* 2008, 41, 1202.
[12] R. D. Mccullough, S. Tristramnagle, S. P. Williams, R. D. Lowe, M. Jayaraman, *J. Am. Chem. Soc.* 1993, 115, 4910.
[13] C. H. Woo, B. C. Thompson, B. J. Kim, M. F. Toney, J. M. Fréchet, *J. Am. Chem. Soc.* 2008, 130, 16324.
[14] Y. Kim, S. Cook, S. M. Tuladhar, S. A. Choulis, J. Nelson, J. R. Durrant, D. D. C. Bradley, M. Giles, I. McCulloch, C. Ha, M. Ree, *Nat. Mater*. 2006, 5, 197.
[15] X. Yang, J. Loos, S. C. Veenstra, W. J. H. Verhees, M. M. Wienk, J. M. Kroon, M. A. J. Michels, R. A. J. Janssen, *Nano Lett.* 2005, 5, 579.
[16] J. K. J. van Duren, X. Yang, J. Loos, C. W. T. Bulle-Lieuwma, A. B. Sieval, J. C. Hummelen, R. A. J. Janssen, *Adv. Funct. Mater.* 2004, 14, 425.
[17] J.-F. Chang, B. Sun, D. W. Breiby, M. M. Nielsen, T. I. Sölling, M. Giles, I. McCulloch, H. Sirringhaus, *Chem. Mater.* 2004, 16, 4772.
[18] W. Ma, C. Yang, X. Gong, K. Lee, A. J. Heeger, *Adv. Funct. Mater.* 2005, 15, 1617.
[19] G. Li, Y. Yao, H. Yang, V. Shrotriya, G. Yang, Y. Yang, *Adv. Funct. Mater.* 2007, 17, 1636.
[20] Y. Yao, J. H. Hou, Z. Xu, G. Li, Y. Yang, *Adv. Funct. Mater.* 2008, 18, 1783.
[21] J. Peet, J. Y. Kim, N. E. Coates, W. L. Ma, D. Moses, A. J. Heeger, G. C. Bazan, *Nat. Mater.* 2007, 6, 497.
[22] V. M. Niemi, P. Knuuttila, J.-E. Österholm, L. Korvola, J. *Polymer* 1992, 33, 1559.
[23] C. Della Casa, E. Salatelli, F. Andreani, P. Costa-Bizarri, *Makromol. Chem. Makromol. Symp.* 1992, 59, 233.
[24] J. Lowe, S. Holdcroft, *Macromolecules* 1995, 28, 4608.
[25] C. Lee, K. J. Kim, S. B. Rhee, *Synth. Met.* 1995, 69, 295.
[26] T. J. J. M. Kock, B. de Ruiter, *Synth. Met.* 1996, 79, 215.

[27] S. C. Ng, P. Fu, W. L. Yu, H. S. O. Chan, K. L. Tan, *Synth. Met.* 1997, 87, 119.
[28] S. C. Ng, Y. F. Ma, H. S. O. Chan, Z. L. Dou, *Synth. Met.* 1999, 100, 269.
[29] L. Zhai, R. L. Pilston, K. L. Zaiger, K. K. Stokes, R. D. McCullough, *Macromolecules* 2003, 36, 61.
[30] E. Zhou, J. Hou, C. Yang, Y. Li, *J. Polym. Sci., Part A: Polym. Chem.* 2006, 44, 2206.
[31] K. K. Stokes, K. Heuze, R. D. McCullough, *Macromolecules* 2003, 36, 7114.
[32] K. Buga, K. Kepczynska, I. Kulszewicz-Bajer, M. Zagórska, R. Demadrille, A. Pron, S. Quillard, S. Lefrant, *Macromolecules* 2004, 37, 769.
[33] M. Lanzi, P. C. Bizzarri, L. Paganin, G. Cesari, *Eur. Polym. J.* 2007, 43, 72.
[34] K. Buga, A. Majkowska, R. Pokrop, M. Zagórska, D. Djurado, J.-L. Oddou, S. Lefrant, *Chem. Mater.*2005, 17, 5754.
[35] K. H. Kim, H. J. Jo, *Macromolecules* 2007, 40, 3708.
[36] L. Zhai, D. W. Laird, R. D. McCullough, *Langmuir* 2003, 19, 6492.
[37] R. D. Mccullough, R. D. Lowe, M. Jayaraman, D. L. Anderson, *J. Org. Chem.* 1993, 58, 904.
[38] R. S. Loewe, S. M. Khersonsky, R. D. McCullough, Adv. Mater. 1999, 11, 250.
[39] T. A. Chen, X. M. Wu, R. D. Rieke, *J. Am. Chem. Soc.* 1995, 117, 233.
[40] R. D. Mccullough, S. Tristramnagle, S. P. Williams, R. D. Lowe, M. Jayaraman, *J. Am. Chem. Soc.* 1993, 115, 11608.
[41] K. A. Murray, A. B. Holmes, S. C. Moratti, R. H. Friend, *Synth. Met.* 1996, 76, 161.
[42] J. Liu, R. D. McCullough, *Macromolecules* 2002, 35, 9882.
[43] M. Jeffries-EL, G. Sauve, R. D. McCullough, *Adv. Mater.* 2004, 16, 1017.
[44] E. E. Sheina, S. M. Khersonsky, E. G. Jones, R. D. McCullough, *Chem. Mater.* 2005, 17, 3317.
[45] K. K. Stokes, K. Heuze, R. D. McCullough, *Macromolecules* 2003, 36, 7114.
[46] X. M. Wu, T. A. Chen, R. D. Rieke, *Macromolecules* 1996, 29, 7671.
[47] J. Liu, E. E. Sheina, T. Kowalewski, R. D. McCullough, *Angew. Chem. Int. Ed.* 2002, 41, 329.
[48] J. S. Liu, E. N. Kadnikova, Y. X. Liu, M. D. McGehee, J. M. J. Frechet, *J. Am. Chem. Soc.* 2004, 126, 9486.
[49] L. Zhai, D. W. Laird, R. D. McCullough, *Langmuir* 2003, 19, 6492.
[50] L. Zhu, R. M. Wehmeyer, R. D. Rieke, *J. Org. Chem.* 1991, 56, 1445.
[51] B. J. Campo, W. D. Oosterbaan, J. Gilot, T. J. Cleij, L. Lutsen, R. A. J. Janssen, D. Vanderzande, in *Proceedings of SPIE*, 2009, 7416, 74161G1
[52] B. J. Kim, Y. Miyamoto, B. Ma, J. M. J. Fréchet, *Adv. Funct. Mater.* 2009, 19, 2273
[53] S. Miyanishi, K. Tajima, K. Hashimoto, *Macromolecules* 2009, 42, 1610.
[54] K. Tamao, S. Kodama, I. Nakajima, M. Kumada, A. Minato, K. Suzuki, *Tetrahedron* 1982, 38, 3347.
[55] P. Bauerle, F. Pfau, H. Schlupp, F. Wurthner, K. U. Gaudl, M. B. Caro, P. Fischer, *J. Chem. Soc. Perk. T. 2* 1993, 489.
[56] J. Dai, J. L. Sellers, R. E. Noftle, *Synth. Met.* 2003, 139, 81.
[57] W. D. Oosterbaan, V. Vrindts, S. Berson, S. Guillerez, O. Douhéret, B. Ruttens, J. D'Haen, P. Adriaensens, J. Manca, L. Lutsen, D. Vanderzande, *J. Mater. Chem.* 2009, 19, 5424.
[58] F. C. Spano, *J. Chem. Phys.* 2005, 122, 234701.
[59] K. J. Ihn, J. Moulton, P. Smith, *J. Pol. Sci. B 1993*, 31, 735-742

[60] Z. Bao, A. Dodabalapur, A. J. Lovinger, *Appl. Phys. Lett.* 1996, 69, 4108.
[61] C. J. Brabec, A. Cravino, D. Meissner, N. S. Sariciftci, T. Fromherz, M. T. Rispens, L. Sanchez, J. C. Hummelen, *Adv. Funct. Mater.* 2001, 11, 374.
[62] N. Camaioni, G. Ridolfi, G. Casalbore-Miceli, G. Possamai, M. Maggini, *Adv. Mater.* 2002, 14, 1735.
[63] L. Reimer, Transmission Electron Microscopy, Springer-Verlag, Berlin 1989.

Supporting information

Supporting figure 1: Solar cell characteristics of **P1** as a function of layer thickness

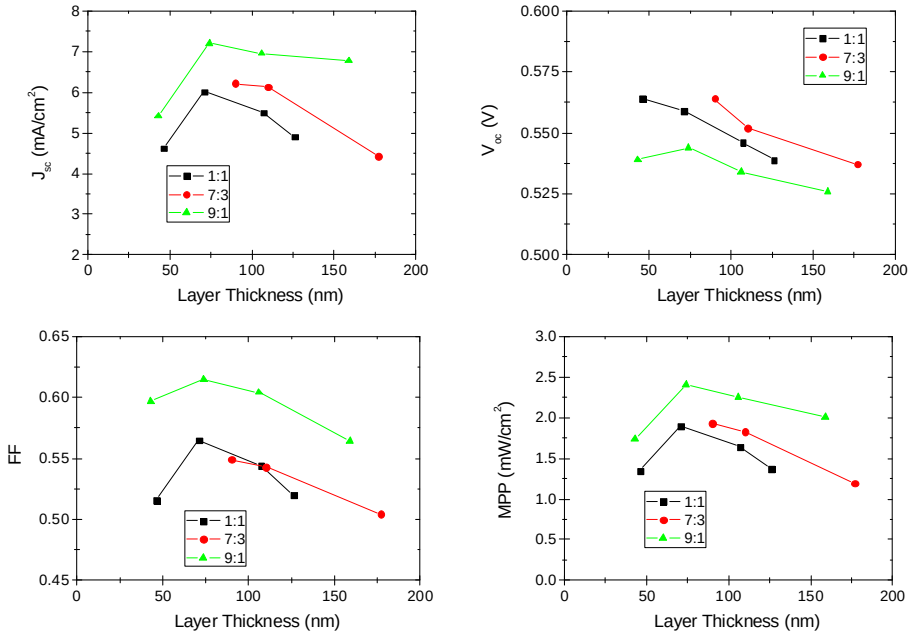

Supporting figure 2: Solar cell characteristics of **P2** as a function of layer thickness

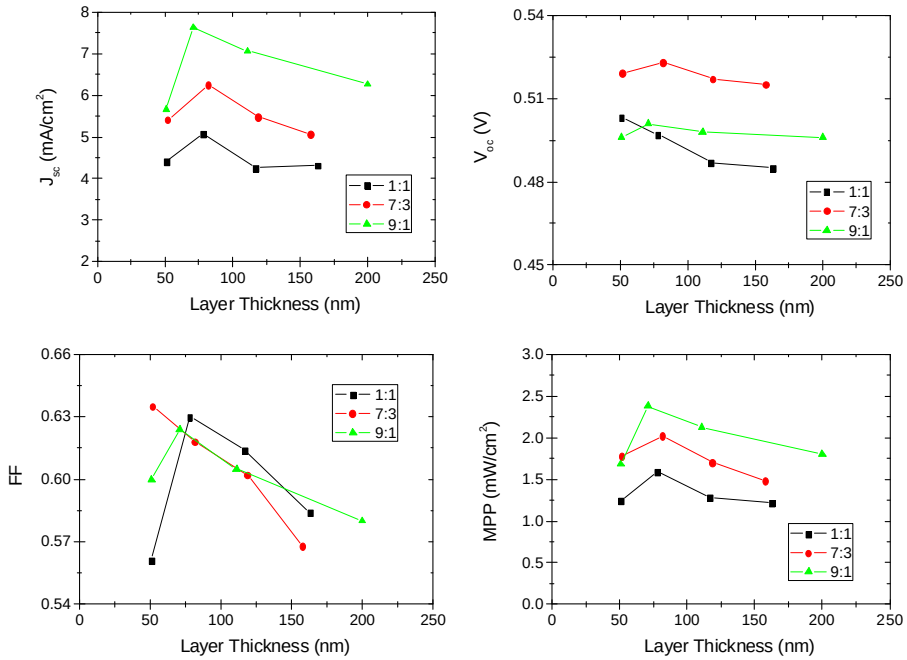

Supporting figure 3: OFET measurements: output current with varying applied voltages at gate (VG) and drain (VD). Here the output is shown for P3HT and the **P1** 9/1 sample. The measured channel width and length were 20 mm and 40 µm; respectively.

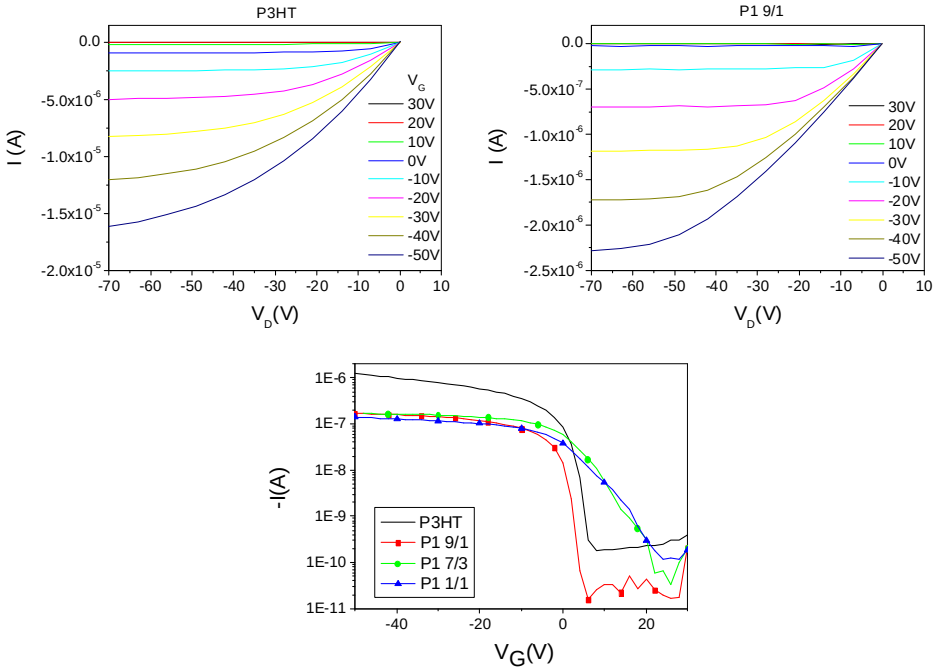

Supporting figure 4: DSC and MTDSC curves of copolymer **P1**

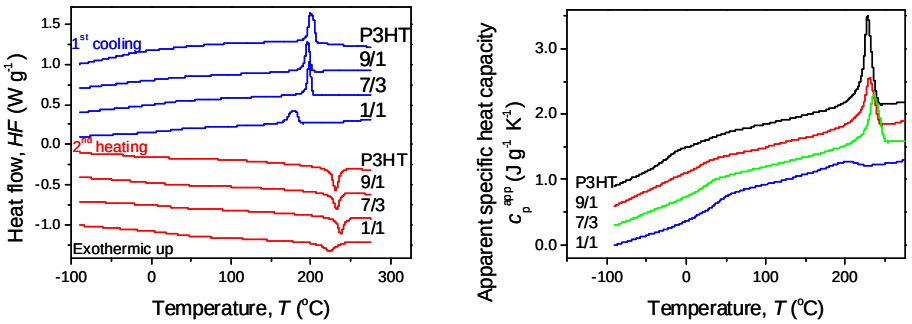

Supporting figure 5: DSC and MTDSC curves of copolymer **P2**

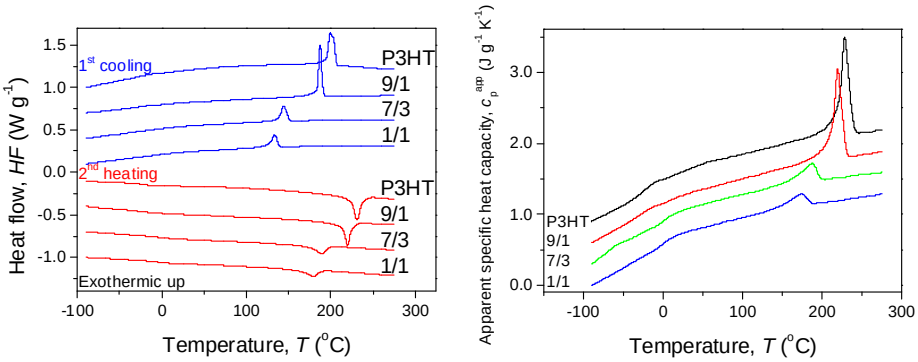

Chapter Five:

Broadening the Absorption Window in Polymer: Fullerene Solar Cells: "Click" Functionalization of Conjugated Polymers with Phthalocyanines[§]

Abstract: The absorption range of the active layer in polymer:fullerene solar cells was expanded by changing the polymer side chains, to increase the device efficiency. Copolymers of poly[2-methoxy-5-(3′,7′-dimethyloctyloxy)-1,4-phenylenevinylene] (MDMO-PPV) and poly(3-hexylthiophene) (P3HT) containing functionalized side chains, synthesized following the sulphinyl precursor route and the Rieke method respectively, were covalently bonded to a Phthalocyanine (Pc). By a post-polymerization click chemistry reaction between alkyne functionalities in the side chains of the MDMO-PPV- and P3HT- based copolymers and an azide functionalized Pc, conjugated polymers with Pc in the side chains were obtained. The resulting poly(*p*-phenylenevinylene)-Pc (PPV-Pc) were obtained with 9% Pc and Polythiophene-Pc (PT-Pc) with 4% or 8% of Pc in the side chains. The presence of the Pc contributes to the extension of the absorption up to 700 nm. Although the polymer-Pc is very well soluble in tetrahydrofurane, the materials solubility in the processing solvent is disturbed. Therefore, the application of the PPV-Pc and PT-Pc in bulk heterojunction solar cells with PCBM results in decreased device conversion efficiency compared to

[§] To be submitted by B. J. Campo, J. Duchateau, J. Gilot, B. Ballesteros, W. D. Oosterbaan, L. Lutsen, T. J. Cleij, G. De la Torre, R. A. J Janssen, D. Vanderzande and T. Torres
J.D. performed all PPV-related synthesis

P3HT:PCBM (1:1) and MDMO-PPV:PCBM (1:4) solar cells. The spectral response however, shows that the Pc absorption contributes to the generation of the photocurrent.

1. Introduction

Polymer:fullerene bulk heterojunction solar cells (BHJSC) are promising candidates for sources of renewable energy.[1-3] A continuous improvement in material properties and device processing has led to devices with efficiencies over 6% in polymer:fullerene solar cells today. [4, 5] Increasing the efficiency and lifetime is a challenge that has to be met to increase the hopes for successful commercialization for this type of solar cells.[1] Often cited examples of polymer:fullerene bulk heterojunction solar cells are the poly[2-methoxy-5-(3′,7′-dimethyloctyloxy)-1,4-phenylenevinylene] (MDMO-PPV):Phenyl-C_{61}-Butyric acid Methyl ester (PCBM) and poly(3-hexylthiophene) (P3HT):PCBM BHJSC, with the polymer acting as electron donor and the fullerene as the electron acceptor. Some intrinsic material properties are limiting the device efficiency, for example the poor overlap between the absorption spectrum of the blend and the emission spectrum of the sun.

Several strategies have been applied to increase the efficiency in BHJSC devices. The open circuit voltage (V_{oc}) and short circuit current densities (J_{sc}) may be improved by tailoring the donor and acceptor energy levels. Because the narrow absorption window of the conjugated polymer limits the efficiency in polymer solar cells, extending the absorption of the organic material will enhance the absorption of the active layer in the device. The increased energy absorption could lead to a higher short circuit current and

efficiency. As mentioned before, other studies aimed to fine-tune the molecular energy levels or to synthesize a low band gap polymer. Another approach to absorb more energy is to design devices with several active layers on top of each other, the tandem solar cells.[6, 7]

Here, we aim to broaden the absorption of the polymer material. A molecule that absorbs longer wavelengths compared to the conjugated polymer is covalently attached to functionalized side chains in the conjugated polymer. MDMO-PPV and P3HT absorb light with wavelengths ranging from 400 to 600 nm (figure 1), therefore the addition of a Phthalocyanine (Pc) absorbing from 600 to 700 nm will cause a broadening of the absorption range and an increased energy absorption. Pc's are highly conductive photoactive materials and display promising properties in combination with fullerene molecules[8-10] and polythiophenes[11]. They have been applied as photo active materials in bulk heterojunction solar cells with fullerenes[12] and metal oxides[13, 14] as well as in dye sensitized solar cells.[15] The combination of conjugated polymers and Pc's in BHJSC is a possible route to a higher photocurrent and increased device power conversion efficiency.

MDMO-PPV is an amorphous conjugated polymer that is usually used in polymer: PCBM (1:4) blends to obtain sufficient phase separation.[16] The synthesis of PPVs has been reported by several routes.[17-19] Ester-functionalized PPV-copolymers appropriate for further post-polymerization functionalization procedures were obtained using the sulphinyl route (Figure 1).[19] Also the synthesis of Poly(3-alkylthiophenes) (P3ATs) has been achieved using various synthetic routes.[20, 21] Functionalized P3HT-based copolymers with 10, 30 and 50% of ester-functionalized alkyl side chains, produced using the Rieke method, were reported previously.[22] The copolymers have a regio-regularity of 90% or higher, comparable to P3HT

homo polymers prepared according to the same method. Regioregular P3ATs have a tendency to self-organize upon (thermal or solvent) annealing, leading to a phase separated blend morphology favouring high energy conversion efficiency in solar cells.[23] Post-polymerization reactions allow synthesis of acid functionalized copolymers (Figure 1), which may be further functionalized with a variety of molecules. By introduction of functional groups on the polymer side chains, the possibilities of several secondary functionalities on this material are explored. To achieve the goal of extending the polymer absorption, Pc's were reacted with the functionalized side chains. MDMO-PPV and P3HT-based copolymers were prepared and further functionalized with an alkyne bond (C≡C). While Pc with solubilising tertiary butyl groups have been reported,[24] a Pc derivative containing three tertiary butyl groups and an azide functionality was used in this work. The reaction between an azide and alkyne functionality is known as the 1,3 Huisgen cycloaddition and proceeds with a high yield.[25] This "click chemistry" reaction was applied before to combine Pc's with carbon nanotubes.[26, 27] Using this reaction, the alkyne functionalities on the polymer side chains were reacted with azide functionalized Pc, and polythiophene-Pc (PT-Pc) and PPV-Pc coupled product with a broader absorption range compared to P3HT or MDMO-PPV were obtained. The polymer-Pc were applied in polymer:PCBM BHJSC with several ratios of PCBM.

2. Results and discussion

2.1 Polymer synthesis and characterization

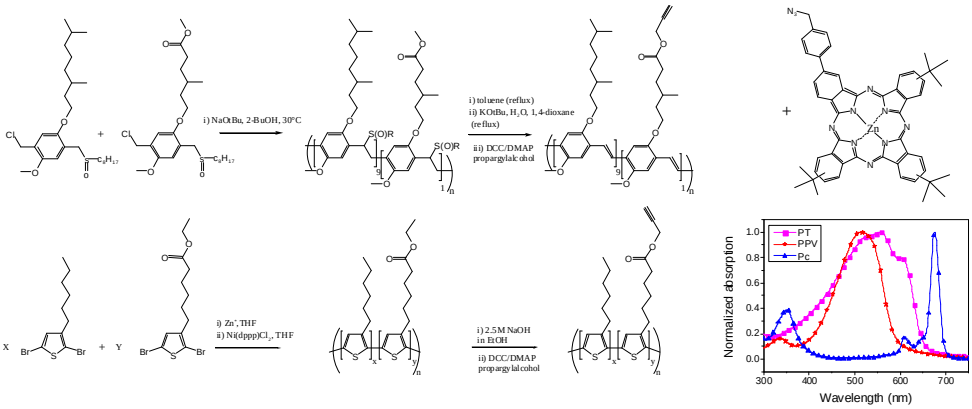

Figure 1: Synthesis of alkyne functionalized conjugated polymers, available for click chemistry reaction with the azide functionalized Phthalocyanine (Pc) and the UV-Vis absorption ranges of a polythiophene (PT), poly(p-phenylenevinylene) (PPV) and a Pc.

2.1.1 Poly(*p*-phenylenevinylene) (PPV) synthesis

A detailed report on the synthesis of (alkyne-)functionalized PPV's will be published elsewhere.[28] The copolymerization reaction of the MDMO monomer and an ester functionalized molecule was done using the sulphinyl precursor route.[19] Although both monomers are a mixture of regio-isomers, for reasons of simplicity only one isomer is depicted in Figure 1. Post-polymerization conversion reactions transformed the ester functionality in the side chains of the copolymer to an acid and then to an alkyne. A copolymer containing 9% of triple bonds in the side chains was obtained, as determined by ^{1}H-NMR.

2.1.2 Polythiophene (PT) synthesis

The synthesis of ester functionalized P3ATs, displayed in figure 1, was done using the Rieke method, as reported previously.[22, 29] The ester functionalities in the alkyl side chains were converted after polymerization to the corresponding acid functions in a 2 M NaOH solution in EtOH. The conversion of ester-functionalized copolymer to acid-functionalized copolymer was complete after stirring for 48 h under reflux. The complete conversion is evidenced in ^{1}H-NMR by the disappearance of the signal originating from the O-CH_2 methylene protons in the ester functionality. Additional proof is the shift of the C=O absorption in FT-IR from 1740 cm^{-1} to 1710 cm^{-1}. A part of the acid functionalized copolymer was extracted with $CHCl_3$ in a Soxhlet setup to obtain in the extract a polymer with 4% acid functionalities (^{1}H-NMR). This way, the original copolymer with 10% and a batch with 4% of acid functional groups were available for further functionalization with propargyl alcohol using the DCC/DMAP protocol in an esterification reaction.[30] The presence of the triple bond at the end of the alkyl side chains is visible in ^{1}H-NMR by the signal originating from the O-CH_2-C≡CH methylene protons. Also the acetylene proton is visible at δ = 2.42 ppm. The C=O stretch on FT-IR shifts from 1710 cm^{-1} in the acid group to 1740 cm^{-1} in the ester group. The percentage of functionalized side chains in this copolymer was calculated as the ratio of the signals integration on ^{1}H-NMR from the O-CH_2 peak (4.7 ppm) for the functionalized side chains and CH_3 groups (0.89 ppm) for the hexyl side chains. The ratios indicate that the acetylene functionalized copolymers contain 8 and 4% C≡C triple bonds in the side chains.

2.1.3 Polymer-Phthalocyanine coupling by click chemistry

The reaction conditions for the Polymer-Pc coupling via click chemistry were adapted from literature procedures.[31] The reaction conditions of two procedures are presented in the experimental section. The polymer and Pc were dissolved in degassed THF. The copper containing compound (CuI or CuBr) and a N-ligand: 2,6-lutidine or N,N,N',N',N",N",N'" pentamethyldiethylenetriamine (PMDETA) were added under nitrogen flow. After work up and purification, the presence or absence of non reacted Pc molecules was verified with thin layer chromatography (TLC). The reaction mixture in tetrahydrofurane (THF) was spotted on a TLC plate and eluted in a THF: hexane (1:2) mixture. Since the polymer does not eluate on the TLC plate, the visible spots with retention factor (R_f) > 0 are due to the smaller molecules present in the reaction mixture. Bright blue Pc spots were visible for both experiments before purification. After work up and purification by rinsing with acetone, no Pc spots were visible in TLC, a positive verification of removal of all non- reacted Pc molecules. UV-Vis absorption in solution displayed the polymer absorption with a maximum around 450 nm for PT and 500 nm for PPV, and the absorption at 675 nm of the covalently bonded Pc (Figure 2). The proof that conversion of the C≡C bonds towards the 1,4-disubstituted -1,2,3-triazole was complete is delivered by ^{1}H-NMR spectrum of the PT-Pc and PPV-Pc. The signal of the CH_2 protons next to the alkyne function at δ = 4.7 ppm completely disappears, indicating that all present alkyne bonds are functionalized with a Pc molecule. New signals, originating from the polymer-Pc units, are visible in the aromatic region.

2.1.4 UV-Vis absorption characteristics of polymer-Pc

The UV-Vis absorption spectra of PPV-Pc solutions in THF and chlorobenzene (CB) are displayed in figure 2a. The absorption between 400 and 550 nm with wavelength of maximum absorption (λ_{max}) around 510 nm is due to the conjugated backbone of the PPV, while the absorption between 600 and 700 nm is due to the Pc molecules covalently attached to the side chains. In THF and CB, the λ_{max} of the Pc absorption is at 676 nm and 691 nm respectively. The absorption of longer wavelengths by the Pc in a solution of CB points to a certain extent of aggregation of the Pc's, indicating that THF is a better solvent for the PPV-Pc system.

In figure 2b, the UV-Vis absorptions of alkyne-functionalized PPV and PPV-Pc (with 9% Pc) in film are given. The absorption of the alkyne-functionalized PPV is - comparable to the absorption of MDMO-PPV – between 400 and 550 nm with λ_{max} at 512 nm. In the PPV-Pc film, the Pc absorption is visible with λ_{max} at 692 nm, while the λ_{max} of the PPV decreases to 494 nm. The shift to lower wavelengths of the PPV absorption in PPV-Pc as compared to PPV-alkyne indicates that the presence of the Pc in the side chains disturbs the polymer organization and lowers effective conjugation length. The shift of the Pc λ_{max} to longer wavelengths in PPV-Pc film (692 nm) compared to the PPV-Pc in solution (676 nm) is an indication of stacking of the Pc in the PPV-Pc film. The presence of this organized Pc in the PPV-side chain can twist the conjugated backbone, explaining the decreased λ_{max} of the PPV contribution in the UV-Vis absorption spectrum.

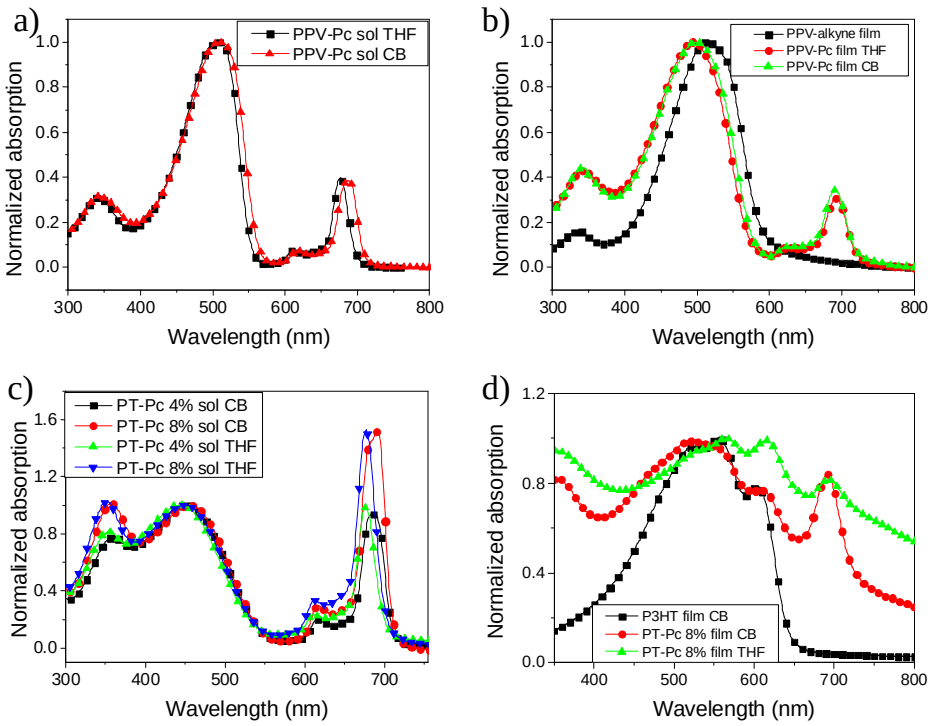

Figure 2: UV-Vis absorption of a) PPV-Pc solutions in THF (squares) and CB (triangles); b) PPV-alkyne film drop-cast from solution in THF (squares), PPV-Pc film drop-cast from solution in CB (circles) and THF (triangles); c) PT-Pc 4% and PT-Pc 8% in solutions of CB and THF; d) polythiophene films drop-cast from solution in CB (P3HT: squares and PT-Pc 8%: circles) and THF (PT-Pc 8%: triangles)

The UV-Vis absorption spectra of PT-Pc solutions in THF and CB are displayed in Figure 2c. The polythiophene absorption has a λ_{max} around 450 nm. The contribution of the Pc in the absorption is visible at λ = 350 nm, and between 600 and 700 nm with λ_{max} around 675 nm. In THF solution, the Pc absorption was at λ_{max} 677 nm while in CB solution the λ_{max} of the Pc was at 685 nm and 691 nm for the PT-Pc 4% and PT-Pc 8%, respectively. The λ_{max} of the Pc absorption was higher in CB, indicating that also in the PT-Pc the Pc units were more aggregated in CB, this means that THF is a better solvent for the PT-Pc.

The UV-Vis absorption of PT-Pc 8% films drop-cast from solution in CB and THF are displayed in Figure 2b, together with the absorption of 96% regio-regular P3HT. Compared to the absorption in solution, the absorption of the polymer increased relative to the Pc absorption, due to π-π stacking of the conjugated polymer backbone. The polythiophene absorption red-shifted compared to the solution to wavelengths between 400 and 600 nm with maximum absorptions at 523 nm for the film drop-cast from CB and 564 nm for the film drop-cast from THF. The contribution of the absorption of the Pc moiety was visible around 690 nm. The higher λ_{max} in films drop-cast from THF compared to the λ_{max} in films drop-cast from CB indicates that the π-π stacking is better in films drop-cast from THF. From the absorption in solution it is known that THF is the better solvent. Films with more organized polymer chains were obtained from solutions in a better solvent. The impact of the large Pc molecules in the alkyl side chains on the structural order in a polymer was limited when a good solvent was used. The maximum in the polymer absorption spectrum, for P3HT at 555 nm, decreased in PT-Pc 8% films drop-cast from CB to 523 nm, indicating that the PT π-π stacking was disturbed by the presence of Pc in the side chains. In films drop-cast from THF, however, the absorption of the PT increased even to 564 nm, evidence for a better organization in films drop-cast from a good solvent.

2.1.5 Cyclic voltammetry

Electrochemical data (mV *vs*. Ag/ AgCl) of the redox process of tetra(*tert*-butyl)phthalocyaninato zinc(II) in *o*-DCB solution ($0.005 moldm^{-3}$ $TBAPF_6$) were obtained from cyclic voltammetry. The first oxidation and reduction potential of the two electron process are used to estimate the energy of the

HOMO and LUMO levels. The estimations were done with relation (1) with respect to the vacuum level, defined as zero. [32]

$$E_{HOMO/LUMO} = -(\varphi_{Ox/\mathrm{Re}d} + /- 4.72)(eV) \qquad (1)$$

The first reduction potential was -1.08 V, the first oxidation potential was 0.61 V. Filling in these values into equation 1 gave the energy levels displayed in figure 3. The HOMO and LUMO energy levels of the (*tert*-butyl)phthalocyaninato zinc(II) were found to be 5.4 eV and 3.7 eV, respectively. The Pc molecules could, apart from acting as an absorber, therefore act as electron acceptor relative to P3HT and as electron donor relative to PCBM. In combination with MDMO-PPV however, there is no energetic driving force for the holes in the Pc to be transported towards the conjugated polymer.

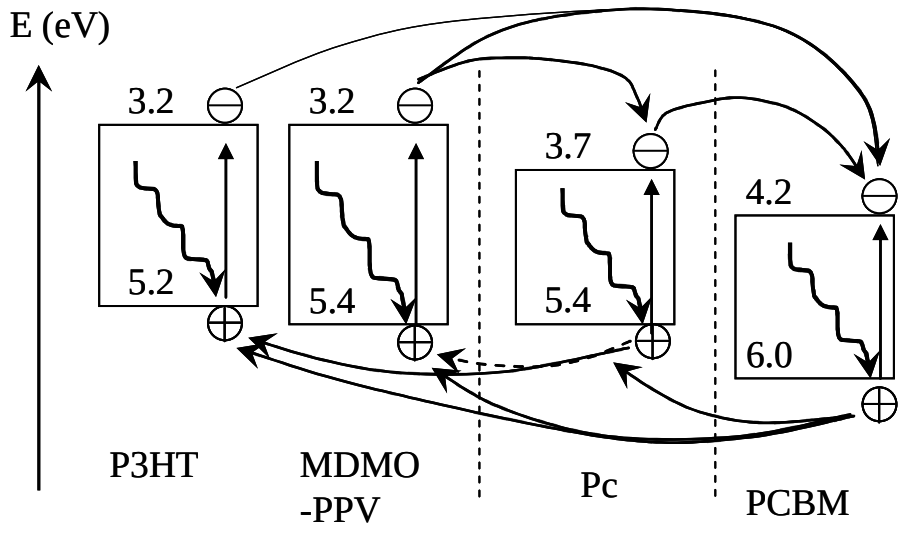

Figure 3: Energy scheme of the absorbing materials in PT-Pc:PCBM and PPV-Pc:PCBM solar cells. Arrows indicate the possible energy absorptions and charge transfers

2.2 Application in photovoltaic devices

The PT-Pc copolymers were mixed in polymer:PCBM 1:1 and 1:2 (w/w) blends, the PPV-Pc in 1:4 blends and applied in a ITO/PEDOT:PSS/polymer:PCBM/LiF/Al BHJSC. Blend solutions were made in CB and spincoated at several spinning speeds to obtain varying layer thicknesses.

2.2.1 Photocurrent generation from a broader absorption window

In the spectral response of a BHJSC with PPV-Pc:PCBM (1:4) active layer in Figure 4a, there is a clear contribution of the covalently bonded Pc molecules in the the external quantum efficiencies (EQE). The contribution of PPV is visible around 500 nm, the Pc around approximately 700 nm. Comparing the *EQE* with the UV-Vis absorption spectrum of a PPV-Pc film, the absorption peaks of the PPV backbone and the Pc remain at the same wavelengths. The height of the Pc peak relative to the PPV signal differs. In the spectral response the relative intensity of the Pc absorption is higher, possibly because of the supramolecular organization. This indicates that the Pc's have a certain structural ordering in the blend, but this disturbs the polymer organization in the solar cell active layer, as was discussed before when the UV-Vis absorption spectra of a PPV-Pc film and a PPV film were compared.

Also in the spectral response of the PT-Pc:PCBM solar cells (figure 4b), the Pc absorptions are clearly present around 700 nm, indicating that the light absorbed by the Pc moiety leads to charge transfer and these charges are extracted. With a higher content of Pc (8% compared to 4%) the EQE at 700 nm increases. The EQE between 550 and 600 nm however, the range where usually only the polythiophene is absorbing, is almost absent, indicating a

lack of polythiophene stacking in the blend with consequently a low hole mobility in the polymer phase. The low values of the EQE between 350 - 550 nm, due to polythiophene:PCBM also indicates a lack of crystalline ordering which is important for higher conversion efficiencies in P3HT:PCBM solar cells.

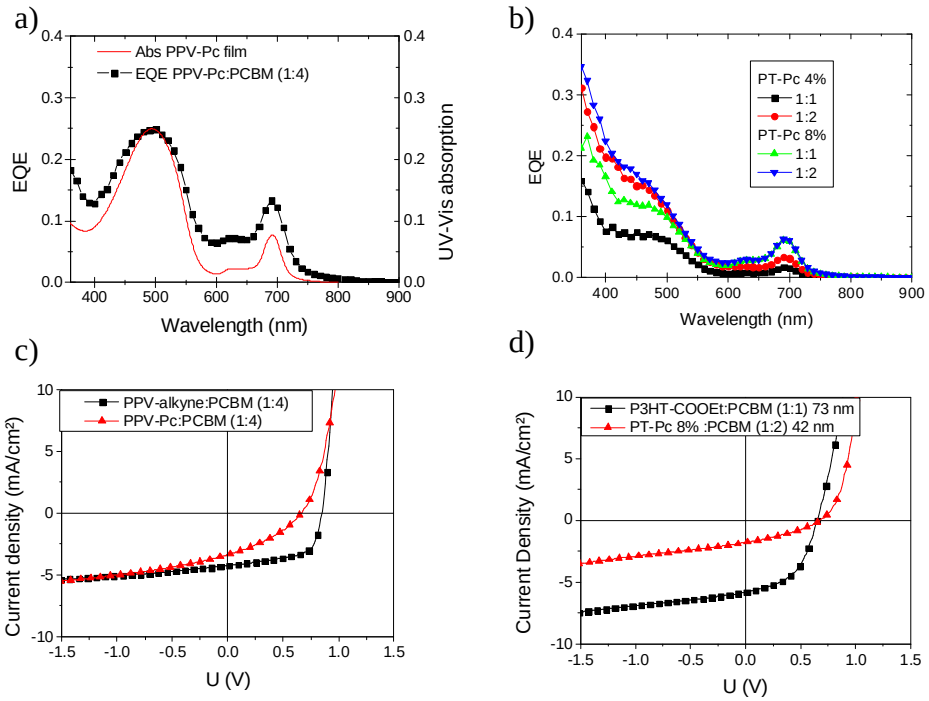

Figure 4: EQE of solar cells with a) PPV-Pc:PCBM (1:4) active layer or b) PT-Pc 4% and PT-Pc 8% in blends with PCBM in a (1:1) and (1:2) weight ratio; and J-V curve of ITO /PEDOT:PSS (~50nm) /polymer:PCBM /LiF /Al with c) PPV-alkyne:PCBM (1:4) (squares) and PPV-Pc:PCBM (triangles); d) esterfunctionalized PT:PCBM (1:1) (squares) and PT-Pc 8%:PCBM (1:2)

2.2.2 Polymer-Pc:PCBM in BHJSC

The *J-V* curves of the best PPV-C≡C:PCBM and PPV-Pc:PCBM solar cells are displayed in figure 4c. The device characteristics of the best solar cells of each copolymer are given in §4.6. The performance of devices with

alkyne-functionalized PPV is quite comparable to what is reported for MDMO-PPV:PCBM (1:4) BHJSCs.[33] The presence of 10% of alkyne functionalized side chains has little or no effect in the device, an efficiency of 2.2% was achieved. In solar cells with PPV-Pc:PCBM (1:4) blends however, there is a decrease in short circuit current (J_{sc}), open circuit voltage (V_{oc}) and fill factor (*FF*). The detrimental effect of the Pc molecule on solubility in CB could be largely responsible for the poor device performance. The presence of the Pc molecules in the side chains of the copolymer and a limited solubility in CB causes a poor polymer organization, as was evidenced in the UV-Vis spectra. This will cause an unfavourable morphology and lower hole mobility in the blend, with consequently a low J_{sc} and *FF*. The origin of the decrease in V_{oc} is unclear.

The J-V curves of the best PT:PCBM and PT-Pc:PCBM solar cells are shown in Figure 4d. The performance in organic solar cells of copolymers containing 10% functionalized side chains was comparable to the performance of P3HT:PCBM solar cells prepared following the same procedures.[29] The best PT-Pc:PCBM solar cell was obtained for a device with a relatively thin layer (42 nm). Better currents and efficiencies were obtained with higher amounts of PCBM. The low J_{sc} compared to P3HT:PCBM solar cells, together with the fact that for very thin layers (thickness < 50 nm) the best currents were obtained, indicated that the charge transport properties in the blend were unfavourable. The low *FF*, and the need of more PCBM to extract the charges indicated that the blend morphology was not favourable. Thermal treatment of P3HT:PCBM solar cells have been reported to result in better hole transport in the polymer phase because of closer stacking of the conjugated polymers backbones and

a phase separated morphology. [34] However, annealing treatments of the PT-Pc devices did not lead to better results. The Pc molecules in the side chains may prevent the PT chains from self-organizing, explaining why no better results were obtained after annealing. A better π-π stacking would be obtained by processing from THF, but the solubility of PCBM in this solvent was too low for device preparation. A better solubility in the processing solvent might lead to a polymer organization in the blend and a blend morphology that is favorable for high efficiency power conversion.

3. Conclusion

Conjugated polymers decorated with Pc molecules (PT-Pc and PPV-Pc) were obtained by post-polymerization functionalization reactions using click chemistry to couple an azide functionalized Pc to PPV and PT containing alkyne functions in the side chains. Relative to the number of alkyl side chains in the PT, integration on ^{1}H-NMR indicated that copolymers with 4% and 8% of covalently bonded Pc were obtained, PPV-Pc was obtained with 9% Pc's. These products were applied in bulk heterojunction solar cells (BHJSC) with PCBM in 1:4 blends for PPV and 1:1 and 1:2 blends for PT. The spectral response showed the contribution of the Pc around 700 nm. Thus, the Pc in the alkyl side chains absorbed light and contributed to the generation of photocurrent. A broader absorption of the active layer in polymer solar cells was achieved, but material solubility in chlorobenzene (the processing solvent) and therefore also the electrical properties of the processed materials in the device were affected in such a way that device efficiency decreased. However, continued efforts in materials design can lead to more processable polymer-Pc materials, what will facilitate the

device preparation, improve electrical properties of spincoated layers and this can result in more efficient devices.

4. Materials and methods

4.1 General experimental procedures

^{1}H-NMR spectra were recorded on a Varian Inova 300 MHz spectrometer in a 5 mm probe using deuterated chloroform or tetrahydrofurane, obtained from Cambridge Isotope Laboratories. Chemical shifts are reported in ppm downfield from tetramethylsilane (TMS) using the peak of residual $CHCl_3$ as an internal standard at δ = 7.24 ppm in chloroform, or the polythiophene aromatic proton peak at δ = 6.96 ppm in tetrahydrofurane. Fourier transform infrared spectroscopy (FT-IR) was performed on a Perkin Elmer Spectrum One FT-IR spectrometer using pellets in KBr or films drop-cast on a NaCl disk from solution in chlorobenzene or tetrahydrofurane. Gas chromatography/mass spectrometry (GC-MS) was carried out on TSQ-70 and Voyager mass spectrometers. UV-Vis spectra were recorded on a Varian CARY 500 UV-Vis-NIR spectrophotometer from 200 to 800 nm at a scan rate of 600 nm min^{-1}. Size exclusion chromatography (SEC) was done with a 1 mg mL^{-1} polymer solution in THF, which was filtered with a 0.45 µm pore PTFE syringe filter. A Spectra Physics P100 pump equipped with two mixed-B columns (10 µm, 30 cm x 7.5 mm) Polymer Labs and a Shodex refractive index detector at 40°C in THF at a flow rate of 1.0 ml min^{-1} were used. Molecular weight distributions were measured relative to polystyrene standards and toluene was used as a flow rate marker. Solar cells were made on glass substrates (3 x 3 cm) with patterned ITO electrodes. The substrates were sonicated in acetone, cleaned with soapy

water and isopropanol and treated with UV/O_3 for 15 minutes. Typically, 50 nm poly(ethylenedioxythiophene): poly(styrenesulfonate) (PEDOT: PSS) (Clevios™ P VP AI 4083, HC Starck) was spin-coated at 3000 rpm. 7.5, 10 and 15 mg mL^{-1} solutions of PCBM in chlorobenzene were added to the polymer in (1:1), (1:2), (1:4) (w/w) ratios respectively. The solutions were stirred at 50 °C before they were spin-coated at several spinning speeds to investigate the influence of active layer thickness. The preparation of P3HT:PCBM solar cells was done with P3HT obtained from Rieke Metals. 1 nm of LiF and 100 nm of Al were evaporated in high vacuum (p = 10^{-7} mbar). J-V curves were measured under simulated solar light (100 mW cm^{-2}) from a tungsten-halogen lamp filtered by a Schott GG385 UV filter and a Hoya LB120 daylight filter using a Keithley 2400 source meter. Spectral response was measured with monochromatic light from a 50 W tungsten halogen lamp (Philips focusline) in combination with a monochromator (Oriel, Cornerstone 130) and a lock-in amplifier (Stanford research Systems SR830). A calibrated Si cell was used as reference. The device was kept behind a quartz window in a nitrogen filled container. To measure the cell under appropriate operation conditions, the cell was illuminated by a bias light from a 532 nm solid state laser (Edmund Optics).

4.2 Polythiophene synthesis

The preparation of monomers and the copolymerization reaction are reported elsewhere. The copolymer poly([3-hexylthiophene-2,5-diyl]-*co*-[3-(6-ethoxy-6-oxohexyl)thiophene-2,5-diyl]) containing 10% of functionalized side chains was obtained and characterized. (3.77 g, 74%) GPC M_w: 76 700, M_w/M_n: 1.9; FT-IR (KBr, cm^{-1}): 3053, 2954 (s), 2925 (vs), 2855 (s), 1738, 1562, 1509, 1455, 1377, 1261, 1180 1094, 1030, 821,

725; ^{1}H NMR (300 MHz, $CDCl_3$): 6.96 (1H, s, Th), 4.10 (2H, OCH_2), 2.79 (2H, H-T α-CH_2), 2.56 (2H, s, H-H α-CH_2), 2.31 (2H, CH_2COOEt), 1.69 (2 H, β-CH_2), 1.48 – 1.20 (10 H, m, γ, δ, ε-CH_2 3-HT and γ, δ-CH_2), 0.90 (6 H, CH_3); UV-Vis (λ_{max}) 555, 602 nm

To hydrolyze the ester functions in the side chains, 1.00 g of the 9/1 copolymer was stirred for 48 h in 100 mL of a 2 M NaOH solution in EtOH under reflux. The mixture was poured out in a MeOH/2 M HCl mixture and filtrated. The isolated copolymer was dried to obtain 0.95 g (96 %) of poly([3-hexylthiophene-2,5-diyl]-*co*-[3-(6-carboxyhexyl)thiophene-2,5-diyl]) and characterized. GPC M_w: 51 00, D: 1.7; FT-IR (KBr, cm^{-1}): 2954, 2924 and 2853, 1710, 1635, 1507, 1457, 1377, 1261, 1077, 820, 803, 725; ^{1}H NMR (300 MHz, $CDCl_3$): 6.96 (1H, s, Th), 2.79 (2H, t, H-T α-CH_2), 2.56 (H-H α-CH_2), 2.37 (2H, m, CH_2COOH), 1.70, 1.42, 1.34 and 1.25 (γ, δ, ε-CH_2), 0.90 (3 H, CH_3) A part of the acid functionalized copolymer was extracted with $CHCl_3$. After precipitation of the extract, a lower molecular weight fraction was filtered off. A copolymer with 4% (on ^{1}H-NMR) of acid functionalized side chains was obtained. Mw = 38 600, M_w/M_n: 2.1

The acid functionalized copolymer (100 mg of the (x/y) 0.90/0.10 and 150 mg of the (x/y) (0.96/0.04)) was dissolved in chlorobenzene before addition of the alcohol, DCC and DMAP (respectively 90 mg, 80 mg and 4 mg for the 0.90/0.10 and 135 mg, 120 mg and 6 mg for the 0.96/0.04 copolymer). The reaction was stirred for 48 h at 50 °C. The mixture was precipitated in MeOH, stirred for 1 h and filtrated to obtain 60 mg and 135 mg of the alkyne-functionalized copolymers poly([3-hexylthiophene-2,5-diyl]-*co*-[3-(6-(prop-2-yn-oxyl)-6-oxohexyl)thiophene-2,5-diyl]). GPC Mw: 31 800,

M_w/M_n: 1.9; FT-IR (KBr, cm^{-1}): 3055, 2956 (s), 2926 (vs), 2855 (s), 1746, 1656, 1562, 1509, 1455, 1377, 1261, 1156, 1092, 1021, 820, 801, 725; ^1H NMR (300 MHz, $CDCl_3$): (x/y) = 0.92/0.08, δ = 6.96 (1H, s, Th), 4.65 (2H, OCH_2), 2.78 (2H, H-T α-CH_2), 2.54 (2H, H-H α-CH_2), 2.42 (1H, s, CHC≡C), 2.37 (2H, t, CH_2COOR), 1.69, 1.42 and 1.32 (β, γ, δ, ε-CH_2), 0.89 (3H, CH_3)

GPC Mw: 38 600, M_w/M_n: 2.1; FT-IR (KBr, cm^{-1}): 2956 , 2926, 2855, 1739, 1656, 1597, 1509, 1455, 1377, 1260, , 1092, 1020, 801; ^1H NMR (300 MHz, $CDCl_3$): (x/y) = 0.96/0.04, δ = 6.96 (1H, s, Th), 4.65 (2H, OCH_2), 2.78 (2H, H-T α-CH_2), 2.54 (2H, H-H α-CH_2), 2.42 (1H, s, CHC≡C), 2.37 (2H, t, CH_2COOR), 1.88, 1.66, 1.42 and 1.32 (β, γ, δ, ε-CH_2), 0.89 (3H, CH_3)

4.3 PPV synthesis

The synthesis of monomers, the copolymerization and post-polymerization reactions are reported elsewhere. Characterization of alkyn functionalized copolymer which was used to react with Pc is given to enable interpretation of results: poly([2-methoxy-5-(3′,7′-dimethyloctyloxy)-1,4-phenylenevinylene]-*co*-[2-methoxy-5-(6-oxo-6-(prop-2-yn-oxyl)hexyloxy)-1,4-phenylenevinylene]) GPC (THF) M_w = 380 000, M_w/M_n = 5.2; FT-IR (KBr, cm^{-1}): 3058, 2954, 2927, 2868, 1745, 1505, 1464, 1414, 1384, 1352, 1258, 1158, 1092, 1037, 969, 860; ^1H NMR (300 MHz, $CDCl_3$): 7.6-7.4, 7.2-7.1, 4.65, 4.1-3.8, 2.43, 2.4-2.3, 1.8-0.6; UV-Vis (λ_{max}) in THF solution = 507 nm

4.4 Phthalocyanine synthesis and characterization

The measured potentials in *o*-DCB solution (0.005 mol dm^{-3} $TBAPF_6$): E_{red}^1: -1084 mV, E_{red}^2: -1376 mV, E_{ox}^1: 609 mV, E_{ox}^2: 1261 mV

4.5 Polymer-Pc coupling: click chemistry reactions

Dry THF was degassed by sonicating while an Argon flow was sent continuously through the solvent. The polymer was dissolved in THF by stirring at 50 °C, before adding the azide-functionalized Pc and other reagents. Two methods were used, both giving complete functionalization. Equivalents were calculated relative to the number of alkyne functions present in the copolymer. The reactions were stirred in the dark under reflux and inert atmosphere.

Method 1: CuI (2.5 eq.) and 0.2 eq. 2,6-lutidine were added to the dissolved polymer and 2.5 eq. Pc in a total volume of 5 mL THF. To stop the reaction, THF was evaporated, the mixture was dissolved in $CHCl_3$ and extracted with a saturated NH_4OH solution. The product was precipitated in MeOH, stirred and washed with 3x 100 mL acetone before filtration and drying.

Method 2: CuBr (0.1 eq) and PMDETA (0.1 eq.) were added to the polymer with 2 eq. Pc in 10 mL THF. The work-up was done by filtering the reaction over Al_2O_3 and washing with THF and CH_2Cl_2 (PPV-Pc) or $CHCl_3$ (PT-Pc). Subsequently, the total volume was reduced to 15 mL by evaporation under reduced pressure and the resulting solution was precipitated drop wise in MeOH. The resulting copolymer was filtered off, washed extensively with MeOH and acetone and dried at room temperature under reduced pressure.

PT-Pc 4% (Method 1) 50 mg copolymer and 22 mg of Pc-azide were dissolved with 0.2 mg 2,6-lutidine and 5 mg CuI to obtain 48 mg of PT-Pc after purification. GPC (THF): Mw: 40 200, M_w/M_n: 2.2; FT-IR (KBr, cm^{-1}): 2956 (s), 2926 (vs), 2857 (s), 1739, 1645 (br), 1513 (w), 1487 (w), 1455, 1391(w), 1376 (w), 1363 (w), 1331 (w), 1261, 1231 (w), 1186 (w), 1154 (w), 1092, 1046, 1020, 920 (w), 816, 800, 748 (w); ^{1}H NMR (300 MHz, $CDCl_3$): 8.18, 7.58, 6.97, 6.89, 6.83, 6.79, 5.60, 5.06, 3.86, 3.70, 3.64, 3.47, 2.80, 2.56, 2.40, 2.02, 1.67, 1.53, 1.32 and 1.23, 0.89; UV-Vis (λ_{max}) in THF solution 355, 443, 677 nm, in CB solution 360, 452, 685 nm, in film drop-cast from THF: 348, 555, 692 nm, in film drop-cast from CB: 361, 515, 692 nm

PT-Pc 8% (Method 2) 60 mg copolymer was dissolved with 61 mg of Pc-azide, 0.6 mg PMDETA and 0.2 mg CuBr. After purification, 36m g of PT-Pc was obtained. GPC (THF): Mw: 58 600, M_w/M_n: 1.8; FT-IR (NaCl, cm^{-1}): 2957 (s), 2927 (vs), 2856 (s), 1739, 1644 (br), 1511 (w), 1487 (w), 1456, 1390 (w), 1363 (w), 1331 (w), 1261, 1231 (w), 1186 (w), 1152 (w), 1092, 1048, 1024, 920, 820, 800, 748; ^{1}H NMR (300 MHz, THF-d_8): 8.14, 7.97, 7.76, 7.44, 7.35, 6.96, 6.89 6.83, 6.79, 5.60, 5.06, 2.80), 2.67, 2.40, 2.04, 1.91, 1.77, 1.34 and 1.27, 0.91; UV-Vis (λ_{max}) in THF solution 352, 459, 677 nm, in CB solution 358, 458, 691 nm, in film drop-cast from THF: 564, 694 nm, in film drop-cast from CB: 523, 692 nm

PPV-Pc (Method 1) 50 mg copolymer, Pc-azide (38 mg, 0.043 mmol), 2,6-lutidine (0.3 mg, 0.0036 mmol) and Cu(I)I (8 mg, 0.043 mmol) were stirred 42 h at reflux temperature. After purification 55 mg PPV-Pc was isolated (82 % yield). GPC (THF) M_w: 217 000, M_w/M_n: 3.2; FT-IR (NaCl, cm^{-1}):

3059, 2959, 2927, 2870, 1736, 1504, 1464, 1414, 1385, 1352, 1260, 1206, 1027, 971, 863, 800; ^{1}H-NMR (300 MHz, THF-d_8): δ = 9.58-9.38, 8.30, 8.11, 7.90, 7.55-7.4, 7.3-7.1, 5.70, 5.21, 4.1-3.8, 2.4-2.3, 1.8-0.7; UV-Vis (λ_{max}) in THF solution 509 nm

PPV-Pc (Method 2) 50 mg copolymer was dissolved before adding. Pc-azide (31 mg, 0.036 mmol), distilled PMDETA (0.3 mg, 0.0018 mmol) and Cu(I)Br (0.3 mg, 0.0018 mmol). 60 mg PPV-Pc was isolated (89 % yield). GPC (THF) M_w: 302 000, M_w/M_n: 4.0; FT-IR (NaCl, cm^{-1}): 3058, 2959, 2927, 2869, 1737, 1504, 1464, 1414, 1385, 1351, 1260, 1205, 1027, 970, 862, 800; ^{1}H-NMR (300 MHz, THF-d_8): δ = 9.58-9.38, 8.30, 8.11, 7.90, 7.55-7.4, 7.3-7.1, 5.70, 5.21, 4.1-3.8, 2.4-2.3, 1.8-0.7; UV-Vis (λ_{max}) in THF solution 509 nm

4.6 Solar cell characteristics of best devices of each polymer: PCBM combination

Polymer:PCBM	J_{sc} (mA/cm²)	V_{oc} (V)	*FF*	*MPP*	Layer thickness (nm)
PT-COOEt 10% (1:1)	5.81	0.65	0.49	1.86	73
PT-Pc 8% (1:2)	1.79	0.67	0.34	0.41	42
PT-Pc 8% (1:1)	1.46	0.68	0.33	0.32	33
PT-Pc 4% (1:2)	1.52	0.70	0.31	0.33	45
PT-Pc 4% (1:1)	0.75	0.70	0.28	0.15	22
PPV-C≡C (1:4)	4.25	0.85	0.62	2.22	80
PPV-Pc (1:4)	3.36	0.66	0.35	0.77	100

Acknowledgements

The authors gratefully acknowledge the funding of the Ph.D. grant of B. J.C. by the Institute for the Promotion of Innovation through Science and Technology in Flanders (IWT-Vlaanderen), as well as the received support from the European Science Foundation (ESF) for the activity entitled 'New Generation of Organic based Photovoltaic Devices'.

5. References

[1] G. Dennler, M. C. Scharber, C. J. Brabec, *Adv. Mater.* **2009**, *21*, 1323.
[2] B. C. Thompson, J. M. J. Frechet, *Angew. Chem. Int. Edit.* **2008**, *47*, 58.
[3] M. C. Scharber, D. Wuhlbacher, M. Koppe, P. Denk, C. Waldauf, A. J. Heeger, C. L. Brabec, *Adv. Mater.* **2006**, *18*, 789.
[4] M. A. Green, K. Emery, Y. Hishikawa, W. Warta, *Progr. Photovoltaics* **2009**, *17*, 320.
[5] Y. Y. Liang, D. Q. Feng, Y. Wu, S. T. Tsai, G. Li, C. Ray, L. P. Yu, *J. Am. Chem. Soc.* **2009**, *131*, 7792.
[6] A. Hadipour, B. de Boer, P. W. M. Blom, *Adv. Funct. Mater.* **2008**, *18*, 169.
[7] J. Y. Kim, K. Lee, N. E. Coates, D. Moses, T. Q. Nguyen, M. Dante, A. J. Heeger, *Science* **2007**, *317*, 222.
[8] A. de la Escosura, M. V. Martinez-Diaz, D. M. Guldi, T. Torres, *J. Am. Chem. Soc.* **2006**, *128*, 4112.
[9] G. Bottari, D. Olea, C. Gomez-Navarro, F. Zamora, J. Gomez-Herrero, T. Torres, *Angew. Chem. Int. Ed.* **2008**, *47*, 2026.
[10] M. Quintiliani, A. Kahnt, T. Wolfle, W. Hieringer, P. Vazquez, A. Gorling, D. M. Guldi, T. Torres, *Chem. - Eur. J.* **2008**, *14*, 3765.
[11] M. V. Martinez-Diaz, S. Esperanza, A. De la Escosura, M. Catellani, S. Yunus, S. Luzzati, T. Torres, *Tetrahedron Lett.* **2003**, *44*, 8475.
[12] M. K. R. Fischer, I. Lopez-Duarte, M. M. Wienk, M. V. Martinez-Diaz, R. A. J. Janssen, P. Bauerle, T. Torres, *J. Am. Chem. Soc.* **2009**, *131*, 8669.
[13] D. Placencia, W. N. Wang, R. C. Shallcross, K. W. Nebesny, M. Brumbach, N. R. Armstrong, *Adv. Funct. Mater.* **2009**, *19*, 1913.
[14] Y. Y. Lin, T. H. Chu, S. S. Li, C. H. Chuang, C. H. Chang, W. F. Su, C. P. Chang, M. W. Chu, C. W. Chen, *J. Am. Chem. Soc.* **2009**, *131*, 3644.
[15] B. C. O'Regan, I. Lopez-Duarte, M. V. Martinez-Diaz, A. Forneli, J. Albero, A. Morandeira, E. Palomares, T. Torres, J. R. Durrant, *J. Am. Chem. Soc.* **2008**, *130*, 2906.
[16] J. K. J. Van Duren, X. Yang, J. Loos, C. W. T. Bulle-Lieuwma, A. B. Sieval, J. C. Hummelen, R. A. J. Janssen, *Adv. Funct. Mater.* **2004**, *14*, 425.
[17] H. G. Gilch, W. L. Wheelwright, *J. Polym. Sci.: A* **1966**, *4*, 1337.
[18] R. A. Wessling, *J. Polym. Sci. Pol. Sym.* **1985**, *72*, 55.
[19] L. Lutsen, P. Adriaensens, H. Becker, A. J. Van Breemen, D. Vanderzande, J. Gelan, *Macromolecules* **1999**, *32*, 6517.
[20] I. Osaka, R. D. McCullough, *Acc. Chem. Res.* **2008**, *41*, 1202.

[21] R. D. McCullough, *Adv. Mater.* **1998**, *10*, 93.
[22] B. J. Campo, W. D. Oosterbaan, J. Gilot, T. J. Cleij, L. Lutsen, R. A. J. Janssen, D. Vanderzande, in *Proceedings of SPIE*, **2009** 7416-53.
[23] Y. Kim, S. Cook, S. M. Tuladhar, S. A. Choulis, J. Nelson, J. R. Durrant, D. D. C. Bradley, M. Giles, I. McCulloch, C. Ha, M. Ree, *Nat. Mater.* **2006**, *5*, 197.
[24] B. Ballesteros, G. de la Torre, T. Torres, G. L. Hug, G. M. A. Rahman, D. M. Guldi, *Tetrahedron* **2006**, *62*, 2097.
[25] V. V. Rostovtsev, L. G. Green, V. V. Fokin, K. B. Sharpless, *Angew. Chem. Int. Ed.* **2002**, *41*, 2596.
[26] B. Ballesteros, G. de la Torre, C. Ehli, G. M. A. Rahman, F. Agullo-Rueda, D. M. Guldi, T. Torres, *J. Am. Chem. Soc.* **2007**, *129*, 5061.
[27] S. Campidelli, B. Ballesteros, A. Filoramo, D. D. Diaz, G. de la Torre, T. Torres, G. M. A. Rahman, C. Ehli, D. Kiessling, F. Werner, V. Sgobba, D. M. Guldi, C. Cioffi, M. Prato, J. P. Bourgoin, *J. Am. Chem. Soc.* **2008**, *130*, 11503.
[28] J. Duchateau, L. Lutsen, D. Vanderzande, T. J. Cleij, **2009**.
[29] B. J. Campo, J. Gilot, H. J. Bolink, J. Zhao, J. C. Bolsée, W. D. Oosterbaan, S. Bertho, B. Ruttens, J. D'Haen, T. J. Cleij, J. Manca, L. Lutsen, G. Van Assche, R. A. J. Janssen, D. Vanderzande, **2009**, as in chapter 4
[30] B. Neises, W. Steglich, *Angew. Chem. Int. Ed.* **1973**, *17*, 522.
[31] T. L. Benanti, A. Kalaydjian, D. Venkataraman, *Macromolecules* **2008**, *41*, 8312.
[32] J. Hou, L. Hou, C. He, C. Yang, Y. Li, *Macromolecules* **2005**, *39*, 594.
[33] S. E. Shaheen, C. J. Brabec, N. S. Sariciftci, F. Padinger, T. Fromherz, J. C. Hummelen, *Appl. Phys. Lett.* **2001**, *78*, 841.
[34] F. Padinger, R. S. Rittberger, N. S. Sariciftci, *Adv. Funct. Mater.* **2003**, *13*, 85.

Chapter Six:

Increased morphological stability in side-chain functionalized poly(3-alkylthiophene):fullerene bulk heterojunction solar cells[5]

Abstract: In P3HT:PCBM solar cells, the BHJ morphology of the interpenetrating network in the active layer is critical for high device efficiency. Here, an increased thermal stability of morphology is presented in blends of PCBM with side chain functionalized P3HT-based random copolymers. The increased thermal morphological stability is visualized in optical micrographs of the blend and results in a more stable J_{sc} and efficiency when devices are kept at 100 or 125 °C for at least 100 h. Decreased crystalline order in the copolymer:PCBM blends compared to P3HT:PCBM is visible in XRD. The crystallization kinetics in the blend are affected, as illustrated by DSC measurements, slowing down phase separation and resulting in thermally more stable active layers in solar cells.

1. Introduction

Recently, solar cells with a polymer:fullerene blend in the active layer and power conversion efficiencies (PCE) above 6% have been reported.[1, 2] Design and synthesis of materials, combined with new device architectures and processing techniques are responsible for the consecutive improvements that pave the way towards commercialization.[3-8] Because of the limited

[5] To be submitted by B. J. Campo, J. Zhao, S. Bertho, B. Ruttens, W. D. Oosterbaan, G. Van Assche, J. Manca, J. D'Haen, T. J. Cleij, L. Lutsen, B. Van Mele and D. Vanderzande

exciton diffusion length in organic semi conductors (typically ~10 nm), the nano-scale interpenetrating bulk heterojunction (BHJ) network of the polymer (electron donor) and fullerene (electron acceptor) is essential to dissociate created excitons and to collect charges at the electrode.[9, 10] A blend for which the morphology has been thoroughly investigated is poly(3-hexylthiophene) (P3HT): [6,6]-phenyl-C_{61}-butyric acid methyl ester (PCBM).[9, 11, 12] Regioregular P3HT tends to self-organize, favoring a phase separated morphology and stacking of the polymer chains, resulting in efficient exciton dissociation, high charge mobility and PCE.[4, 13, 14] PCBM, a soluble C_{60} derivative, forms crystalline needles in the P3HT:PCBM blend upon prolonged heating, indicating the intrinsic thermal instability of the blend morphology that endangers the long term device stability.[12, 15] The tendency for the P3HT and PCBM to crystallize and extensive phase separation to occur, depends on polymer characteristics such as regioregularity, the weight fraction of PCBM and the temperature to which the device is exposed.[13, 14, 16-18] The ongoing phase separation decreases the surface of the donor/acceptor interface, so there are less excitons separated and therefore the current and efficiency in the solar cell decrease in time.[19] It has been reported that the morphological stability may be increased by the use of non crystalline fullerene derivatives,[20] compatibilizing compounds,[21, 22] materials with high T_g[19, 23] or by crosslinking the material in the active layer.[24-26] In this communication, solar cells with blends of side chain functionalized P3HT-based copolymers and PCBM with an increased thermal morphological stability are reported.

2. Experimental part

Monomer and polymer synthesis is reported elsewhere.[27] Synthesis that has not been described before and characterization for **P3** is added to the supporting information (Supporting figure 1). All blends of polymer:PCBM were made in a 1/1 ratio (w/w). Optical micrographs were taken from blends spin-coated on silicon substrates. Solar cells were made on glass ITO-patterned substrates. All substrates were cleaned with sonicating in soapy water, Mili-Q water, acetone and heated in isopropanol followed by a UV/O_3 treatment. To prepare solar cells, a PEDOT:PSS (Baytron P) layer was spincoated from aqueous solution on the ITO electrode. The polymer:PCBM (1:1) blend was spincoated from a 10 mg mL^{-1} polymer solution in chlorobenzene and annealed for 15 minutes at 100 °C on a hotplate. As a cathode, typically 20 nm Ca and 80 nm Al were deposited in high vacuum (p = 1.10^{-6} mbar). *I-V* measurements were performed in N_2 atmosphere under AM 1.5G simulation, using an Oriel simulator equipped with a 150 W Xenon short arc lamp.

Accelerated life testing was done in a heating chamber which was developed for this purpose. The solar cells were kept in the dark, lighting only for *I-V* characterization every 30 minutes, while the experiments' temperature was kept constant. Solar cell characteristics are given relative to their initial value at time t_0 at the experiments' temperature. XRD measurements were done on a Siemens D5000 diffractometer in θ-2 θ mode. The incident beam used is the CuKα1 line of a Ge(111) monochromator, with a λ = 0.154056 nm. Differential scanning calorimetry (DSC) was done to measure the melting temperature (T_m) and melting enthalpy (ΔH_m) on a TA Instruments Q2000 (Tzero™) with Refrigerator Cooling System (RCS)

and nitrogen 50 mL min^{-1}, aluminum Tzero crucible at a scan rate of 10.0 K min^{-1}. The first cooling and second heating run were used for discussion.

3. Results and discussion

The synthesis and application in BHJ solar cells of the P3HT-based random copolymers poly[(3-hexylthiophene-2,5-diyl)-*co*-(3-[R]thiophene-2,5-diyl)] with R = 2-acetoxyetheyl (**P1**), 2-hydroxyethyl) (**P2**) and 2-cinnamoyloxyethyl (**P3**) (Figure 2) is reported elsewhere.[27, 28]

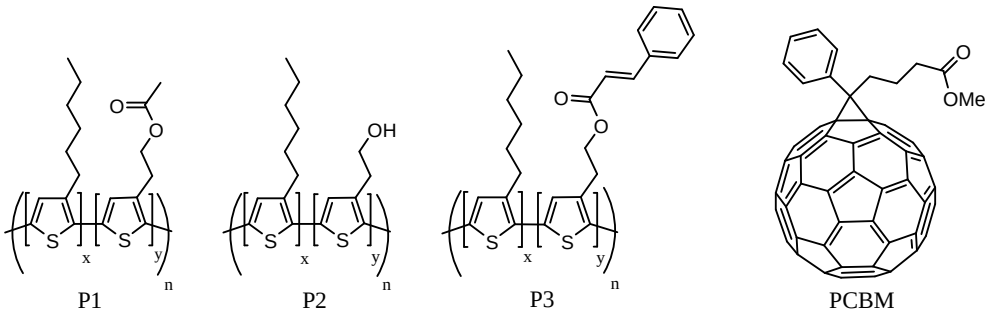

Figure 1: Structures of the side chain functionalized P3HT-based random copolymers and the soluble C60 derivative PCBM

The thermal stability of the side-chain functionalized copolymers as measured with TGA is somewhat lower compared to P3HT (Supporting figure 2), but thermal degradation starts only well above the testing temperatures used for BHJSC. The performance of these copolymers in BHJ solar cells depends on the percentage of the functionalized side chains in the copolymer. The short circuit current (J_{sc}) and PCE decrease with a higher percentage of functionalized side chains, due to the disturbing effect of the functionalized side chains on polymer organization because they - partially - prevent the stacking of the conjugated backbones.[28] Lower melting enthalpies of the copolymers compared to P3HT, measured with Differential Scanning Calorimetry (DSC), indicate a lower percentage of crystalline

material with higher percentages of functionalized side chains. The decreased crystallinity in copolymers causes a lower photocurrent and solar cell power conversion efficiency.[27, 28]

3.2 Decreased PCBM crystallization upon annealing of copolymer:PCBM blends

In optical microscopy pictures of polymer:PCBM (1:1, w/w) blends (figure 2), it is observed that after 15 minutes at 125°C there are plenty of µm-scale PCBM crystals visible for the P3HT:PCBM blend. These needle-like crystals are created when PCBM diffuses out of the blend and crystallizes.[18] In blends of the copolymers with PCBM however, the needle formation is suppressed. After 15 minutes at 125 °C for **P2** 9/1 there are no needles visible at all, for **P3** 9/1 occasionally a PCBM needle can be found.

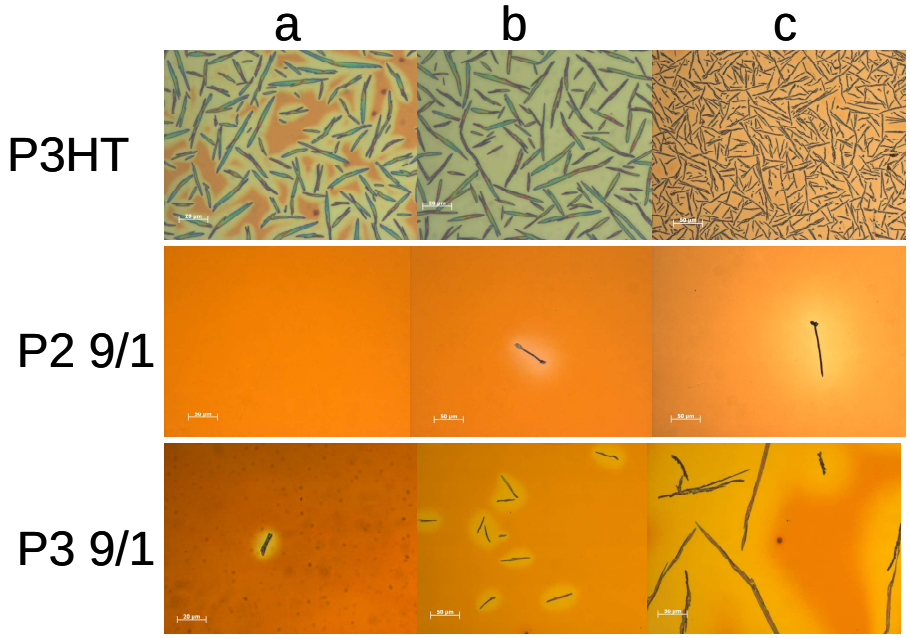

Figure 2. Needle-like PCBM crystals in optical micrographs of polymer:PCBM (1:1) blends annealed at 125°C for a) 15 minutes b) 2 hours and c) 24 hours. The scale bar is 50 µm.

With longer annealing times, the number of PCBM crystals increases strongly in the P3HT:PCBM blend but only slightly in the copolymer:PCBM blends, indicating a thermally more stable morphology in the copolymer blends. It is clear that the decreased crystalline behaviour of the copolymers also decreases the PCBM crystallization when the blends are annealed for a longer time at 125 °C. The lower tendency of the copolymers, compared to P3HT, to self-organize is reflected in an augmented thermal stability of the polythiophene:PCBM blend morphology. That polymer crystallization affects the PCBM crystal formation has been shown before for P3HT in a series with differing regioregularity.[17] Here, when copolymers with a higher percentage of functionalized side chains are used, the polymer stacking is disturbed more strongly. With an increasing degree of functionalization, less PCBM crystals were observed (supporting figure 3).

3.3 Decreased crystallization rate in copolymer:PCBM blends

X Ray Diffraction (XRD) and Differential Scanning Calorimetry (DSC) were performed on copolymer:PCBM blends to collect more information on the crystallization phenomena. In P3HT:PCBM blends spin-coated from chlorobenzene, the lamellar stacking in P3HT with d-spacing around 17.0 Å is in accordance with literature values.[13] Upon annealing, the diffraction peak narrows, caused by a directional alignment of polymer chains. In **P3** 9/1:PCBM blends, no crystalline signal is visible in films spincoated from PCBM. Upon annealing 15 minutes at 125°C, the crystalline diffraction signal was detected but this was broader compared to P3HT, indicating that the orientation of the formed crystallites is less defined.

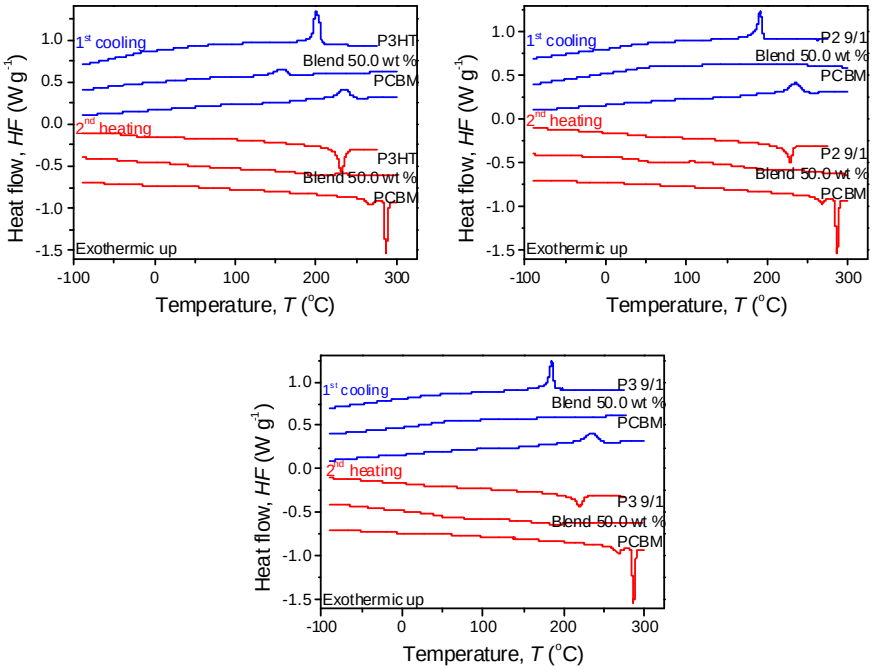

a)

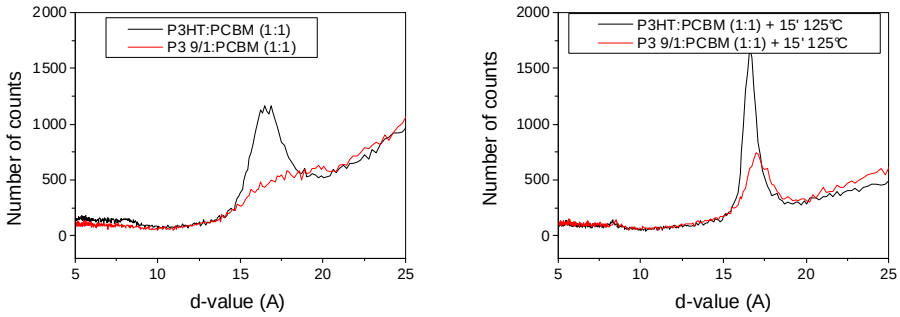

b)

Figure 3: a) DSC curves of P3HT, **P2** 9/1 and **P3** 9/1 and PCBM, and their respective 1:1 (w/w) blends, b) d-values obtained from XRD diffraction patterns of P3HT:PCBM (1:1) blends before and after annealing

The heating and cooling curves for P3HT, the **P2** 9/1 and **P3** 9/1 copolymers and their (1/1) blends with PCBM are displayed in Figure 3 a, b and c, respectively. For P3HT:PCBM blends there is a single crystallization

peak visible in the first cooling curve, comparable to what was reported before.[30] At the same scan rate of 10 K min^{-1} however, no crystallization can be measured for the copolymer:PCBM blends. Although the crystallization of PCBM is visible in optical microscopy and the crystalline stacking in the copolymer was clear in XRD, the presence of functionalized side chains affected the crystallization kinetics of the two materials in the blend in such a way that no melting or crystallization could be detected with DSC.

3.4 Increased thermal stability in copolymer:PCBM solar cells

To verify if the increased thermal morphological stability in the blend was also reflected on the thermal stability of the BHJSC, several ITO/PEDOT:PSS/polymer:PCBM(1:1)/Ca/Al devices were subjected to higher temperatures for a specific time. The efficiencies, relative to the first measurement at the experiments' temperature, are displayed in Figure 4. The relative efficiency of P3HT:PCBM solar cells are displayed in Figure 4a as a function of time for several temperatures. At 80 °C, the device efficiency is fairly constant for at least 100 h. At 100 °C and 125 °C, the efficiency of the P3HT:PCBM device decreases increasingly fast. When looking at the device parameters (supporting information), the degradation of J_{sc} is largely responsible for the decreasing efficiency. As the phase separation continues in the blend morphology, and proceeds increasingly fast with higher temperatures within a certain range, less excitons are dissociated and less current is generated, therefore J_{sc} is the most appropriate parameter to correlate with morphological stability.[29] The decrease in *FF* and V_{oc} may also be related to reorganization effects in the

blend, but other ageing mechanisms can not be excluded at these temperatures and in this time interval.

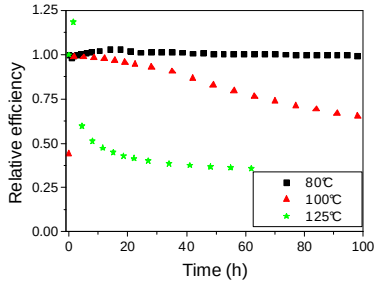

a)

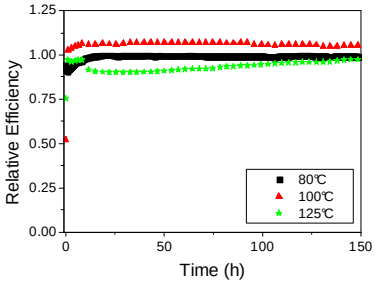

b)

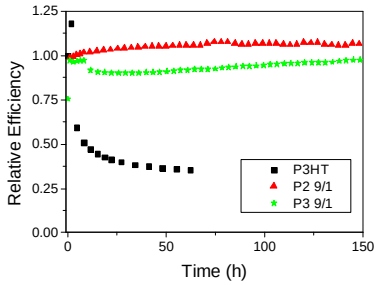

c)

Figure 4. Efficiency as a function of time for ITO/PEDOT/polymer:PCBM (1:1)/Ca/Al solar cells with a) P3HT at 80°C (squares), 100°C (triangles) and 125°C (stars) b) **P3** 9/1 at 80°C (squares), 100°C (triangles) and 125°C (stars) c) P3HT (squares), **P2** 9/1 (triangles) and **P3** 9/1 (stars) at 125°C.

In Figure 3b, the evolution of **P3** 9/1 copolymer solar cells efficiency is given at several temperatures. Here, the efficiency is less dependent on temperature, and is quite stable even at 125 °C for 150 h. From the device parameters (supporting figure 5), the constant J_{sc} points to a thermally more stable morphology in the **P3** 9/1:PCBM solar cells: after 150 h no degradation of the photocurrent could be observed. The *FF* and V_{oc} showed fluctuations of about 10% relative to the initial value throughout the testing period. In Figure 3c, the device efficiency of P3HT solar cells at 125 °C is

compared to that of devices made with **P2** 9/1 and **P3** 9/1 copolymer blends. The J_{sc} and efficiency of the P3HT solar cells decreases much more rapidly compared to the copolymer solar cells. The morphology in a copolymer:PCBM blend is much less sensitive to reorganization compared to P3HT, resulting in the increased thermal stability of copolymer:PCBM solar cells. Introducing 10% of functionalized side chains does not affect the PCE significantly when compared to P3HT:PCBM devices processed according to the same procedure, but increases the morphological stability.

4. Conclusion

Although there is some crystallization in a copolymer:PCBM blends (PCBM crystallization visible with optical microscopy, crystalline P3AT stacking in XRD), the presence of the functionalized side chains slows down the crystallization rate (not visible with DSC at 10 K min^{-1}) which stabilizes the blend morphology. The stable blend morphology in the device leads to a more stable photocurrent in solar cells at 125 °C. The increased thermal morphological stability for the 9/1 copolymers presents a compromise between high efficiency and increased thermal stability in polythiophene:fullerene bulk heterojunction solar cells.

5. References

[1] M. A. Green, K. Emery, Y. Hishikawa, W. Warta, *Progr. Photovoltaics* **2009**, *17*, 320.
[2] Y. Y. Liang, D. Q. Feng, Y. Wu, S. T. Tsai, G. Li, C. Ray, L. P. Yu, *J. Am. Chem. Soc.* **2009**, *131*, 7792.
[3] F. Padinger, R. S. Rittberger, N. S. Sariciftci, *Adv. Funct. Mater.* **2003**, *13*, 85.
[4] G. Li, V. Shrotriya, J. S. Huang, Y. Yao, T. Moriarty, K. Emery, Y. Yang, *Nat. Mater.* **2005**, *4*, 864.
[5] J. Peet, J. Y. Kim, N. E. Coates, W. L. Ma, D. Moses, A. J. Heeger, G. C. Bazan, *Nat. Mater.* **2007**, *6*, 497.
[6] J. Y. Kim, S. H. Kim, H. H. Lee, K. Lee, W. L. Ma, X. Gong, A. J. Heeger, *Adv. Mater.* **2006**, *18*, 572.

[7] N. Blouin, A. Michaud, D. Gendron, S. Wakim, E. Blair, R. Neagu-Plesu, M. Belletete, G. Durocher, Y. Tao, M. Leclerc, *J. Am. Chem. Soc.* **2008**, *130*, 732.
[8] C. N. Hoth, P. Schilinsky, S. A. Choulis, C. J. Brabec, *Nano Lett.* **2008**, *8*, 2806.
[9] X. Yang, J. Loos, *Macromolecules* **2007**, *40*, 1353.
[10] S. H. Park, A. Roy, S. Beaupre, S. Cho, N. Coates, J. S. Moon, D. Moses, M. Leclerc, K. Lee, A. J. Heeger, *Nature Photonics* **2009**, *3*, 297.
[11] H. Hoppe, N. S. Sariciftci, *J. Mat. Chem.* **2005**, *16*, 45.
[12] A. Swinnen, I. Haeldermans, M. vande Ven, J. D'Haen, G. Vanhoyland, S. Aresu, M. D'Olieslaeger, J. Manca, *Adv. Funct. Mater.* **2006**, *16*, 760.
[13] Y. Kim, S. Cook, S. M. Tuladhar, S. A. Choulis, J. Nelson, J. R. Durrant, D. D. C. Bradley, M. Giles, I. McCulloch, C. Ha, M. Ree, *Nat. Mater.* **2006**, *5*, 197.
[14] W. Ma, C. Yang, X. Gong, K. Lee, A. J. Heeger, *Adv. Funct. Mater.* **2005**, *15*, 1617.
[15] M. Jorgensen, K. Norrman, F. C. Krebs, *Sol. Energ. Mat. Sol. C* **2008**, *92*, 686.
[16] K. Sivula, C. K. Luscombe, B. C. Thompson, J. M. J. Fréchet, *J. Am. Chem. Soc.* **2006**, *128*, 13988.
[17] C. H. Woo, B. C. Thompson, B. J. Kim, M. F. Toney, J. M. Fréchet, *J. Am. Chem. Soc.* **2008**, *130*, 16324.
[18] A. Swinnen, I. Haeldermans, P. Vanlaeke, J. D'Haen, J. Poortmans, M. D'Olieslaeger, J. V. Manca, *Eur. Phys. J. Appl. Phys.* **2006**, *36*, 251.
[19] S. Bertho, I. Haeldermans, A. Swinnen, W. Moons, T. Martens, L. Lutsen, D. Vanderzande, J. Manca, A. Senes, A. Bonfiglio, *Sol. Energ. Mat. Sol. C* **2007**, *91*, 385.
[20] Y. Zhang, H. L. Yip, O. Acton, S. K. Hau, F. Huang, A. K. Y. Jen, *Chem. Mater.* **2009**, *21*, 2598.
[21] Z. Y. Zhou, X. W. Chen, S. Holdcroft, , *J. Am. Chem. Soc.* **2008**, *130*, 11711.
[22] K. Sivula, Z. T. Ball, N. Watanabe, J. M. J. Frechet, *Adv. Mater.* **2006**, *18*, 206.
[23] F. C. Krebs, H. Spanggaard, *Sol. Energ. Mat. Sol. C* **2005**, *17*, 5235.
[24] M. Drees, H. Hoppe, C. Winder, H. Neugebauer, N. S. Sariciftci, W. Schwinger, F. Schaffler, C. Topf, M. C. Scharber, Z. G. Zhu, R. Gaudiana, *J. Mater. Chem.* **2005**, *15*, 5158.
[25] S. Miyanishi, K. Tajima, K. Hashimoto, *Macromolecules* **2009**, *42*, 1610.
[26] B. J. Kim, Y. Miyamoto, B. Ma, J. M. J. Fréchet, *Adv. Funct. Mater.* **2009**, *19*, 2273.
[27] B. J. Campo, W. D. Oosterbaan, J. Gilot, T. J. Cleij, L. Lutsen, R. A. J. Janssen, D. Vanderzande, in *Proceedings of SPIE*, **2009** 7416-53.
[28] B. J. Campo, J. Gilot, H. J. Bolink, J. Zhao, J. C. Bolsée, W. D. Oosterbaan, S. Bertho, B. Ruttens, J. D'Haen, T. J. Cleij, J. Manca, L. Lutsen, G. Van Assche, R. A. J. Janssen, D. Vanderzande, **2009**, as in chapter 4
[29] S. Schuller, P. Schilinsky, J. Hauch, C. J. Brabec, *Appl. Phys. A-Mater.* **2004**, *79*, 37.
[30] J. Zhao, A. Swinnen, G. Van Assche, J. Manca, D. Vanderzande, B. Van Mele, *J. Phys. Chem. B* **2009**, *113*, 1587.

Supporting information

Synthesis and characterization of **P3**

Hydrolysis of the ester functions is done post-polymerization by refluxing 1.04, 1.00 and 1.00 g of finely grounded copolymer **P1** 9/1, 7/3 and 1/1 respectively in 100 mL 0.2 M NaOH solution in MeOH for 24h. The mixture is poured out in 600 mL of a MeOH/2 M HCl mixture and stirred, copolymers P2 are filtered off and rinsed with H_2O and MeOH.

P2 9/1 (1.00g, 98%) UV-Vis (λ_{max} ,film) 520, 550infl, 600sh GPC (THF): M_n= 31 100 , M_w= 68 100, D= 2.2; FT-IR (KBr, cm^{-1}): 2953 and 2853 (C-H), 1640, 1508 and 1455 (C=C), 1376 (CH_3), 1292- 1046 and 821 cm^{-1} (C-H), 723 (CH_3) ^{1}H-NMR (300 MHz, $CDCl_3$, δ): 7.03, 7.01, 6.96 (1H, m, Th), 3.95 (2H, t, CH_2-OH), 3.09 (2H, t, α-CH_2CH_2-OH), 2.79 (2H, t, H-T α-CH_2), 2.56 (2H α-CH_2, 1.70 (2 H, m, β-CH_2 3-HT), 1.45 – 1.25 (6 H, m, γ, δ, ε-CH_2), 0.90 (3 H, t, CH_3)

P2 7/3 (0.9g, 95%) GPC (THF): M_n= 21 500, M_w= 42 100 , D= 2.0; ν_{max}(KBr)/cm^{-1} FT-IR (KBr, cm^{-1}): 2951, 2923 and 2853 (C-H), 1639, 1509 and 1455 (C=C), 1376 (CH_3), 1290, 1132, 1042 and 821 cm^{-1} (C-H) 722 (CH_3) ^{1}H-NMR (300 MHz, $CDCl_3$, δ): 7.05, 7.02 and 6.96 (1H, m, Th), 3.96 (2H, t, CH_2-OH), 3.10 (2H, t, α-CH_2CH_2-OH), 2.78 (2H, t, H-T α-CH_2), 2.56 (2H,br s, H-H α-CH_2), 1.69 – 1.23 (8 H, m, β, γ, δ, ε-CH_2), 0.90 (3 H, t, CH_3)

P2 1/1 (1.0g, 100%) GPC (THF): M_n= 9 500, M_w= 17 700, D= 1.9; FT-IR (KBr, cm^{-1}): 2920 and 2850 (C-H), 1639, 1508 and 1455 (C=C), 1376 (CH_3), 1298, 1230, 1142, 1038 and 823 cm^{-1} (C-H); ^{1}H-NMR (300 MHz, $CDCl_3$, δ): 7.02 and 6.96 (1H, m, Th), 3.96 (2H, t, CH_2-OH), 3.09 (2H, t, α-

CH_2CH_2-OH), 2.78 (2H, t, H-T α-CH_2), 1.68 – 1.23 (8 H, m, β, γ, δ, ε-CH_2), 0.90 (3 H, t, CH_3)

Esterification of the alcohol in **P2** was done by dissolving 600, 500 and 300 mg of the 9/1, 7/3 and 1/1 copolymer in THF, respectively. Triethylamine (15 mL) and 10 eq. of cinnamoylchloride were added. The reaction was stirred at room temperature overnight. After precipitation and filtration 610, 600 and 370 mg of the resulting copolymers **P3** were obtained after purification with Soxhlet extraction using acetone.

P3 9/1 UV-Vis (λ_{max} ,film) 553, 600sh; GPC (THF): M_n= 33 100, M_w= 74 500, D= 2.2; FT-IR (KBr, cm^{-1}):2956, 2923, 2853, 1711, 1635, 1505, 1449, 1375, 1306, 1259, 1158, 1075, 818; ^{1}H NMR (300 MHz, $CDCl_3$, δ): 7.70 and 7.65 (d, 1H, C=CH-Ph), 7.47 (m, 2H, CH_{Ph}), 7.32 (m, 2H, CH_{Ph}), 7.06 - 6.96 (m, H_{Th} and H_{ph}), 6.44 and 6.39 (d, 1H, COCH=C), 4.49 (t, 2H, CH_2O), 3.23 (t, 2H, α-CH_2), 2.79 (t, 2H, H-T α-CH_2 3-HT) and 2.56 (α-CH_2 3-HT), 1.70 (m, 2H, β-CH_2 3-HT), 1.46 – 1.25 (m, 6H, γ, δ, ε-CH_2 3-HT), 0.90 (t, 3H, CH_3)

P3 7/3 UV-Vis (λ_{max} ,film) 549 nm, sh 599 nm; GPC (THF): M_n= 25 300, M_w= 47 500, D= 1.9; FT-IR (KBr, cm^{-1}):2956, 2924, 2853, 1712, 1635, 1510, 1449, 1377, 1307, 1262, 1201, 1161, 1090, 1021, 804; ^{1}H NMR (300 MHz, $CDCl_3$, δ): 7.70 and 7.64 (d, 1H, C=CH-Ph), 7.46 (m, 2H, CH_{Ph}), 7.33 (m, 2H, CH_{Ph}), 7.12- 6.96 (m, H_{Th} and H_{ph}), 6.44 and 6.39 (d, 1H, COCH=C), 4.48 (t, 2H, CH_2O), 3.21 (t, 2H, α-CH_2), 2.77 (t, 2H, H-T α-CH_2 3-HT) and 2.56 (α-CH_2 3-HT), 1.67 - 1.31 (m, 6H, γ, δ, ε-CH_2 3-HT), 0.88 (t, 3H, CH_3)

P3 1/1 UV-Vis (λ_{max} ,film) 521; GPC (THF): M_n= 19 800, M_w= 40 300, D= 2.0; FT-IR (KBr, cm^{-1}): 3060, 2954, 2926, 2855, 1714, 1637, 1511, 1495,

1450, 1378, 1327, 1309, 1282, 1202, 1162, 1071, 978,862, 823, 766; ^{1}H NMR (300 MHz, $CDCl_3$, δ): 7.68 and 7.63 (d, 1H, C=CH-Ph), 7.46 (m, 2H, CH_{Ph}), 7.32 (m, 2H, CH_{Ph}), 7.12- 6.96 (m, H_{Th} and H_{ph}), 6.43 and 6.38 (d, 1H, COCH=C), 4.47 (t, 2H, CH_2O), 3.21 (t, 2H, α-CH_2), 2.76 (t, 2H, H-T α-CH_2 3-HT) and 2.56 (α-CH_2 3-HT), 1.67 – 1.23 (m, 2H, β-CH_2 3-HT), 1.30-1.23 (m, 6H, γ, δ, ε-CH_2 3-HT), 0.88 (t, 3H, CH_3)

Supporting Figure 1 a) ^{1}H-NMR spectra, b) DSC cooling and heating curves, c) MTDSC measurements of **P3** 9/1, 7/3 and 1/1 copolymers with respectively 10, 30 and 50 mol % of functionalized side chains

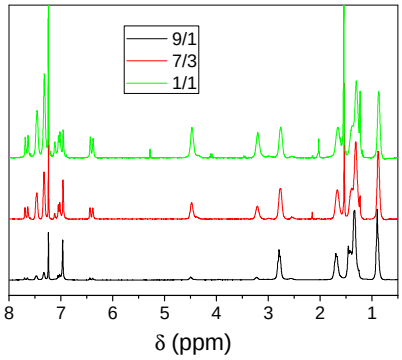

a)

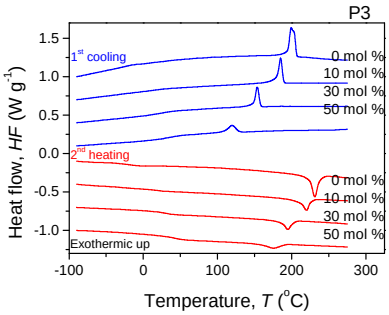

b)

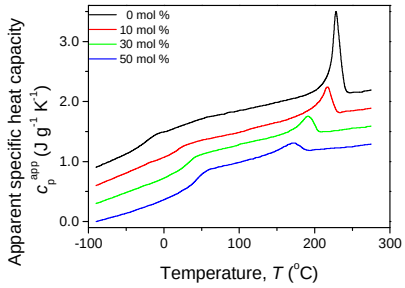

c)

Supporting Figure 2: Thermal Gravimetrical Analysis of copolymers a) **P1**, b) **P2**, and c) **P3**

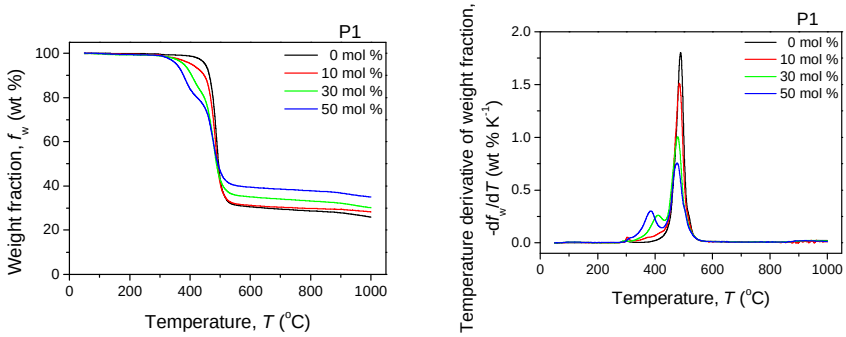

a)

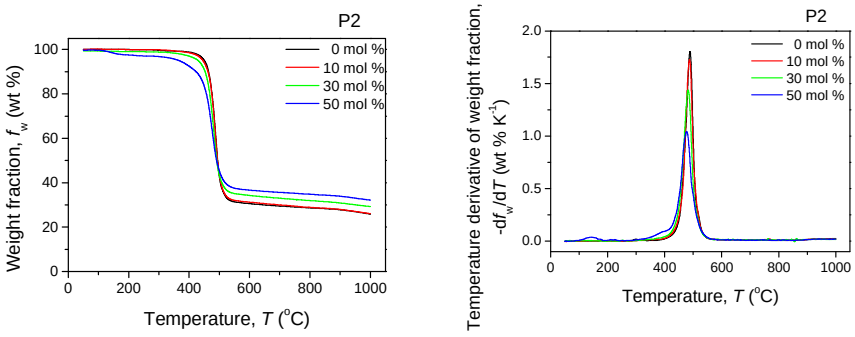

b)

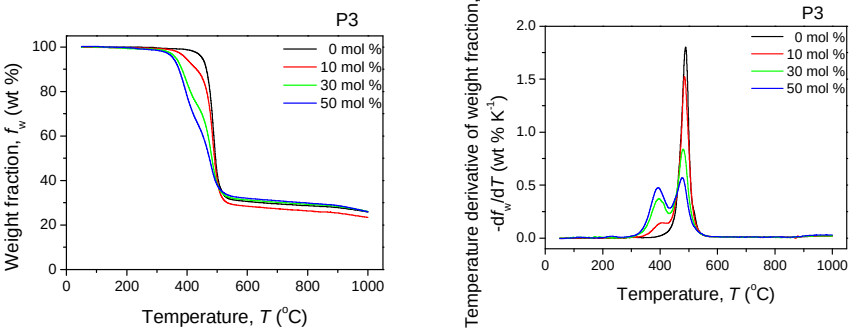

c)

Supporting Figure 3: Optical micrographs of co-polymer:PCBM (1:1, w/w) blends for **P1** (top) and **P3** (bottom) annealed at 125 °C for a) 15 minutes b) 2 hours c) 24 hours

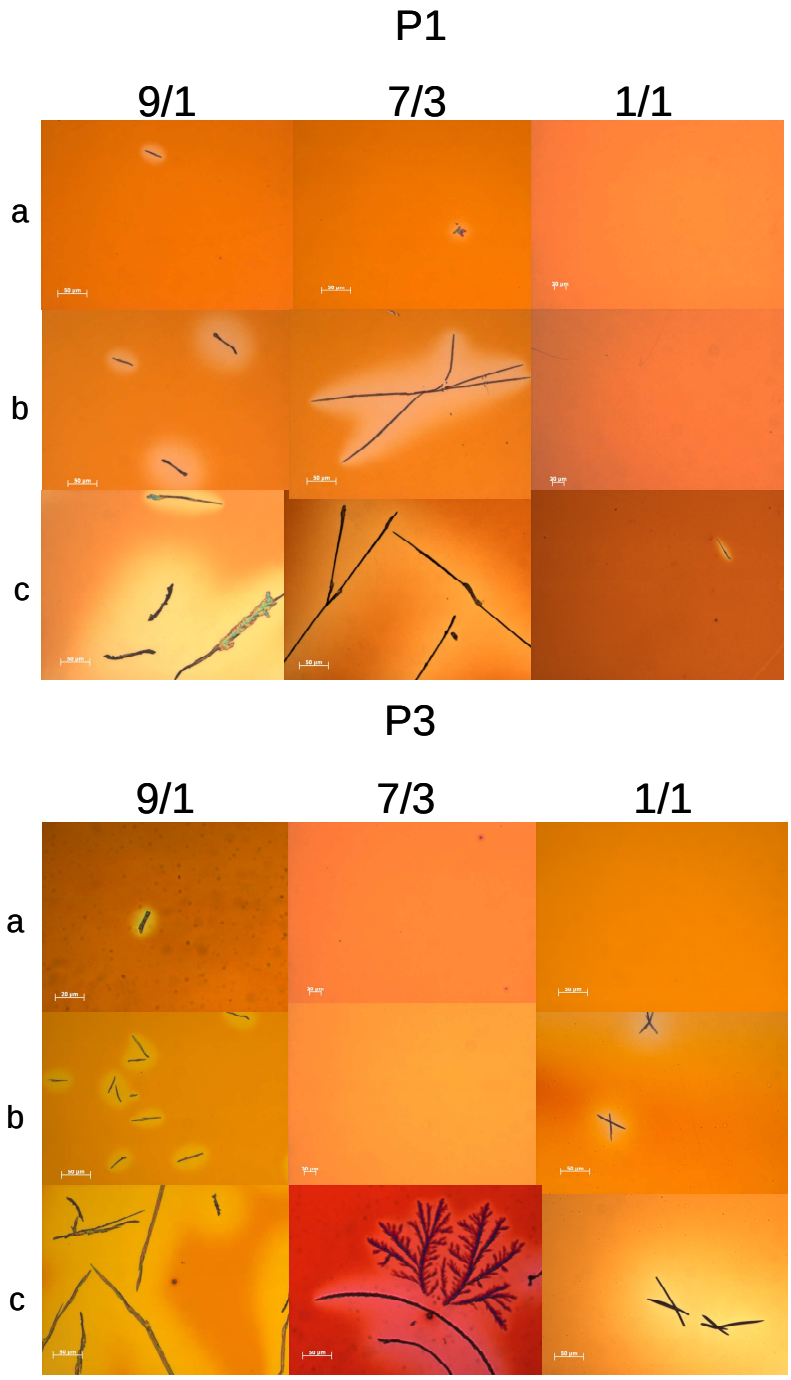

Supporting Figure 4: Characteristics of ITO/PEDOT/P3HT:PCBM (1:1)/Ca/Al solar cells at higher temperature as a function of time

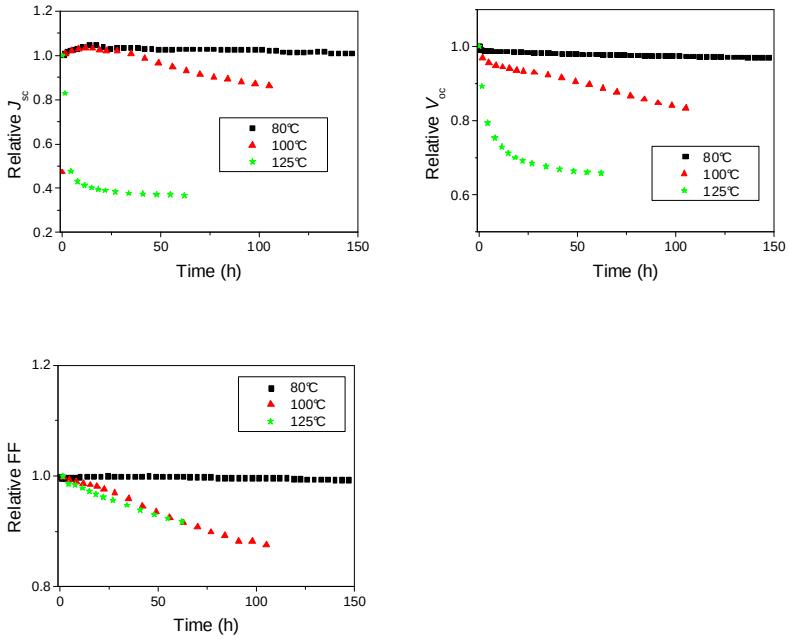

Supporting Figure 5: Characteristics of ITO/PEDOT/**P3** 9/1:PCBM (1:1)/Ca/Al solar cells at higher temperature as a function of time

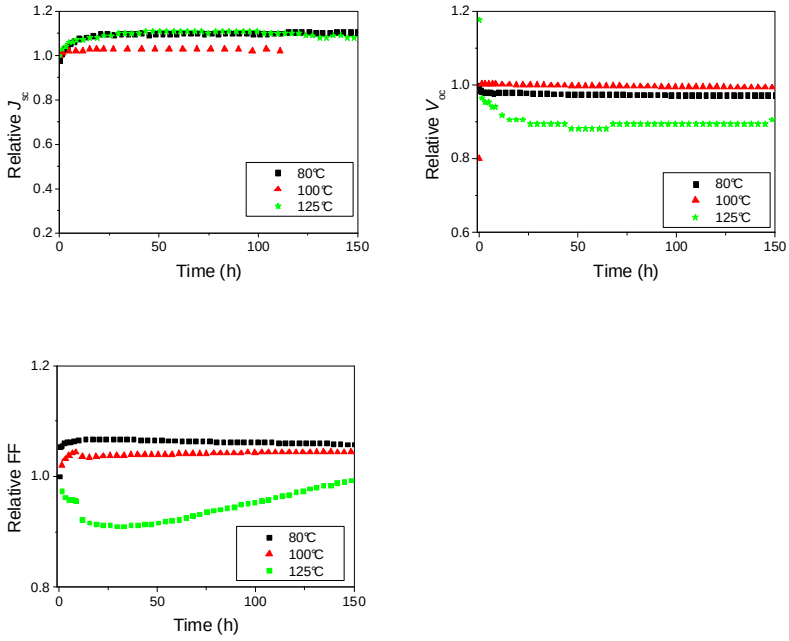

Summary

Conjugated polymers combine semi-conductive electrical properties with desirable mechanical properties such as light weight and high mechanical strength and flexibility. This enables the development of new technologies and applications based on these materials. Poly(3-hexylthiophene) is a conjugated polymer that has been extensively investigated in polymer:fullerene bulk heterojunction solar cells. In **chapter 1**, several synthetic routes and the regioregularity of the resulting polymer structure are discussed. As the most important application of P3HT, the bulk heterojunction solar cell with PCBM is introduced. P3HT-based copolymers are presented as a possible route to further improve the performance of P3HT:PCBM solar cells. Every following chapter is a (draft for) manuscript for publication.

The oxidative polymerization with $FeCl_3$ is used to synthesize copolymers based on P3HT, as reported in **chapter 2**. Non-regioregular copolymers of 3-HT with thiophenes containing the ester analogue of an alcohol or acid groups in the side-chain are synthesized. Generally, the molecular weight and reaction yield lowers with an increasing percentage of functionalized side chains because of a decreasing solubility. The copolymers of the type Poly([3-hexylthiophene-2,5-diyl]-*co*-[3-(R)thiophene-2,5-diyl]) are used as a template for further reactions on the R group: the functionalized side chains. After hydrolysis of the ester groups, the versatile alcohol and acid functions are subjected to functionalization with other molecules. This way, a variety of crosslinkable functional groups is introduced into the polymer side chain. The compatibility of an ester group in the side chain with electronic performance is shown in a polymer LED.

In **chapter 3**, the design and synthesis of the same type of P3HT-based copolymers as in chapter 2 is presented using the Rieke method. This method gives a more regioregular polymer. A preliminary study of the impact of the functionalized side chains on polymer properties is done. The UV-Vis absorption of the polymer and the polymer blends with PCBM is correlated with the performance of these blends in bulk heterojunction solar cells. It is observed that an increasing percentage of functionalized side chains disturb the polymer organization in a polymer film and blend. A larger side chain functional group has a stronger effect on the π-π stacking of the conjugated polymer backbones.

The effect of the introduced side chains is investigated in more detail for two regioregular copolymer series in **chapter 4**. That the produced copolymers are in fact random copolymers is observed in ^{1}H-NMR. The percentage of functionalized co-monomers in the monomer feed varies from 10 to 30 and 50%, corresponding to the percentage of functionalized side chains in the copolymer. Thermal characterization shows that copolymers with a higher percentage of functionalized side chains have a lower melting temperature and enthalpy, an indication of less perfect crystalline ordering. The solid phase-structure of copolymers containing 50% of functionalized side chains is studied with XRD and TEM. A larger functionalized side chain increases the lamellar stacking distance and disturbs the π-π stacking more strongly. The decreasing crystalline order as an effect of the side chain functionalities causes a decrease in hole mobility, as measured in OFETs. With appropriate processing conditions however, the decrease in solar cell performance is limited for smaller side chain functionalities. The copolymers containing 10% of side chains perform even better as compared to devices with P3HT, processed in the same conditions.

A strategy to increase device efficiency is probed in **chapter 5**. Using post-polymerization functionalization, an alkyne functionalized copolymer is synthesized. A Phthalocyanine (Pc) with an azide group allows to use click chemistry so that conversion of triple bonds is complete. The polymer- Pc system absorbs a broader range of wavelengths, as evidenced in the UV-Vis absorption. A broader absorption window allows the active layer in solar cells to absorb more energy. The spectral response shows that the Pc absorption contributes to photocurrent generation. The device performance in polymer-Pc:PCBM solar cells however, is lower as compared to the original polymer:PCBM devices, due to the low solubility of the polymer-Pc in the processing solvent.

Finally, in **chapter 6**, the impact of the functionalized side chains on thermal morphological stability of a polymer:PCBM bulk heterojunction blend is discussed. In optical micrographs, a lower amount of PCBM crystals is visible after thermal annealing in copolymer:PCBM blends as compared to P3HT:PCBM blends. Even for 9/1 copolymers, containing 10% of functionalized side chains, the difference with P3HT is remarkable. In solar cells with copolymer:PCBM blends, the current is stable for a longer time at higher temperatures. DSC and XRD data indicate that 10% of functionalized side chains interfere with polymer crystallization, disturb and thus slow down the reorganization by crystallization. Using 9/1 copolymers of P3HT, a thermally more stable blend morphology is obtained, while comparable efficiencies were reached in chapter 4.

Samenvatting

Geconjugeerde polymeren combineren halfgeleidende elektrische eigenschappen met gewenste mechanische eigenschappen: ze zijn licht, sterk en plooibaar. Dit laat toe om nieuwe technologieën en toepassingen te ontwikkelen, gebaseerd op deze materialen. Poly(3-hexylthiofeen) (P3HT) is een geconjugeerd polymeer dat uitgebreid werd onderzocht voor toepassing in polymeer:fullereen bulk heterojunctie zonnecellen. In **hoofdstuk 1** worden verschillende syntheseroutes en de regioregulariteit van de resulterende polymeren besproken, evenals de belangrijkste toepassing van P3HT: de bulk heterojunctie zonnecel met PCBM. Copolymeren gebaseerd op P3HT worden voorgesteld als een mogelijke route om de prestaties van P3HT:PCBM zonnecellen te verbeteren.

De oxidatieve polymerisatie met $FeCl_3$ wordt gebruikt om copolymeren gebaseerd op P3HT te synthetiseren, zoals voorgesteld in **hoofdstuk 2**. Niet-regioregulaire copoymeren worden gesynthetiseerd van 3-HT met thiofenen die de ester-analogen van een zuur of alcohol-groep in de zijketen bevatten. Algemeen liggen het moleculair gewicht en de reactie opbrengst lager met een toenemend percentage gefunctionaliseerde zijketens, veroorzaakt door een dalende oplosbaarheid. De copolymeren van het type type Poly([3-hexylthiofeen-2,5-diyl]-*co*-[3-(R)thiofeen-2,5-diyl]) worden gebruikt als template voor verdere reacties op the R groep. Na hydrolyse van de esterfuncties, wordt de chemische veelzijdigheid van de zuur- en alcoholgroep geïllustreerd door verdere reactie met verschillende moleculen. Alzo wordt een verscheidenheid aan vernetbare functionele groepen in de zijketen gebouwd. De compatibiliteit van een ester groep met een elektronische toepassing wordt aangetoond voor een polymere LED.

In **hoofdstuk 3** wordt het ontwerp van hetzelfde type copolymeren als in hoofdstuk 2 voorgesteld, samen met de synthese door de Rieke methode. Deze methode leidt tot een meer regioregulair polymeer. Een studie van de impact van de gefunctionalizeerde zijketens op de eigenschappen van het polymeer wordt gedaan door correlatie van de UV-Vis absorptie van het polymeer en de polymeer blends met PCBM enerzijds met de prestatie van deze blends in bulk heterojunctie zonnecellen anderzijs. Een hoger percentage functionele groepen verstoort de organisatie van het polymeer in film en in blend. Een grotere gefunctionaliseerde zijketen heeft een sterkere invloed op de π-π ordening van de geconjugeerde polymeerketen.

Het effect van de ingevoerde zijketens wordt meer gedetailleerd onderzocht in **hoofdstuk 4** voor twee reeksen regioregulaire copolymeren. Deze copolymeren zijn random copolymeren, zoals geobserveerd in ^{1}H-NMR. Het percentage aan gefunctionaliseerde co-monomeren in het monomeer mengsel komt overeen met het percentage functionele groepen in het copolymeer en wordt gevarieerd van 10 naar 30 en 50%. Thermische karakterisatie toont dat copolymeren met een hoger percentage aan gefunctionaliseerde zijketens een lagere smelttemperatuur en enthalpie hebben in vergelijking met P3HT, een indicie van een minder perfecte kristallijne ordening. De structuur in vaste fase van copolymeren met 50% functionele groepen wordt bestudeerd met X-straal en elecrond diffractie. Een grotere gefunctionaliseerde zijketen veroorzaakt een toename van de afstand tussen twee lagen en verstoort de π-π ordening. De dalende orde heeft een lagere gaten mobiliteit als gevolg, gemeten in OFETs. Met aangepaste omstandigheden tijdens de verwerking tot zonnecellen is het effect op de prestatie van de zonnecelen eerder beperkt. Copolymeren met

10% functionele groepen presteren zelfs beter in vergelijking met P3HT in zonnecellen, als deze gemaakt worden volgens zelfde procedure.

Een strategie om de efficientie in zonnecellen te verhogen wordt aangereikt en uitgediept in **hoofdstuk 5**. Door middel van post-polymerisatie functionalisatie wordt een alkyn-gefunctionaliseerd copolymeer verkregen. In cominatie met een azide bevattend Phthalocyanine (Pc) wordt “click chemie” toegepast om volledige reactie van de driedubbele binding te verkrijgen. Het polymeer-Pc gekoppelde systeem heeft een bredere absorptie, hetgeen wordt aangetoond met UV-Vis spectroscopie. Omdat er meerdere golflengtes geabsorbeerd worden, kan de zonnecel meer energie opnemen. De spectrale respons toont dat de Pc absorptie ook daadwerkelijk in elektrische energie wordt omgezet. De efficientie van polymeer-Pc:PCBM ligt echter lager dan de efficientie van polymeer:PCBM in zonnecellen omwille van de lagere oplosbaarheid in het gebruikte solvent.

Tenslotte wordt in hoofdstuk 6 het effect van de gefunctionaliseerde zijketens op de thermische stabiliteit van de polymeer:PCBM morfologie besproken. Na annealing zijn met optische microscopie een lager aantal PCBM kristallen zichtbaar in copolymeer:PCBM blends in vergelijking met P3HT:PCBM blends. Zelfs voor 9/1 copolymeren, met 10% functionele groepen, is het verschil met P3HT opmerkelijk. In zonnecellen met copolymeer:PCBM blends is de stroom gedurende een langere tijd stabiel op hogere temperatuur. DSC en X-straal diffractie wijzen erop dat 10% gefunctionaliseerde zijketens interfereren met de ordening in het polymeer, en de reorganisatie in blends vertragen door het verstoren van de krisatllisatie. Gebruik makend van een 9/1 copolymeer worden efficienties bereikt vergelijkbaar met P3HT, gecombineerd met een verhoogde stabiliteit van de morfologie in de blend.

Dankwoord

Aan het eind van een vierjarige periode in mijn leven, die leerrijk was op vele vlakken en waarbij ik heb het plezier en het genoegen heb mogen smaken om te leren over de wetenschap, over mijzelf en andere mensen, wens ik een aantal mensen te eren, want “eren” zit in “doctoreren”. Ik hoop dat ik alle zaken die ik ervaren en geleerd heb, een goede plaats in mijn leven zal kunnen geven.

Allereerst wens ik mijn promotor, Prof. Dr. Dirk Vanderzande te danken voor de kans om aan een project te beginnen waarvan dit boekje het resultaat is, voor de gegronde voorbereiding die me in staat stelde om een IWT-beurs te behalen, voor het ter beschikking stellen van je drukbezette tijd in wetenschappelijke en andere discussies en voor de onvergetelijke zeiltochten. Alsook mijn co-promotoren Prof. Dr. Thomas Cleij en Dr. Laurence Lutsen, wens ik te danken voor hun begeleiding. Laurence, je voudrais vous remercier pour les conseils que vous avez donné pendant les quatres années, spécifiquement en préparant les stages à l’étranger.
De grote mate van vrijheid, zowel wetenschappelijk als organisatorisch, heb ik naar beste vermogen ingevuld en was een stimulans om uit te kijken naar nieuwe initiatieven, mogelijkheden en ervaringen. Samenwerking en correspondentie met mensen uit andere organisatie hebben mij bemoedigd en veel bijgebracht.

Onderzoek vereist financiering, waarvoor ik de vier jaar lange steun van het IWT-vlaanderen zeer apprecieer. Alsook de finianciële steun van het ESF,

zonder dewelke de buitenlands uitwisselings projecten niet mogelijk zouden zijn geweest, werd zeer gewaardeerd.

Henk Bolink van de Universidad Valencia ben ik speciale dank verschuldigd. Het verblijf in Valencia betekende voor mij een stap vooruit qua vaardigheden in onderzoek, maar ook menselijk heb ik hier veel uit geleerd. Het was geweldig om een andere cultuur te mogen beleven. Michele, I would like to thank you for sharing some great moments – with or without whiskey.
Also my stay at the Universidad Autonoma de Madrid is worth to remember and was a good experience. Thanks to Tomas, Gema and Beatriz, the cooperation became an asset to this thesis. Stefan Oosterbosch en Jan Gilot uit de groep van René Janssen (TUe), jullie vakkundige toepassing van materialen en enthousiasme was steeds leerrijk en motiverend. Afshin Hadipour (IMEC), veel dank voor de deskundige raadgevingen tijdens de hartelijke bezoeken.The thermal characterization done by Dr. Jun Zhao in the group of Dr. Guy van Assche and Prof. Bruno Van Mele and valued discussions about the results are a valuable addition, therefore: many thanks!

Dit doctoraatsproject had ik nooit kunnen vervullen zonder de deskundige hulp en raadgevingen die ik mocht ontvangen van verschillende mensen aan de Universiteit Hasselt: Kristof, dank voor het bijbrengen van enkele vaardigheden maar toch vooral de spirit, bij mijn aankomst aan de Uhasselt. Wibren, dank voor de bereidwilligheid waarmee je je ruime ervaring en expertise hebt gedeeld, waardoor ik ontzettend veel heb geleerd en de kwaliteit van mijn onderzoek en dit boekje heb kunnen verbeteren. Verder

dank ik vooral de collega's van de organische chemie voor de goede sfeer in het labo en op bureau. Mensen die al weg zijn: Juliette, Lien, Ine, Sofie, Fateme, Jerome, Burak, Liesbet, Zarina, Jimmy, Steven en mensen die er nog zijn Sarah, Joke, Hanne, Iris, Veerle, Raoul, Lidia, Ans, Fre, Elif en nu ook Suleyman, Toon, Brecht en Inge. Arne verdient een aparte vermelding, wegens de vriendschap, het jaar samen wonen en omdat hij mij duidelijk maakte dat ik best wel naar Hasselt zou kunnen komen. Jan (het samen afzien, dat schept een band) en Wouter, voor de voetbaluitslagen per SMS, voetbal- en andere uitstappen per auto of vliegtuig, eilandhumor en Bosporus/Koelen-momenten. Sylvain, mon ami, merci pour tous les moments dans un café ou pas, à Hasselt ou n'importe où. Je me souviendrai ce trip magnifique et désorganisé en Californie pour longtemps.
Naast de sfeerverzorging waren de collega's ook daar voor het wetenschappelijk gedeelte: Iris en Veerle voor GPC metingen. Peter Adriaensens, Koen en Raoul: dank voor de opname van vele NMR-spectra. Huguet stond steeds klaar voor UV-Vis en IR. Technische- en glasproblemen werden dan weer opgelost door Jos en later door Tim. Niets van dit alles zou mogelijk geweest zijn zonder de gewaardeerde werking van de mensen op het secretariaat en Christel.

Een fascinerend deel van dit doctoraatswerk was voor mij het toepassen van de materialen die ik zelf gemaakt heb. Daarom zou ik graag de collegae-doctorandi van de materiaalfysica willen danken voor de samenwerking. Sabine: de geheimen van het plaatjes schoonmaken, spincoaten, zonnecellen maken, stabiliteitsmetingen, TEM en andere microscopie heb ik allemaal aan jou mogen ontfutselen, tussen de grappige gesprekken door. Jean-Christophe, merci beaucoup pour l'atmosphere agréable pendant la

préparation des OFETS. Bart Ruttens dank ik voor de karakterisatie dmv XRD, Geert Lekens voor de raadgevingen wat betreft de verouderingsexperimenten. Dr. Jan D'Haen, Prof. Jean Manca, Dr. Abay Gadisa en Koen Vandewal waren ook steeds te vinden voor leerrijke discussies. Verder was de sfeer in het IMO-gebouw en daarrond aangenaam, waarvoor dank aan Rob,Ronald, Ilse, Ann, Bert, Wouter, Evi, Lars en Jan.

Dan resteren nog de belangrijkste mensen in mijn leven, mijn vrienden en familie. De vrienden uit Brussel, die zich langzaam aan het verspreiden zijn over België en daar stilaan vervallen in volwassen zaken zoals samenwonen, trouwen en kinderen krijgen. Jullie zijn steeds een geweldige motivatie om waar dan ook samen te komen om - al dan niet aan den toog – het nodige plezier te beleven. Gedurende het doctoreren waren ook steeds de WK-activeiten memorabele hoogtepunten en momenten van reflectie en ontspanning. Iemand die tijdens de eerste jaren van deze periode een speciale plaats heeft ingenomen is Katleen. De herinnering aan die tijd en aan de vele verblijven in hotel Hens zijn mij dierbaar. Camille, de voorbije jaren waren een droom voor mij, het sprookje dat ik zocht. Onze ervaring samen in Spanje, de wederzijdse liefde, het vertrouwen en respect, de spirit die er was in onze relatie, zijn dingen waar ik energie zal blijven uithalen.

Mijn familie, P Jef, Bomma en Bobonne, Ma en Arnold, Pa en Anneke. Peter, Ward en Mie. De weekends thuis of familiale activiteiten in Hasselt of elders– ook al vallen die verdacht veel samen met caféachtige bezigheden - zijn momenten waar ik veel plezier en voldoening uit haal en zaken die ik koester. Ik ben steeds trots en blij als ik alle broers en zusje samenzie.

Dank u!

ANOVA: ANALYSIS OF VALUE

IS YOUR RESEARCH WORTH ANYTHING?

Developed in 1912 by geneticist R.A. Fischer, the Analysis of Value is a powerful statistical tool designed to test the significance of one's work.

am i wasting my time?

Significance is determined by comparing one's research with the **Dull Hypothesis**:

$$H_o: \mu_1 = \mu_2 \ ?$$

where,

- H_o: the Dull Hypothesis
- μ_1: significance of your research
- μ_2: significance of a monkey typing randomly on a typewriter in a forest where no one hears it.

WWW.PHDCOMICS.COM

The test involves computation of the *F'd* ratio:

$$F'd = \frac{\text{sum(people who care about your research)}}{\text{world population}}$$

This ratio is compared to the F distribution with I-1, N_r degrees of freedom to determine a *p(in your pants)* value. A high *p(in your pants)* value means you're on to something good (though statistically improbable).

Type I/II Errors

The Analysis of Value must be used carefully to avoid the following two types of errors:

- Type I: You incorrectly believe your research is not Dull.
- Type II: No conclusions can be made. Good luck graduating.

Of course, this test assumes both Independence and Normality on your part, neither of which is likely true, which means *it's not your problem.*